Technische Universität Dresden

High-Throughput Air-to-Ground Connectivity for Aircraft

Sandra Hoppe (geb. Hofmann), M. Sc.

der Fakultät Elektrotechnik und Informationstechnik der Technischen Universität Dresden

zur Erlangung des akademischen Grades

Doktoringenieur

(Dr.-Ing.)

genehmigte Dissertation

Vorsitzender: Prof. Dr.-Ing. habil. Frank Ellinger
Gutachter: Prof. Dr.-Ing. Dr. h. c. Frank Fitzek
Gutachter: Prof. Dr. Jonathan Rodriguez
Gutachter: Prof. Dr. Christian Bettstetter

Tag der Einreichung: 05.10.2020
Tag der Verteidigung: 19.04.2021

"The airplane became the first world wide web, bringing people, languages, ideas and values together."

Bill Gates

Acknowledgements

Pursuing a PhD degree can be compared to a journey, from the very first idea to the final publication. As a journey, it is full of ups and downs, delight and challenges. I am not enjoying travelling alone and luckily many people accompanied me on this journey in one way or another. I want to thank everyone who contributed to my work with their motivation and support.

Thanks to Airbus and TU Dresden for providing the opportunity of doing a PhD in industry. I enjoyed the balance between academia and industrial research and can only encourage future students to do the same.

Thanks to Prof. Dr.-Ing. Dr. h.c. Frank H. P. Fitzek for accepting to supervise my thesis, his guidance and valuable comments. Thanks for inviting me to become a part of the ComNets family, and for making me a feel as a full member despite the physical distance.

Thanks to Dr.-Ing. Dominic Schupke, for his guidance and his patience in seemingly endless discussions. In particular, thanks for his encouragement and support, his advice on my research and my personal development have been invaluable.

Thanks to my fellow PhD students and colleagues, both at Airbus and ComNets teams, for inspiring discussions, providing support and a positive working environment. In particular, thanks to Adrian Exposito Garcia, Divya Tati and Aygün Baltaci, the "wireless" PhD students, for their for friendship and positive mindset even during frustrating times. Thanks to all my co-authors for the great joint work and collaboration, in particular to the KTH ICARO-EU team.

Lastly, thanks to my family and friends for their unconditional support, in particular, to Nils Hoppe, for being at my side and supporting and motivating me. Finally, thanks to my parents Dagmar and Heinz Hofmann for their continuos support and encouragement wherever my path has lead me and their unconditional support wherever it will lead to in the future.

Abstract

Permanent connectivity to the Internet has become the defacto standard in the second decade of the 21st century. However, on-board aircraft connectivity is still limited. While the number of airlines offering in-flight connectivity increases, the current performance is insufficient to satisfy several hundreds of passengers simultaneously. There are several options to connect aircraft to the ground, i.e. direct air-to-ground, satellites and relaying via air-to-air links. However, each single solution is insufficient. The direct air-to-ground coverage is limited to the continent and coastal regions, while the satellite links are limited in the minimum size of the spot beams and air-to-air links need to be combined with a link to the ground. Moreover, even if a direct air-to-ground or satellite link is available, the peak throughput offered on each link is rarely achieved, as the capacity needs to be shared with other aircraft flying in the same coverage area. The main challenge in achieving a high throughput per aircraft lies in the throughput allocation. All aircraft should receive a fair share of the available throughput. More specifically, as an aircraft contains a network itself, a weighted share according to the aircraft size should be provided. To address this problem, an integrated air-to-ground network, which is able to provide a high throughput to aircraft, is proposed here. Therefore, this work introduces a weighted-fair throughput allocation scheme to provide such a desired allocation. While various aspects of aircraft connectivity are studied in literature, this work is the first to address an integrated air-to-ground network to provide high-throughput connectivity to aircraft.

This work models the problem of throughput allocation as a mixed integer linear program. Two throughput allocation schemes are proposed, a centralized optimal solution and a distributed heuristic solution. For the optimal solution, two different objectives are introduced, a max-min-based and a threshold-based objective. The optimal solution is utilized as a benchmark for the achievable throughput for small scenarios, while the heuristic solution offers a distributed approach and can process scenarios with a higher number of aircraft. Additionally, an option for weighted-fair throughput allocation is included. Hence, large air-

craft obtain a larger share of the throughput than smaller ones. This leads to fair throughput allocation with respect to the size of the aircraft. To analyze the performance of throughput allocation in the air-to-ground network, this work introduces an air-to-ground network model. It models the network realistically, but independent from specific network implementations, such as 5G or WiFi. It is also adaptable to different scenarios. The aircraft network is studied based on captured flight traces. Extensive and representative parameter studies are conducted, including, among others, different link setups, geographic scenarios, aircraft capabilities, link distances and link capacities. The results show that the throughput can be distributed optimally during high-aircraft-density times using the optimal solution and close to optimal using the heuristic solution. The mean throughput during these times in the optimal reference scenario with low Earth orbit satellites is 20 Mbps via direct air-to-ground links and 4 Mbps via satellite links, which corresponds to 10.7% and 1.9% of the maximum link throughput, respectively. Nevertheless, during low-aircraft-density times, which are less challenging, the throughput can reach more than 200 Mbps. Therefore, the challenge is on providing a high throughput during high-aircraft-density times. In the larger central European scenario, using the heuristic scheme, a minimum of 22.9 Mbps, i.e. 3.2% of the maximum capacity, can be provided to all aircraft during high-aircraft-density times. Moreover, the critical parameters to obtain a high throughput are presented. For instance, this work shows that multi-hop air-to-air links are dispensable for aircraft within direct air-to-ground coverage. While the computation time of the optimal solution limits the number of aircraft in the scenario, larger scenarios can be studied using the heuristic scheme. The results using the weighted-fair throughput allocation show that the introduction of weights enables a user-fair throughput allocation instead of an aircraft-fair throughput allocation. As a conclusion, using the air-to-ground model and the two introduced throughput allocation schemes, the achievable weighted-fair throughput per aircraft and the respective link choices can be quantified.

Contents

List of Figures

List of Tables

Symbols

a	aircraft
a_h	aircraft selected for handover
a_i	aircraft i
A	set of aircraft connected to own base station
alt_1	altitude of aircraft 1
alt_2	altitude of aircraft 2
$A_{\lambda_{s,t}}$	defines if capacity threshold β is exceeded
BW	bandwidth
β	capacity threshold
b_h	base station selected for handover
b	neighbor BSs
b_j	neighbor BSs j
B	set of neighbor BSs
c_{maxAir}	maximum capacity of A2A links
c_o	own capacity
c_{DA2G}	maximum capacity of DA2G links
c_{GEO}	maximum capacity of GEO links
c_{LEO}	maximum capacity of LEO links
c	speed of light
D_{air}	maximum nodal degree for A2A links
D_{da2g}	maximum nodal degree for DA2G links
D_n	nodal degree for node n
D_{sat}	maximum nodal degree for satellite links
D	antenna diameter
d	vector with directions of aircraft a to BSs b
$d_{a_i b_j}$	direction of aircraft a_i to BS b_j
d_o	vector with directions of aircraft a to own BS

d_{TX-RX}	distance between transmitter and receiver
d_1	maximum link distance between aircraft 1 and tangent point on ground
d_2	maximum link distance between aircraft 2 and tangent point on ground
d_{max}	maximum link distance
E_{AIR}	set of A2A edges
E_{DA2G}	set of DA2G edges
E_{GEO}	set of GEO edges
E_{GND}	set of edges from satellite and BSs to ground
E_{ISL}	set of ISL edges
E_{LEO}	set of LEO edges
E	set of edges
η	efficiency
$f_{i,j}^{\lambda_{s,t}}$	traffic flow on each edge (i, j) from source s to destination t
f	frequency
G	antenna gain
G_{RX}	gain of receive antenna
G_{TX}	gain of transmit antenna
h_a	vector with headings of aircraft a
$h_{i,j,step}$	binary helper variables per step
$I_{i,j}^{k,l}$	received interference of link (i, j) by link (k, l)
k_B	Boltzmann constant
Λ	set of data rates
$\lambda_{s,t}$	throughput from the source s to destination aircraft t
l_{des}	desired load per aircraft
Δl	vector with difference of own load to neighbor loads
l_e	vector with estimated new load difference
$l_{e_{ij}}$	estimated new load difference of aircraft a_i to BS b_j
l_o	own load
l_a	vector with loads of aircraft a
l_b	vector with loads of base station b
L_{other}	additional losses
l_{step}	upper 1/SINR limits per step
N_{ofdma}	number of OFDMA symbols
N_0	thermal noise power
N_{PRB}	number of resource blocks

N_{slots}	number of slots
N_{sub}	number of subcarriers
$N_{symbols}$	number of symbols per second
n_s	number of steps
OH	overhead
$\pi_{i,j}$	penalty of a link (i, j)
$\Phi(s_{i,j})$	capacity step function in terms of 1/SINR
p_a	vector with positions of aircraft a
p_b	vector with positions of BSs b
$P_{i,j}$	received power at aircraft j from aircraft i
P_{RX}	receive power
P_N	total noise power consisting of thermal noise power and interference
P_{TX}	transmit power
ψ	beam width
R_{4G}	4G data rate
R_{earth}	radius of the Earth
r_d	ranks of d
r_l	ranks of l_e
ρ_{AC}	aircraft density
ρ_{BS}	BS density
SE	symbol efficiency
$s_{i,j}$	1/SINR at aircraft j from link (i, j)
s_{thresh}	SNR threshold needed for respective modulation format
s	source node
t	destination node
T	temperature
θ	steering angle
t	times
T	set of times
V	set of vertices
v_{layers}	number of layers
v_{step}	capacity values per step
w_a	vector with weights of aircraft
w_{min}	minimum weight of aircraft
$z_{i,j}$	topology variable, defining if edge (i,j) is selected

Acronyms

3GPP	3rd Generation Partnership Project
a/c	aircraft
A2A	air-to-air
A2G	air-to-ground
AAC	Aeronautical Administrative Communication
AANET	aeronautical ad-hoc network
ADS-B	Automatic Dependent Surveillance - Broadcast
ADSL	asymmetric digital subscriber line
AOC	Aeronautical Operational Control
AODV	Ad-hoc On-demand Distance Vector
APC	Aeronautical Passenger Communication
ATC	air traffic control
ATSC	Air Traffic Service Communication
ATM	air traffic management
ATSSS	Access Traffic Steering, Switching and Splitting
BATMAN	Better Approach To Mobile Adhoc Networking
BS	base station
D2D	device-to-device
DA2G	direct air-to-ground
DL	downlink
DSR	Dynamic Source Routing

DYMO	Dynamic MANET On-demand
E2E	end-to-end
EAN	European Aviation Network
eNB	evolved NodeB
EIRP	Equivalent Isotropically Radiated Power
FANET	flying ad-hoc network
GEO	geostationary Earth orbit
gNB	Next Generation NodeB
GND AP	ground access point
GNSS	global navigation satellite system
GPS	Global Positioning System
GPSR	Greedy Perimeter Stateless Routing
HAPS	high-altitude pseudo satellite
HEO	high elliptical orbit
HF	high frequency
HTS	high throughput satellite
IATA	International Air Transport Association
ICAO	International Civil Aviation Organization
IoT	Internet of Things
ISL	inter-satellite links
ISM	industrial, scientific and medical
LB-G	load balancing ground
LB-S	load balancing satellite
LEO	low Earth orbit
LOS	line of sight
MANET	mobile ad-hoc network
MEO	medium Earth orbit
MILP	mixed integer linear program
MIMO	multiple-input multiple-output
MP-TCP	Multipath Transmission Control Protocol
NGMN	Next Generation Mobile Networks
NR	5G new radio

NTN	non-terrestrial network
QAM	quadrature amplitude modulation
QoS	quality of service
QUIC	Quick UDP Internet Connections
QPSK	quadrature phase shift keying
RAN	radio access network
SDN	software-defined networking
SNR	signal-to-interference ratio
SINR	signal-to-interference-plus-noise ratio
SON	self organized network
TCP	Transmission Control Protocol
UAV	unmanned aerial vehicle
UE	user equipment
UL	uplink
V2X	vehicle-to-everything
VHF	very high frequency
VDL	VHF data link

1 Introduction

This chapter gives an introduction and background on high-throughput air-to-ground (A2G) connectivity. Firstly, studying high-throughput A2G connectivity is motivated. Subsequently, the used terminology is introduced. Furthermore, all A2G link options and their respective properties are stated. The relevant A2G services and their requirements are defined as well. Moreover, the related work is studied. Lastly, the contributions of this thesis are stated and the related publications are presented.

1.1 Motivation

Connectivity has become essential in our everyday lives. People expect to be connected anywhere, at home or while travelling. In 2018, the global average mobile network throughput was 13.2 Mbps and is expected to increase to 43.9 Mbps for mobile networks and 91.6 Mbps for WiFi networks until 2023 [1]. While the average throughput includes rural areas, the peak throughput is significantly higher. The IMT-2020 requirements for 5G networks define a user experienced data rate of 100 Mbps and a peak data rate of up to 20 Gbps [2]. The number of airlines offering in-flight internet connectivity to passengers is also increasing. Operators, such as Viasat, advertise a peak throughput of up to 100 Mbps per aircraft [3]. Given that this throughput has to be shared by all passengers on an aircraft, 100 Mbps is insufficient for satisfying all passengers simultaneously. Moreover, the peak throughput cannot be reached at all times. Measurements [4] show that the throughput is below 10 Mbps in approximately 90% of all measured time instants, in 50% it is even below 1 Mbps.

Users expect a certain minimum throughput in order to be satisfied with the connectivity. The main limitation for aircraft is that it contains an on-board network on its own, with a high number of passengers demanding connectivity to servers or users on the ground.

Beside passengers, the crew as well as other services can benefit from additional connectivity, e.g. collecting sensor data from the aircraft. Therefore, 100 Mbps per aircraft, as stated above, is insufficient for the number of users on the aircraft. The Next Generation Mobile Networks (NGMN) estimates that 1.2 Gbps on the downlink (DL) and 600 Mbps on the uplink (UL) will be needed per aircraft [5].

The A2G connectivity performance depends on several factors. To serve a high number of passengers, a high throughput is needed. Additionally, A2G connectivity should provide coverage throughout the flight. Besides that, some services also demand a low delay. For passenger connectivity, throughput is the main challenge due to the large number of users on-board. Therefore, high-throughput connectivity for aircraft is investigated here. There are different options to provide connectivity today, for instance using geostationary Earth orbit (GEO) satellites. Recently, several new low Earth orbit (LEO) constellations, such as OneWeb or StarLink, have been announced with the aim of providing high throughput worldwide. The goal of improving connectivity is also pursued by using high-altitude pseudo satellite (HAPS), for instance by projects such as Google Loon. Hence, there is a trend of moving high-throughput communication networks toward the sky. Likewise, combining space, aerial and terrestrial networks is investigated in research to improve the performance of ground users. These concepts can also be applied to aircraft connectivity. The seamless support for different A2G links is pursued by the Seamless Air Alliance, consisting of major players such as operators, airlines and manufacturers [6]. Additionally, companies like SITA present their vision of a multi-network mobile inflight connectivity [7]. Achieving a high throughput per aircraft not only depends on the link throughput. Aircraft need to share the capacity offered within the same area. Hence, depending on the time of day and flight route, the throughput varies. Therefore, multiple links should be used simultaneously to obtain the optimal throughput, which will be studied within this work.

Lastly, for a high performance, the achievable throughput should be as stable as possible over the flight. A highly fluctuating throughput leads to a low user satisfaction. Additionally, the users on aircraft have to be taken into account, as large passenger aircraft transport more passengers than small aircraft. Hence, the achievable throughput per aircraft should be weighted. It needs to be determined, which links have to be chosen in order to to achieve this. Consequently, this study investigates the achievable weighted throughput per aircraft over time by using multiple links.

1.2 Terminology and definitions

The different links from the aircraft to the ground can be referred to as A2G links. This definition includes both directions, from the aircraft to the ground and from the ground to the aircraft. It also includes paths consisting of multiple hops, for instance from one aircraft to another aircraft to the ground. Multiple A2G links form an A2G network.

A simplified view on the A2G network is depicted in Figure 1.1. In cellular networks, the link from the user to the BS is defined as UL and the link from the BS to the user as DL. In the A2G network, the same terminology is used. Therefore UL refers to the link from the aircraft to the BS, while the physical direction is down toward the ground. For consistency, the same definition can be applied to the satellite and air-to-air (A2A) links, centering on the receiving or transmitting aircraft. Additionally, the focus of this study is on the A2G network, as the achievable throughput per aircraft is limited by the A2G links. It is assumed that the ground network is properly dimensioned to relay traffic to and from the A2G network. Therefore, the ground network is modeled as a single source or sink node, excluding the detailed network structure. This is depicted by the purple links in Figure 1.1.

The A2G architecture can be analyzed from different perspectives. The system architecture contains full information about the network connectivity as well as its entities, for instance authentication, subscription management or mobility management. The connectivity architecture states the network topology, i.e. nodes and links. Here, A2G architecture means the connectivity architecture due to the focus on the connectivity. Furthermore, it allows to study the network independently of specific implementations. Due to this reason, the primary metric is the maximum achievable throughput per aircraft. Depending on the network technology or implemented protocols, the goodput will be lower. However, the selected network technology depends on multiple, also non-technical factors. Therefore, the throughput is used as a general property of any link, independent of the implementation.

The A2G network is designed for users on the aircraft, which includes different types of services. A service is defined as a specific application that can be utilized by users on the aircraft, for instance video streaming for passengers. These services include different requirements in terms of throughput, delay and end-to-end (E2E) reliability of the service. In this case, E2E reliability means that the service can be offered during the whole flight without disruptions. The services are utilized by multiple users simultaneously, hence requirements of different services need to be fulfilled simultaneously.

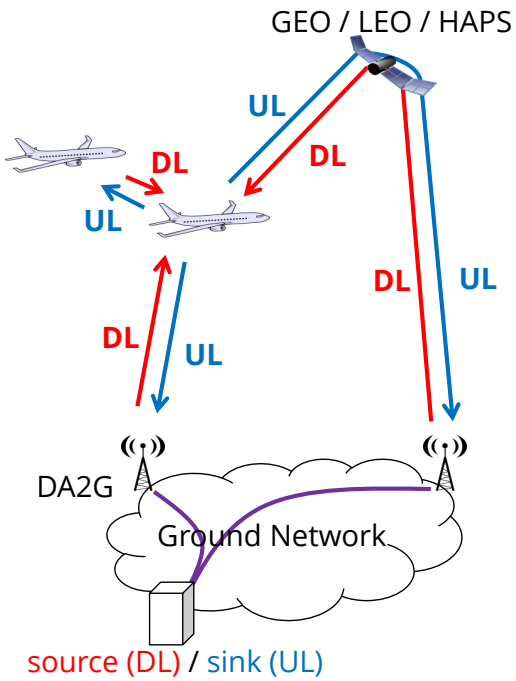

Figure 1.1: A2G connectivity architecture, defining UL and DL directions and the simplified ground network.

1.3 Air-to-ground link options and properties

The different options for aircraft connectivity are presented in Figure 1.2. Worldwide connectivity can be provided by satellites. HAPS can provide additional capacity for specific areas. Over the continent, direct air-to-ground (DA2G) networks are available. Moreover, direct links between aircraft, namely A2A links, can be used for relaying data. In the following, these different link options are introduced including a detailed description as well as properties of currently deployed systems.

1.3.1 Satellites and high-altitude pseudo satellites

Today, satellites are the most widely used option for A2G connectivity. The reason lies in their wide area coverage, offering almost worldwide coverage. A satellite acts as a relay node between the user and the terrestrial network. Depending on the type of satellite, relaying via multiple hops is also feasible. Several frequency bands are available for satellite connectivity worldwide. Satellite services include a wide range of applications, for instance communication, navigation or television. Due to the available bandwidth, different satellite frequency bands are suitable for different types of applications. For high-capacity connectivity, Ka- and Ku-bands are most commonly used. The Ku-band ranges from 12 GHz to 18 GHz and the Ka-band spans 26 - 40 GHz.

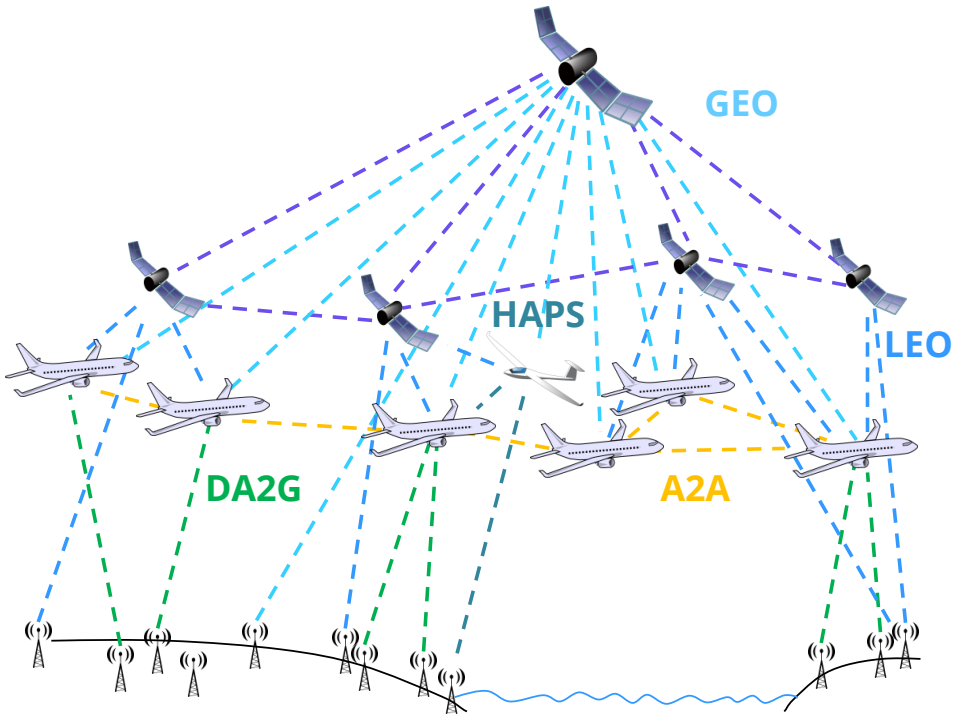

Figure 1.2: Options for A2G connectivity (extended version from [P1] ©2019 IEEE).

Satellites can be classified according to their orbit, namely GEO, medium Earth orbit (MEO) and LEO satellites. Additionally, high elliptical orbit (HEO) specifies elliptical orbits, which can be used to provide polar coverage. Furthermore, HAPS are unmanned objects which fly in the stratosphere at an altitude of about 20 km. They are technically not a satellite, but from the connectivity perspective they act similar to a satellite. Therefore they are included in this section.

GEO satellites are placed in an altitude of 35.786 km, enabling a geostationary position of the satellite. Due to their high altitude, GEO satellites cover a large area, which can be up to one third of the Earth's surface, excluding polar areas. However, the high altitude causes a high propagation delay. The propagation delay is approximately 119 ms for one way from the Earth to the satellite. Including additional delays, such as processing delays and communication protocol overhead, the E2E delay can exceed 500 ms. Additionally, the cost of building, launching and operating a satellite is high, resulting in high cost for the connectivity. To utilize the available bandwidth efficiently, high throughput satellite (HTS) use spot-beam technology. The beams can be fixed or steerable, depending on the capabilities of the satellite. For instance, the Inmarsat-5 satellites implement 89 fixed beams with 40 MHz each and 6 steerable beams while up to 72 beams can be active concurrently [8]. Today, several operators provide aircraft connectivity via GEO satellites. A comparison of advertised peak capacities

is presented in Table 1.1. Today, the peak capacity can be up to 100 Mbps, while operators are working on improving the capacity. For instance, Inmarsat showed 330 Mbps in a trial to a terminal on ground [9]. Moreover, more advanced HTS satellites are currently planned. While the Viasat-2 satellites offer 300 Gbps total capacity, the next generation Viasat-3 will provide 1 Tbps total capacity [10]. Additionally, the next generation Eutelsat satellite will provide 500 Gbps total capacity [11]. Nevertheless, the total capacity needs to be shared among all users. Therefore the achievable capacity per user will be less, in particular for moving users like aircraft. From the aircraft perspective, GEO satellites are suitable due to their worldwide coverage without frequent handovers. However, disadvantages are high delay and cost.

MEO satellites cover the altitudes from the GEO altitude to approximately 2000 km. compared with GEO, the MEO is not geostationary, hence a constellation of satellites is needed provide a worldwide coverage at all times. One example of a MEO constellation is Global Positioning System (GPS). For communication satellites, MEO is rarely used. SES O3b mPower is one example for high-throughput connectivity. In a recent trial, they achieved 256 Mbps between the ground and an aircraft in flight via a combined GEO/MEO network [12]. The advantage of MEO constellations is their nearly global coverage with a small amount of satellites and with a reduced delay compared with GEO satellites.

LEO satellites are starting from the MEO altitude, reaching down to some hundreds of kilometers. Due to the low orbit, a constellation with a large number of satellites is needed to provide sufficient coverage. Additionally, frequent handovers between satellites in the order of tens of minutes are necessary, due to the high relative speed between the satellite and the surface of the Earth. Moreover, LEO satellites offer low delay connectivity. For an altitude of 1200 km, the one-way propagation delay from the Earth to the satellite is 4 ms. Existing LEO constellations, like Iridium or Globalstar, focus on worldwide connectivity services rather than on high capacity. Lately, LEO constellations, are being discussed for high-capacity connectivity.

Several companies announced high-capacity LEO constellations, aiming to build an Internet of satellites. While some efforts are highlighted here, a comprehensive list of announced and operational LEO constellations can be found in [13]. The OneWeb constellation is planned to consist of 650 satellites at 1200 km altitude and they intent to reach up to 400 Mbps per user [14]. This capability has already been tested in a trial using a part of the constellation which has already been launched [15]. OneWeb also plans to implement beam hopping to redirect capacity to hot spots [16]. The largest constellation, StarLink, has been announced by SpaceX, planning to launch a constellation with over 4000 LEO satellites to provide gigabit speeds [17]. During a trial, they achieved 610 Mbps to a military aircraft [18].

Telesat and Leosat also plan LEO constellations with speeds in the range of Gbps. Telesat showed 370 Mbps [19]. However, the mentioned constellations are not yet fully operational, hence the capacity they can offer in an operational network is still to be determined. An overview on the current status is presented in Table 1.1. LEO constellations are particularly interesting for aeronautical connectivity as they offer worldwide coverage and low latency connectivity. The main challenges are handling numerous handovers, spectrum availability and connecting mobile terminals with a high throughput.

HEO is an uncommon orbit for communication satellites. Nevertheless, the Molniya orbit is a special HEO, where the satellite is positioned over the polar region most of the time. As such, HEO can be a complement to GEO satellites, which lack coverage of polar regions due to the angle to the horizon [20]. However, as the HEO is not widely used, it is not further investigated here.

HAPS are objects flying in the stratosphere. Different types of objects are feasible, such as unmanned aerial vehicles (UAVs), airships or balloons. Airbus Zephyr is one example for a solar-powered UAV which can fly 25 days without landing and provide 100 Mbps [21]. Project Loon [22] is another approach using balloons. Their goal is to connect people without internet connection. The balloons are using the wind for navigation, which changes the direction at certain altitudes. HAPS are designed to provide coverage to a defined area on the ground. Therefore they act similar as GEO satellites, but with a significantly reduced coverage area. The advantage of HAPS is the flexible deployment and capacity enhancement for a specific area. The object needs to be able to provide a stable position over the desired area and to achieve a long flight time in the order of multiple months. A survey on types of aerial platforms, regulatory environment, architecture, technology advances, services, potentials and challenges can be found in [23]. From the connectivity perspective, new worldwide available frequencies have been allocated to be used for HAPS connectivity at the world radio conference 2019 [24]. For the aircraft connectivity use case, HAPS are interesting for high-aircraft-density areas, such as airports or frequently used air corridors.

An overview on satellite operators which are available for mobile broadband and aircraft today as well as announced constellations are summarized in Table 1.1. The announced constellations can be identified by “n/a” in the application column. The table includes the peak capacity per aircraft as well as throughput showcased in trials. Table 1.1 shows that the throughput achieved in trials is significantly higher than the currently available peak capacity. Therefore, an increase in throughput provided by satellites can be expected. Nevertheless, other factors besides peak capacity have to be taken into account, such as the number of aircraft and the size of spot beams, as studied in Chapter 2.

Table 1.1: Overview on satellite operators for mobile broadband for aircraft and the respective peak capacities.

Operator	Orbit	Application	Peak capacity per aircraft	Trials
Inmarsat	GEO	GlobalXpress	50/5 Mbps (DL/UL) [8]	330 Mbps [9]
Viasat	GEO	Viasat In-flight Internet	100/20 Mbps (DL/UL) [3]	n/a
Intelsat	GEO	Intelsat Epic NG	100 Mbps (DL) [25]	n/a
Eutelsat	GEO	Eutelsat Broadband	20 / 6 Mbps (DL/UL) [26]	n/a
Hughes	GEO	HughesNet Gen5	25/3 Mbps (DL/UL) [27]	n/a
SES / O3B	GEO/MEO	Signature Aero/ O3b mPower	n/a	256 Mbps [12]
Iridium	LEO	Iridium Certus	1.4 / 0.512 Mbps (DL/UL) [28]	n/a
GlobalStar	LEO	GlobalStar	256 kbps [29]	n/a
OneWeb	LEO	n/a	400/30 Mbps (DL/UL) [14]	400 Mbps [15]
StarLink	LEO	n/a	Gigabit speeds [17]	610 Mbps [18]
Telesat	LEO	n/a	Gigabit speeds [17]	370/110 Mbps [19] 1.2 Gbps [30]
Leosat	LEO	n/a	5.2 Gbps [31]	n/a

1.3.2 Direct air-to-ground

In contrast to satellite connectivity, DA2G specifies the direct connectivity between the aircraft and the ground. DA2G can be partitioned into two types of connectivity: low-throughput and high-throughput connectivity. A typical example for low-throughput connectivity is air traffic control (ATC), where mainly high frequency (HF) or very high frequency (VHF) spectrum is used. The advantage of HF and VHF spectrum is the high range. However, due to the small bandwidth available, these frequencies are unsuitable for high-throughput connectivity. This work focuses on broadband DA2G, therefore HF and VHF are out of the scope.

In terms of high-capacity connectivity, several commercial DA2G networks have been built in the US and Europe, respectively. An overview of the achievable peak capacities can be found in Table 1.2. Gogo has been the first operator, they provide up to 9.8 Mbps to aircraft using the 800 MHz frequency band [32]. They also announced plans on deploying a 5G network in the 2.4 GHz industrial, scientific and medical (ISM) band. The new network is expected to increase the capacity to more than 100 Mbps per aircraft [33]. Smartsky is the second operator in the US, using 4G in the 2.4 GHz ISM band. The network is not yet fully operational, nevertheless, they showcased a throughput of 21 Mbps to an aircraft [33]. In Europe, up to 75 Mbps per aircraft are offered by the European Aviation Network (EAN), using 30 MHz in the S-band satellite spectrum [34]. The network consists of 300 BSs. China Mobile conducted trials in China, reaching up to 75 Mbps per aircraft and plan to build a 5G network in China [35]. In Japan, 141.7 Mbps have been shown in trials using 100 MHz in the millimeter wave spectrum [36]. The advantage of DA2G compared with satellites is the easy maintenance and upgrades. More BSs can be easily added to the network. Also high throughput can be provided with low delay. The one-way propagation delay is only 0.035 milliseconds. The disadvantage is the coverage limitation to the continent and areas close to the shore. As aircraft also travel over oceans, an alternative needs to be selected there. The enabler for high-capacity DA2G is a high available bandwidth. Operators in the US partially utilize unlicensed bands, while the EAN uses the satellite S-band. Additionally, candidate DA2G frequency bands have been identified in Europe [37]. The frequencies are in the range of 1.9 GHz and 5.8 GHz. Whereas the 1.9 GHz frequency is a licensed band, the 5.8 GHz frequency needs to ensure coexistence with other users.

1.3.3 Air-to-air

A2A connectivity refers to the communication link between two aircraft. There are two different types of A2A connectivity. The first type is the direct connectivity between two aircraft. One example is Automatic Dependent Surveillance - Broadcast (ADS-B), where aircraft broadcast their position and other specific information about the flight. While ADS-B is only

Table 1.2: Overview on DA2G operators and the respective peak capacities.

Operator	Area	Spectrum	Peak capacity / aircraft	Trials
EAN	EU	S-band	75 Mbps [34]	n/a
GoGo	US+Alaska	800 MHz	9.8 Mbps [32]	n/a
Smartsky	US	2.4 GHz	n/a	21 Mbps [33]
China Mobile	China	n/a	n/a	75 Mbps [35]
n/a	Japan	46.8/44.45 GHz (UL/DL)	n/a	141.7 Mbps [36]

implementing one-way connectivity, also use cases with bidirectional connectivity are possible. The second type of A2A connectivity is relaying. Aircraft can connect to each other to relay data from the satellite or DA2G network. With this procedure, aircraft without satellite or DA2G connectivity could receive additional throughput from other aircraft via A2A links. This type of A2A is unused today, therefore reference implementations are unavailable. Nevertheless, InfinitusSuperHighway proposed utilizing A2A connectivity to build a global backhaul network [38]. Additionally, A2A connectivity has been investigated in research, as introduced in Section 1.5. The advantage of A2A connectivity is to provide additional throughput in areas with poor coverage. However, A2A depends on a changing topology and thus it is difficult to guarantee a certain delay or throughput. Furthermore, the availability of other aircraft depends on the route and time of flight. From now on, A2A connectivity refers to the second type, i.e. relaying, as a direct communication between two aircraft is unsuitable for A2G connectivity. As a conclusion, A2A is interesting to enhance the throughput for aircraft with a poor coverage. However, challenges include topology formation and how to distribute available capacity among aircraft. Table 1.3 summarizes the properties of the discussed A2G links.

1.4 Air-to-ground services

On aircraft, different use cases demand A2G connectivity. The International Civil Aviation Organization (ICAO) defines four types of connectivity, namely Air Traffic Service Communi-

Table 1.3: Overview on A2G link properties.

Properties	Throughput	Delay	Coverage
DA2G	High	Low	Continental
GEO	High	High	Worldwide
LEO	High	Medium	Worldwide
HAPS	High	Low	Regional
A2A	Time / position dependent	Low/Medium	Time / position dependent

cation (ATSC), Aeronautical Operational Control (AOC), Aeronautical Administrative Communication (AAC) and Aeronautical Passenger Communication (APC) [39]. ATSC combines all applications related to ATC as well as closely related functions, such as reporting the position of the aircraft. AOC and AAC are related to connectivity used by the airline. AOC defines safety related information exchange, such as communication with the authorities. AAC contains the non-safety related connectivity used by the airline, such as catering information. Lastly, APC includes all types of passenger connectivity. These connectivity types group aircraft connectivity with regard to the application. However, when focusing on high-throughput A2G connectivity, a different clustering of A2G services is more suitable. High-throughput services origin from three types of users, namely passengers, the crew and the aircraft itself. These three user groups, their type of services and requirements are detailed in the following. As this work focuses on A2G connectivity, services without an A2G component, i.e. ground-to-ground, aircraft-to-aircraft and within one aircraft, are omitted.

Connectivity from the passengers to the ground can be partitioned into three groups, i.e. multimedia connectivity, internet connectivity and voice connectivity. Multimedia connectivity includes video streaming, video phone calls and conferences. From the connectivity perspective, streaming and conferences can be distinguished by their link usage. While streaming uses mostly the DL, conferences are relying on both, UL and DL. In general, the throughput demand of multimedia connectivity is high. For video phone calls and conferences, a low delay and a stable E2E connection is necessary to ensure realtime interactions. For streaming, the delay requirements can be relaxed, as the video can be buffered. Internet connectivity includes surfing the Internet, sending and receiving emails and short messages. The requirements differ with the exact application. However, in general the requirements for Internet connectivity are relaxed. Voice connectivity is another passenger service. Voice is vulnerable to high delays. The throughput requirement is low but long interruptions on the connection should be avoided. In general, passenger services are uncritical for the operation of the aircraft, hence, disruptions can be tolerated.

Crew connectivity include all A2G connectivity used by the crew. The requirements of the described crew services are similar to Internet and voice connectivity for passengers. Nevertheless, crew connectivity should be handled with priority compared with passenger applications.

The third type of connectivity originates from the aircraft itself. Data collected by sensors on the aircraft can be used to improve the operation and maintenance of the aircraft. The data can be used to actively monitor the state of the aircraft or collected for a full analysis. From the connectivity perspective, two implementation options exist. The first option is to send all aircraft data to the ground for analysis. The second option is to analyze some data

on the aircraft and generate reports to be sent to the ground. These options depend on the specific sensor data and the criticality of the application. The communication is on the UL and depending on the implementation a large amount of data can be generated during the flight. In terms of requirements, sensor data transmission and realtime monitoring needs to be distinguished. Sensor data transmission is delay tolerant while realtime monitoring has to be transmitted with a reduced delay.

The described services differ in terms of their requirements. A high throughput is needed for multimedia applications, while telephony and monitoring need a short delay and good reliability to ensure the reception of live information. Reliability is defined in terms of ensuring a stable E2E connection. Sensor data and Internet connectivity are least demanding in terms of throughput, delay and reliability. The mapping of links to services is presented in Table 1.4. Most links are suitable for most services. The limitations are the coverage of DA2G and HAPS and the high delay of GEO satellites. Furthermore, A2A capabilities are challenging to predict as they depend on the time and route of the flight. The coverage limitation of DA2G can be relaxed, if the flight does not leave the network coverage. However, while the general comparison of the requirements is promising, the number of users needs to be taken into account. An aircraft transports multiple hundreds of passengers. While each link can easily transmit one multimedia streaming flow, multiple hundred streams in parallel are challenging to provide. Therefore, there is a bottleneck in satisfying the requirements of all aircraft users simultaneously. According to NGMN, 1.2 Gbps on the DL and 600 Mbps on the UL will be needed per aircraft to satisfy passenger requirements. Therefore, the achievable throughput per link will be investigated in the following chapters.

Table 1.4: Comparison of requirements of the A2G services and A2G link properties, ✓: suitable, ✗: unsuitable, ❍: suitable under stated condition.

Application	User	DA2G	GEO	LEO	HAPS	A2A
Multimedia streaming	passenger	✓[1]	✓	✓	✓[1]	❍[3]
(Video-) telephony	passenger	✓[1]	✗	✓	✓[1]	❍[4]
Internet connectivity	passenger, crew	✓[1]	✓	✓	✓[1]	✓
Sensor data	aircraft	✓[1]	✓	✓	✓[1]	✓
Real-time monitoring	aircraft	✓[1]	❍[2]	✓	✓[1]	❍[4]

[1]coverage limited, [2]if delay suits application, [3]if sufficient throughput, [4]if E2E route is ensured

1.5 Related work

Research in aerial connectivity covers a large field. The A2G network includes different types of networks, with specific challenges for each of the networks. Additionally, there are different types of aerial vehicles, such as aircraft or drones. As this work studies high-throughput connectivity for aircraft, only related work with a focus on aircraft connectivity is presented. This section is divided into five categories. The first category is integrated space-aerial-terrestrial networks, aiming at combining space, terrestrial and aerial networks to improve the overall performance. The second category is aircraft networking, which consists of aeronautical ad-hoc networks and aircraft networking in general. The third category is satellite networking. The fourth category is DA2G networking. Lastly, as the A2G network is a heterogeneous network, related work on heterogenous networking is introduced as well.

1.5.1 Integrated space-aerial-terrestrial networks

The area of integrated space-aerial-terrestrial networks has gained attention since 2016. The main motivation is to integrate terrestrial and non-terrestrial networks to enhance the performance in the terrestrial network, such as overcoming coverage problems of the terrestrial network by using a satellite. While the network architecture is similar throughout different publications, the name of the network varies, i.e. ACN, AWMN, GIG, ISTN, MLSTIN, SAGIN, SIN and SSAGV. In general, the network consists of three different layers, i.e. space, air and ground layers. The space layer contains different types of satellites. The aerial layer contains HAPS, aircraft and infrequently also UAVs. The layers are mostly interconnected within and between each other. In contrast to this work, the benefit of the integrated network is designed for terrestrial users.

Surveys on the potential and challenges of integrated space-aerial-terrestrial networks are presented by [40, 41]. The survey by [40] provides an extensive overview containing physical layer characteristics, mobility management and routing as well as system integration and performance analysis. The authors identify the complexity of multi-layered networks and coordination of routing, scheduling and spectrum allocation as open challenges. The survey by [41] focuses on the properties and challenges of high altitude platforms and low altitude platforms and investigates the integrated architecture. Among others, the authors identify networking and integrated network design as future challenges. In contrast to this document, both surveys consider aircraft as a part of the network itself and not as the end user of the integrated network.

The other publications can be clustered into two areas: architecture and networking. The area of the architecture includes different variations of the architecture, while the area of

networking includes routing, resource allocation and service quality. For the area of the architecture, an integrated architecture consisting of radio frequency links between different layers and laser links within layers is studied by [42]. The authors propose different techniques for multiple antennas and cooperative transmission and show the feasibility of their approach. Bidirectional offloading is studied by [43]. This includes offloading of computation tasks from space to the ground as well as offloading of terrestrial data to the satellite. The authors show a performance gain and cost reduction for their architecture. One of the first publications in the area of integrated space-aerial-terrestrial networks is [44]. The authors focus on military networks, in particular on enhancing the satellite layer by adding LEO satellites. The applications of remote sensing, navigation and communication in an integrated satellite and terrestrial network are studied by [45]. The authors describe the necessary architecture for these applications. Integration of software-defined networking (SDN) into the architecture is investigated by [46,47]. A cross domain SDN architecture, taking into account the different abilities of the layers, is proposed by [46]. A similar SDN based architecture is proposed by [47], which is applied to a car network. An architecture, where aircraft are used as network nodes is proposed by [48]. In their architecture, aircraft are included in the network, not to receive throughput, but to provide connectivity to users on the ground. The authors propose to use millimeter wave A2A links and free space optics links between aircraft and satellites as well as for inter-satellite links.

In the area of networking, [49–51] focus on optimizing the capacity. The cross layer gateway selection problem is investigated by [49]. The authors optimize the expected transmission count and show the potential of their proposed algorithms. Deep learning is introduced by [50] to improve the network throughput and packet loss rate. Real-time service are studied by [51]. The authors focus on maximizing the effective capacity subject to quality of service (QoS) requirements. The efficiency of the network is investigated by [52,53]. Efficient resource utilization focusing on resource mobility in space information networks is investigated by [52]. Energy and spectral efficiency is optimized by [53]. Tools to model integrated space-aerial-terrestrial networks are developed by [54–56]. A model using network fixed point theory is introduced by [54]. It improves network organization and dynamic characteristics. A domain spatio-temporal consistency language to model observation of satellites is proposed by [55]. Their approach is beneficial for modeling and verifying network requirements. A simulation tool for integrated space-aerial-terrestrial networks is introduced by [56]. The authors developed a simulator combining several existing simulation tools, such as STK and ns-3. They present a case study of an integrated UAV, satellite and terrestrial network. The perspective of routing is investigated by [57, 58]. Content-size based routing is studied by [57] to improve the experienced latency in a hybrid asymmetric digital subscriber line (ADSL)-satellite network. A routing framework for delay tolerant data is proposed by [58]. The authors show that their algorithm improves the delivery ratio, E2E delay and power con-

sumption. Different options for connecting flying vehicles in terms of capacity is analyzed by [59]. The studied connectivity options are satellite, DA2G and A2A. The authors conclude that integrating the three connectivity options improves the overall available capacity and has the opportunity of overcoming the disadvantages of single technologies.

1.5.2 Aeronautical ad-hoc networks

Since 2009, aeronautical ad-hoc networks (AANETs) have been researched. The term AANET is derived from mobile ad-hoc network (MANET), which describes ad-hoc networking between mobile nodes. In the case of AANETs, the mobile node is an aircraft. Sometimes, the term flying ad-hoc network (FANET) is also used for aircraft, although flying node is normally referring to UAVs and drones. The concepts in these areas are similar, however, parameters such as channel conditions and mobility are different for aircraft nodes.

Aeronautical ad-hoc networks have been surveyed by [60–62]. The earliest survey is [60]. It has been part of the SANDRA project, which focused on seamless and integrated aeronautical networking, mainly for air traffic management, but also partly for passenger internet. The authors provide an overview on the aeronautical network modeling as well as routing and scheduling problems. More recently, [61] provides an extensive overview on all parts of the AANET, including applications, scenarios, requirements and challenges. While focusing on FANETs, [62] includes AANETs as well. The authors include mobility models, routing techniques and protocols.

The publications within AANETs can be partitioned into three groups: routing, feasibility and theoretical analysis. The theoretical analysis focuses on the theoretically achievable throughput, delay and connectivity for AANETs. Wang et. al. [63–65] derive analytic formulas for the throughput and delay for one and two-hop aeronautical networks. The capacity of an AANET in a corridor is analyzed by [66]. The authors conclude that the capacity scales with flight length, aircraft density and number of height levels. The connectivity of aircraft is investigated by [67, 68]. Aircraft connectivity prediction using a Fuzzy C clustering algorithm is presented by [67]. Additionally, the authors in [68] calculate the connectivity for one-way and two-way tracks and determine a minimum link range from a given connectivity.

References [69–82] investigate the feasibility of AANETs. The main focus lies on the connectivity of the nodes, the resulting topology and the number of nodes that can be connected under different parameter settings. Büchter et. al. [69–72] analyze flight schedules to obtain the connectivity of aircraft over time. Furthermore, the authors simulate the global airspace including an optical AANET with and without satellite links. They present results for connectivity and nodal degree. A connectivity analysis based on flight data is also presented by [73].

The authors analyze the resulting mesh network and compare the performance of topology algorithms. The connectivity over France is analyzed by [74]. The authors show that a higher throughput compared with VHF data link (VDL) can be achieved using an AANET. The link probability over the North Atlantic is evaluated by [75] through modeling the nearest neighbor distribution. The authors find a 99% probability of being able to connect to links with less than 250 km range with at least 40 aircraft in the area. As a summary, references [69–75] present connectivity figures from 80% up to 99% of the aircraft depending on the link distance and location. A general evaluation of AANETs is conducted by [76]. The authors develop a mobility model and optimize the aircraft topology. The connectivity of oceanic and continental scenarios is assessed by [77, 78]. The authors simulate the achievable throughput. Additionally, they propose a connectivity architecture and analyze the channel access and routing challenges. The management and optimization of the backbone core with a focus on military networks is evaluated by [79]. The authors define an optimization problem and provide a heuristic solution. With a focus on military networks, [80] analyze the link availability, data rate and latency. Their findings show that short links should are beneficial for high stability and multiple radios are necessary to fullfil the requirements. A combined AANET and HAPS system is proposed by [81]. The authors propose HAPS for monitoring of AANETs. They show that this reduces the probability of disconnections, as HAPS provide areas with improved connectivity. An AANET architecture consisting of three different links, as well as HAPS and ground stations is defined by [82]. The three link types are VDL, high speed radio frequency and free space optical links. The authors evaluate different MANET protocols on this architecture.

The majority of publications in the area of AANETs focuses on routing. An overview on the proposed routing protocols is presented in Table 1.5. The routing protocols differ in terms of type of protocol and the metric used for choosing a specific route. They can be partitioned into basic studies, position-based, relative-velocity based and QoS-based protocols. A comparison of different MANET routing protocols and their applicability to AANETs is conducted by [83, 84]. The comparison by [83] includes Ad-hoc On-demand Distance Vector (AODV) and Greedy Perimeter Stateless Routing (GPSR) using a random distribution of aircraft. On the other hand, [84] compares AODV, Dynamic MANET On-demand (DYMO) and Better Approach To Mobile Adhoc Networking (BATMAN) using realistic aircraft traces. Both conclude that AODV is the best performing of the compared protocols. Basic routing protocols based on the hop count are evaluated by [85,86] and [87]. In the study of [85,86], the Dijkstra algorithm is used to find the shortest path and show the feasibility for the applications in terms of delay and loss percentage. A centralized optimal joint routing and scheduling algorithm is proposed by [87]. The authors also propose a heuristic based on a genetic algorithm to minimize the average packet delay. They show that the genetic algorithm performs well.

Table 1.5: Overview on proposed routing protocols for AANET, the first group is based on basic studies, the second group includes position-based approaches, the third group is based on the relative velocity and in the fourth group on QoS.

Reference	Year	Name	Protocol Metric	Aircraft data
[83]	2018	n/a	compare	random
[84]	2010	n/a	compare	realistic
[85, 86]	2010/11	n/a	hop count	realistic
[87]	2013	joint routing and scheduling	hop count	random
[88]	2010	GLSR	position, congestion	random
[89]	2011	AeroRP	velocity, position, time to intercept	random
[90]	2018	PPMAC	position, delay	random
[91]	2006	ARPAM	position	random
[92]	2008	n/a	position	realistic
[93]	2008	MARP	topology	unknown
[94]	2009	n/a	position	realistic
[95]	2009	MAToC	topology	unknown
[96]	2010	GRAA	position	random
[97]	2012	GRHAA	position	random
[98, 99]	2016/7	NoDe-TBR	trajectory	realistic
[100, 101]	2006	MUDOR	relative velocity	random
[102]	2012	DASR	queuing delay, relative velocity	realistic
[103]	2013	A-GR	position, relative velocity	random
[104]	2014	LEBR	link availability	mobility model
[105]	2006	(QoS-)MUDOR	relative velocity, QoS	random
[106]	2009	n/a	delay	random
[107]	2009	gateway selection scheme	route availability, capacity, latency	random
[108]	2017	MQSPR	route availability, capacity, latency	mobility model
[109]	2019	SD-ABN	reliability	random

Position-based routing is studied by [88–99]. References [88–90] introduce further parameters in addition the position, i.e. congestion [88], velocity and time to intercept [89] or delay [90]. The proposed protocols are evaluated using simulation in terms of packet delivery ratio and latency as well as overhead, reachability and path lifetime. All references show a performance gain of their proposed protocol. While [88–91, 97] use random aircraft positions for their evaluation, [92, 94, 98, 99] use real aircraft traces.

Routing based on relative velocity between aircraft is studied by [100–104]. The doppler shift as a routing metric is proposed by [100, 101]. The authors show that they outperform Dynamic Source Routing (DSR) in terms of handoffs. The relative velocity plus queuing delay is the metric in [102]. They show that this metric leads to a more stable routing, less handoffs, decreased delay and higher packet delivery rate compared with [101] and DSR. In addition to relative velocity, ADS-B data is used by [103]. The authors present a decreased routing overhead, better packet delivery ratio and E2E delay compared with [96] and GPSR. Calculating link availability based on link lifetime is proposed by [104]. Their routing protocol is based on AODV including the link lifetime. The authors present an improved throughput, E2E delay and overhead.

Reliability and QoS are additional metrics in [105–109]. Reference [105] extends their previously proposed protocol in [100, 101] in order to additionally meet QoS constraints. The delay is used as a QoS metric in [106] This metric is used additionally to the hop count. Their findings show that the performance is increased compared with a single hop count metric and utilization based gateway selection. Gateway selection is also studied by [107]. To select a gateway node, the authors propose multiple E2E QoS parameters, such as route availability period, route capacity and route latency. They show an increased throughput and packet delivery ratio with improved energy consumption. Path availability period, available path load capacity and path latency is combined by [108]. The authors conclude that their protocol achieves a high ground connectivity and outperforms AODV and GPSR in terms of routing stability and path load balancing. Reliable path routing for military networks is studied by [109]. The authors propose a software-defined airborne backbone network architecture. For routing, they apply a segment routing and traffic scheduling algorithm based on multiple reliable paths. They validate their proposal by simulations.

1.5.3 Aeronautical connectivity

Several studies focus on connectivity for aeronautical applications. A survey on the e-enabled aircraft is conducted by [110]. The authors focus on the airspace system, including on-board as well as off-board connectivity. They include regulations and standards as well as open challenges. They show that achieving future performance targets depends on communica-

tion, networking and security capabilities of the aircraft. The elements of airborne networks are analyzed by [111, 112]. The study includes several possible architectures, requirements as well as link budgets for different types of links. Many studies on the airborne connectivity architecture have been conducted within the SANDRA project [113–116]. The focus lies on air traffic management (ATM) applications, but also take passenger communication into account. The architecture uses multiple access networks and includes mobility solutions in order to ensure a seamless service. The authors validate their architecture with simulations, testbed and flight trials. IP mobility in the area of aeronautical networks is studied by [117, 118]. Connectivity requirements of the aircraft are studied by [119]. Additionally, the authors analyze the market and potential architectures. However, as the study is from 2003, some parts are already outdated. A focus on passenger connectivity is laid by [120]. The authors survey the current network and services including capacity requirements. They calculate the maximum and minimum required capacity per aircraft, which is 29.71 Mbps to 300 Mbps depending on the aircraft. Capacity modeling for safety applications is presented by [121]. The authors determine the traffic distribution and compare towards satellite and terrestrial system capabilities. A different approach is used by [4]. The authors measure the in-flight passenger connectivity on multiple flights within the US, for satellites as well as DA2G. Their measurements include loss, throughput, latency and application performance. The result shows high loss rates of 7% in the median and 40% at the 95^{th} percentile. Additionally, they observe that Quick UDP Internet Connections (QUIC) is better suitable for satellite connectivity than Transmission Control Protocol (TCP). These measurements provide an insight into the current status. Multi-path connectivity for tactical networks has been investigated by [122]. The authors optimize a tactical ad-hoc network without any infrastructure such as ground stations or satellites. They show capacity gains by using multi-path connectivity. A model for the air-to-ground link for ATM is developed in [123]. This model is used to obtain link requirements to ensure that ATM user requirements are met. A central cognitive radio architecture is proposed by [124]. The architecture is used for flexible channel assignment while maintaining safety requirements. The authors conclude that interference can be reduced while ensuring safety. The connectivity architecture for ship networks is studied by [125]. The authors propose a hybrid satellite and terrestrial architecture including a connectivity manager to ensure QoS. While the study is focusing on ships, the same open challenges are present for aircraft. The focus of the presented publications lies mainly on ATM-type applications. Only [4, 119, 120] focus on passenger connectivity.

1.5.4 Satellite connectivity for aircraft

Satellite networking includes a large research area. This section only highlights research on satellite networking with relevance to aircraft connectivity. One challenge, in particular for GEO satellites is the high delay. The expected delay for GEO and LEO satellites has been

studied in [126]. The authors provide a model for the delays, which results in a delay of 250 to 500 ms for GEO satellites. An overview on satellite systems for aeronautical applications is given by [127]. The authors discuss multiple topics, such as spectrum, signalling and architectures, mainly focussing on ATM applications. Using SDN for satellite applications is proposed by [128]. The authors evaluate different scenarios and use cases, and discuss the benefits and challenges. They conclude that SDN for satellites is promising. Another important topic is routing in satellite networks. Classical satellite connectivity uses a bent-pipe approach. However, in particular for non-GEO satellite constellations, routing plays an important role ensure low delay and high packet delivery rate. These issues are analyzed by [129–135]. A predictive concept is proposed by [129–131]. The authors utilize the predicted trajectories of satellites in order to improve the routing mechanisms. They validate their concept with simulations. The delay in LEO satellite networks is optimized in [132]. The authors determine that propagation delay is the largest factor. Therefore, they propose an optimization using multi-commodity flow formulation. They show that the optimization increases the performance compared with shortest path routing. Multi-layered satellite networks are studied by [133]. The authors propose a reliable traffic distribution model and show that their routing method is more effective in terms of improved throughput and lower number of packet drops. Congestion in non-GEO satellite routing is investigated by [134]. The proposed scheme avoids congested paths by using an alternative path resulting in an improved performance. The concept of an Internet of satellites is introduced by [135]. The Internet of satellites is designed as an overlay network on satellites. The authors conduct a survey on the architecture and identify a set of suitable routing algorithms. As a conclusion, several publications are proposing improvements for satellite connectivity. An improved satellite network is able to provide a higher throughput to aircraft.

1.5.5 Direct air-to-ground connectivity

DA2G connectivity has been studied from different aspects. The required bandwidth and throughput for different services has been studied by [136]. While the proposed method can still be applied, the study has been conducted based on 3G and is therefore outdated. The application of cellular technologies, i.e. 4G and 5G, for DA2G has been studied by [35, 137–139]. An experimental verification of 4G/5G technology is conducted by [35]. The results focus on China, however a detailed technical description of the results is unavailable. The authors conclude that 4G/5G technology has a large potential for DA2G. The challenges and solutions for using cellular networks for DA2G is analyzed by [137]. The authors conduct a link budget analysis and propose beamforming and steering as well as multiple-input multiple-output (MIMO) and A2A as possible solutions. The opportunities of 4G for DA2G have been studied by [138]. The authors include business models and deployment considerations as well as flight trial results. The link budget, coverage and throughput are analyzed

by [139]. Their proposal is a 4G system using hierarchical antenna consisting of four antennas to optimize the aerial coverage. A study on possible DA2G improvements is conducted by [140–144]. The topic of interference coordination and the radiation patterns of the antennas is studied by [140]. The authors show that interference coordination and scheduling can improve the capacity from 1-3 Mbps to 15 Mbps. An interference avoidance scheme is also proposed by [141]. The authors introduce a coordinated beam selection and spectrum allocation scheme to avoid interference between neighboring BSs. They show that the available capacity per aircraft can be improved by 60% using this scheme. The DA2G range is studied by [142]. The authors propose to use a large number of antennas at the BS to extend the range. They develop a tool to dimension the number of antennas based on the range and signal-to-interference ratio (SNR) requirement. High-capacity DA2G connectivity of 1.2 Gbps is studied by [143]. The authors show that with multi-user beam forming and 1000 antenna elements, 53 dBm transmit power and 50 MHz, this goal could be reached. The achievable user throughput with 5G is studied by [144]. The authors evaluate the user throughput of a 5G DA2G system. They consider different frequency bands and show that the throughput can be enhanced by using 5G radio access. The handoff rate in a DA2G system is investigated by [145]. The authors derive a closed form expression for the handoff rate and conduct with a simulation of different parameters.

1.5.6 Heterogenous networking

Heterogenous networking is a large research area. One of the main challenges in heterogeneous networks is which link to choose in which case. This problem is called network selection. A survey on available mathematical models for network selection is given in [146]. The authors introduce different schemes, using utility theory, multiple attribute decision making, fuzzy logic, game theory, combinatorial optimization and Markov chain. An overview on different network selection schemes is given by [147]. Their application is a heterogenous network based on drones and terrestrial networks. In the following, research in heterogeneous networking with relation to aircraft connectivity is introduced. Network assisted optimal data link selection for a heterogenous aeronautical network is proposed by [148]. Their scheme uses a centralized algorithm and is based on SDN. The authors prove the effectiveness of their proposed scheme. In [149], the authors extend their work and investigate dual connectivity for aircraft. They assume a satellite and a line of sight (LOS) link. Specifically, they focus on traffic scheduling using an SDN controller. They formulate an optimization model to stabilize the traffic queue backlog. The handover overhead is used as a measure. As a result, they show the feasibility and efficiency of their approach using two example scenarios, meteorological information fetching and real time services. A data link selection scheme for air traffic management is proposed by [150]. The authors introduce a multi-attribute decision making method based on an intelligent method. They include several different parameters,

such as QoS, security, data rate, bit error rate and cost. Their results show a cost, throughput and resource utilization improvement. A combined terrestrial and satellite network for resilience is investigated by [151]. The authors study the traffic distribution under different link conditions such as link failure in the terrestrial network. They model a heuristic algorithm to minimize the impact of a link failure. They show that the utility can be increased by steering satellite resources.

1.6 Contribution

This work investigates high-throughput connectivity for aircraft based on an integrated A2G network. This includes the quantification of the achievable throughput to each aircraft during the flight as well as the necessary link choices to obtain this throughput. The goal is to provide the optimal throughput per aircraft while ensuring a weighted fairness between aircraft. The optimal distribution of throughput among all aircraft contributes to a stable throughput during the flight, which determines user satisfaction. As the aircraft consists of a network itself, the weighted fairness ensures that fairness can be applied based on the users in the aircraft.

To provide a solution to this problem, an A2G network model is developed. The model is implemented for a generic A2G network. Consequently, the achievable throughput can be studied independently of specific implementations, which differ among operators. If implementation specific parameters are known, they can be injected as well. Based on the A2G network model, a centralized optimal and a distributed heuristic throughput allocation scheme are proposed. Using these schemes, various parameter studies are conducted to show the influence on the achievable throughput per aircraft. Additionally, potential implementations for the A2G network are discussed. For instance, a 5G network is a suitable option for the distributed throughput allocation. As a conclusion, with the developed A2G model and the optimal and distributed solutions, an overall study of high-throughput A2G networks is conducted, which is adaptable to implementation specific parameter settings.

In comparison with the related work introduced in Section 1.5, high-throughput A2G connectivity has been studied rarely. In the area of aircraft connectivity, the focus of the related work lies on ATM applications. Publications studying high-throughput connectivity for aircraft, are focusing on single link solutions. The same applies for the area of AANETs. While there are many publications on integrated space-aerial-terrestrial networks, the goal is increasing the performance ground users, with different requirements compared with aircraft users. DA2G and satellite related work focus on implementation specific problems. Their solutions can increase the capacity on the links, however, aircraft throughput allocation needs to be solved separately. Problems in the area of heterogenous networking are closely re-

lated. However, high throughput is not the main focus in the related work. Nevertheless, the introduced concepts could be part of an implementation of the studied network.

1.7 Publications

Within the scope of A2G connectivity, several different aspects have been studied by the author. The structure of the complete scope of the author's work is presented in Figure 1.3. The scope can be partitioned into A2G connectivity, ground network, general studies, services, in-cabin and measurements. The main focus of this thesis and the content presented here, is the A2G connectivity perspective. This consists of four papers [P1–P4]. Hence, parts of the content of Chapters 2, 3, 4 and 5 have been published in [P1–P4]. More specifically, the throughput analysis is conducted in [P1] and included in Chapter 2. The A2G model and the optimal throughput allocation is presented in [P2, P3] and included in Chapters 3 and 4. Lastly, the heuristic throughput allocation is presented in [P4] and included in Chapter 5.

The additional areas, which are not covered in this thesis are the following. The ground connectivity at airports has been investigated in [P5]. The joint optimization of the ground network and the A2G network has been studied in [P6, P7]. General studies on A2G network aspects have been conducted in [P8, P9], with [P8] focusing on a performance study of 4G and 5G for DA2G including a comparison with satellite and [P9] focusing on business models for high-capacity A2G connectivity. The problem of A2A topology formation and rate allocation over the Atlantic ocean has been studied in [P10]. The investigation from the services perspective, i.e. link selection based on the type of service was presented in [P11]. Options to ensure throughput distribution to users within the cabin were presented in [P12]. Lastly, measurements studies on DA2G for aircraft and drones have been conducted in [P13, P14].

1.8 Conclusion

This chapter motivates the study of high-throughput A2G connectivity. The used terminology and definitions are introduced. The description of the A2G links and their state of the art highlights the advantages and disadvantages of each link. The currently available peak throughput per aircraft is 100 Mbps. As this is insufficient, multi-link A2G connectivity is studied. The related work in aircraft connectivity and related areas is introduced. While different aspects have already been researched, high-throughput multi-link A2G connectivity has not been studied before. The main contribution is the implementation independent study of high-throughput A2G connectivity, more specifically providing a weighted-fair throughput allocation for aircraft and improves throughput stability during the flight. The work presented

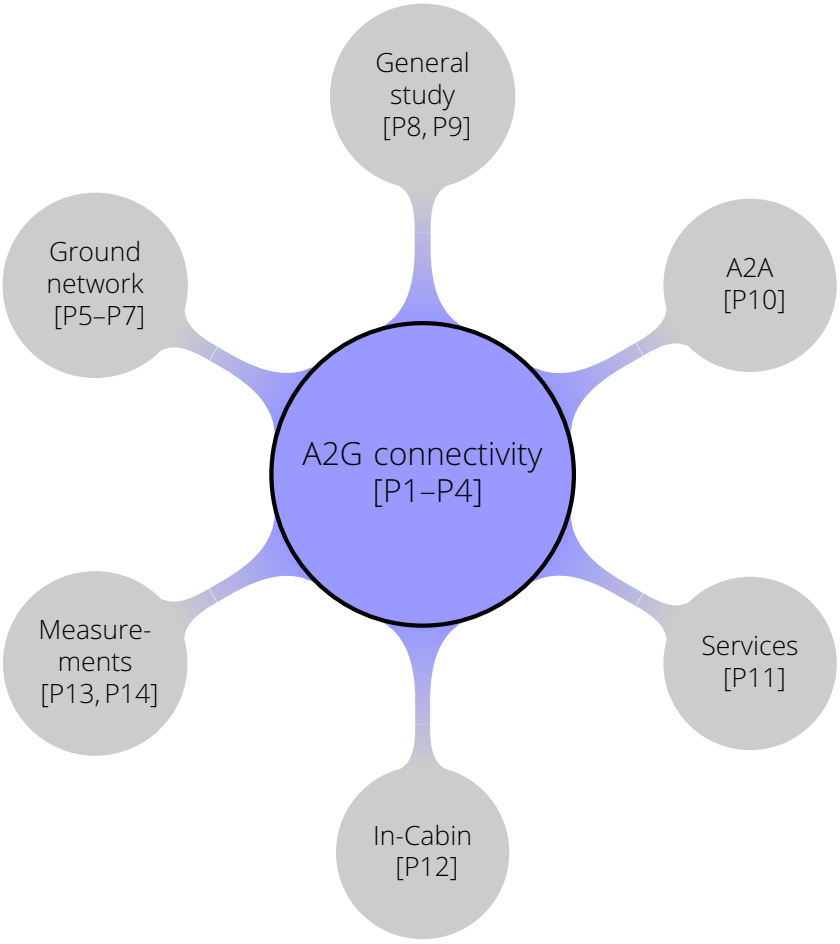

Figure 1.3: Overview on areas of publications by the author, this thesis focuses on the A2G connectivity depicted in the center.

in this thesis has partly been published in [P1–P4], which is stated at the beginning of the respective chapters.

The remainder of this thesis is structured as follows. In Chapter 2, an analysis of the achievable throughput based on aircraft traces is conducted and the integrated A2G system architecture is introduced. In Chapter 3, the A2G network model and the underlying modeling assumptions are defined. The analysis of the optimal achievable throughput under different scenarios and parameter settings is presented in Chapter 4. The distributed heuristic throughput allocation is studied in Chapter 5. Lastly, Chapter 6 concludes the thesis.

2 Throughput analysis and connectivity architecture

Connectivity to aircraft can be provided through different deployed or planned A2G networks as presented in the state of the art in Chapter 1. However, most of these networks, especially the satellite networks, are not designed for varying aircraft densities on different flight routes. Therefore, the achievable throughput per aircraft varies with the aircraft position depending on the flight route. In this chapter the achievable throughput in areas of different sizes is investigated based on real aircraft traces. The relevant parameters for offering a high throughput to aircraft are analyzed and discussed. Additionally, an outlook to future performance with increasing air traffic is given.

In the second part, the integrated A2G architecture is introduced, which combines all different types of links. The different components of the A2G architecture are discussed and the respective challenges are highlighted. Finally, 5G is presented as a candidate network solution, implementing features, such as non-terrestrial network (NTN), which can overcome most of the discussed challenges.

Parts of the content in this chapter have been published by the author in the following papers:

- Section 2.1:
  "Connectivity in the Air: Throughput Analysis of Air-to-Ground Systems" [P1]

- Section 2.2:
  "Distributed Resource Allocation and Load Balancing in Air-to-Ground Networks" [P4]

2.1 Throughput analysis

The focus of this analysis lies on the sharing of available capacity between aircraft, as presented in Figure 2.1. Several different parameters determine the peak throughput that can be provided by each DA2G cell or satellite spot beam, for instance utilized bandwidth, antennas or radio access schemes. Additionally, the share of the peak throughput that one aircraft can obtain depends on the aircraft density in the specific area at a certain instant in time. Therefore, the achievable throughput per aircraft during the flight is analyzed in this study. This is implemented by using aircraft traces. Furthermore, the achievable throughput is defined in terms of percentage of the maximum throughput without sharing, to remain independent of the respective absolute throughput. Based on this analysis, the performance of currently available A2G networks is studied and an outlook on future advancements is given. Additionally, the parameters influencing the throughput per aircraft are studied, and capabilities and limitations of DA2G and satellite networks are discussed. In order to achieve a high throughput per aircraft, the peak throughput per spot or cell needs to be provided to one aircraft, cf. [P1].

2.1.1 Methodology

The analysis is implemented in MATLAB using aircraft traces from FlightRadar24 [152]. More, specifically, worldwide flights between 03/11/2017 and 10/11/2017 have been analyzed. Besides aircraft trajectories, the data set contains additional information about the flight, such as airline or destination and departure airport. A detailed description of the flight traces and the full list of parameters can be found in Section 4.1.2, cf. [P1].

Efficient use of bandwidth is paramount to provide a high throughput to users. Therefore, a HTS partitions its coverage area into small spot beams, within the available spectrum can be reused. The same principle applies to DA2G networks, by dividing the area into cells. As both concepts are similar, DA2G cells and satellite spot beams will both be referred to as ”spots” from now on, cf. [P1].

The peak throughput of the network is available per spot. As depicted in Figure 2.1, aircraft located in the same spot need to share the available capacity and are labeled with A in Figure 2.1. In this case, depending on the number of aircraft in the same spot, the achievable throughput changes during the flight. During some time of the flight, aircraft can be alone in a spot, thus obtaining the peak throughput. These aircraft are labeled with B in Figure 2.1. Therefore, the peak throughput as advertised by operators is inadequate to study the throughput that can be obtained by aircraft. In this study, captured flight traces are utilized to obtain the aircraft density, and therefore the achievable throughput per aircraft during the flight. The study takes multiple parameters into account, such as spot size, the

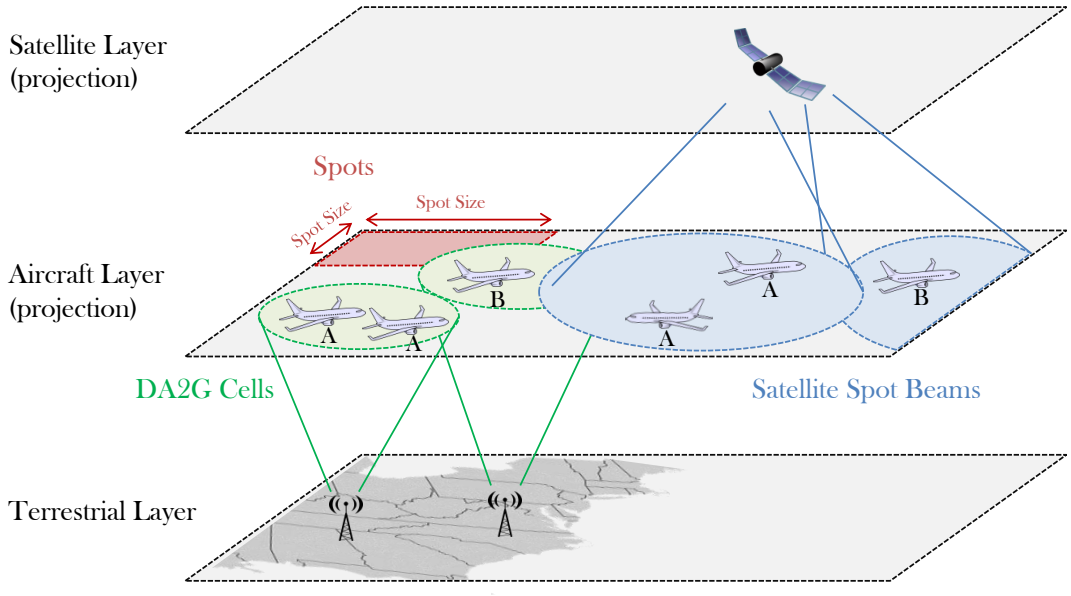

Figure 2.1: Coverage of DA2G cells and satellite spots on the aircraft layer, aircraft labelled with A have to share the capacity while aircraft labelled with B obtain peak capacity [P1] ©2019 IEEE.

continent, the flight time, the percentage of connected aircraft, land and oceanic areas as well as using multiple systems. These parameters are detailed in Table 2.1, cf. [P1].

The achievable throughput per aircraft is obtained by analyzing the number of aircraft per spot in 15 minutes intervals. Aircraft on the ground are discarded. The spots are assumed to be square-shaped, as shown in Figure 2.1. This assumption allows an implementation independent study of the aircraft density, as exact spot positions depend on the A2G network and are subject to change with upgrades of the network, cf. [P1].

The division of the Earth in rectangular spots is not straightforward. A position on the earth can be defined in terms of longitude and latitude. The longitude, ranging from -180 to 180°, specifies the position towards the east or west in relation to the prime meridian. The latitude ranges from -90 to 90° and specifies the position in direction north or south in relation to the equator. While one degree of latitude covers always the same distance of approximately 111 km, the distance of one degree of longitude varies with the latitude. The largest distance of one degree of longitude is 111 km at the equator, decreasing towards the poles. For instance, in Germany one degree of longitude is approximately 75 km.

To create a map of the Earth, the globe needs to be projected onto a flat surface. There are many different types of map projections, preserving different properties such as area or angles. A very common projection is the Mercator projection, where latitudes and longitudes

Table 2.1: Relevant parameters for analyzing the throughput [P1] ©2019 IEEE.

Variable	Description
Spot Size	Different spot sizes between 70 and 2500 km have been considered. By fitting a curve also other spot sizes can be evaluated.
Continent	The flights have been grouped according to their destination and departure continents: Europe, Asia, Africa, Oceania, North America and South America. This yields to 21 different groups.
Flight Time	The flights have been grouped into short (<2h), medium (2h - 7h) and long-range (>7h) flights.
Percentage of Connected Aircraft	As there are multiple A2G operators, not all aircraft have to be connected to the same system. Thus only a percentage of aircraft actually needs to share the capacity. This percentage of connected aircraft can be varied. Raising the percentage of connected aircraft also enables an estimation of future air traffic.
Land and Ocean	Using coastal lines, it can be determined whether the aircraft is over land or ocean. This is relevant for DA2G studies.
Multiple Systems	One aircraft can use either one connectivity system or multiple connectivity systems in parallel, e.g. GEO and DA2G.

are depicted parallel to each other. While dividing this projected map into squares is easy, areas with the same degree of latitude and longitude are not equally sized. Hence, using this projection, spots closer to the poles seem bigger than spots on the equator, even if they cover the same area.

In order to create equally sized spots, the map is divided into small pieces first. These are determined using a 3D histogram based on latitudes and longitudes. The histogram bins correspond to 10 by 10 km at the equator. As described above, this leads to pieces of different size, from 100 km^2 at the equator to some 10s of km^2 in the north or south. As only real aircraft positions are taken into account, the poles are excluded. In order to create equally sized spots from the pieces, a mask is designed to combine multiple pieces to obtain the desired area. In direction of latitude, the number of pieces is chosen according to the desired size of the spot. On the longitude, the resulting area is then divided into similar sized spots. An example mask for a spot size of 1500 km is shown in Figure 2.2. Each differently colored area corresponds to one spot equally sized spot. As explained above, the spots at the equator seem to be smaller than the ones at the poles due to the projection. For additional properties, such as defining land and ocean areas, similar masks are created.

As the generated spots are not exactly same size, the error between the spot area in the mask and the desired spot area is evaluated, which is determined by squaring the spot size. The relative error in percent is presented in Figure 2.3. The figure shows that the error is always less than 5%, in most of the cases it is even below 1%. The error is lowest for 200 km

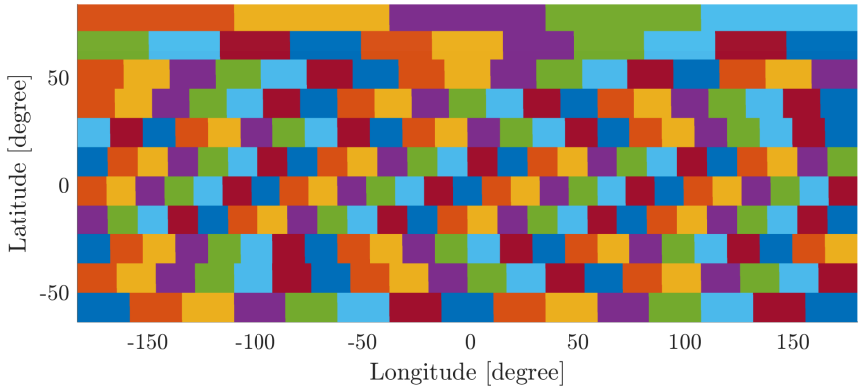

Figure 2.2: Mask for equally sized spots of 1500 km in terms of latitude and longitude, each differently colored area corresponds to one spot.

spot size, and increasing with other spot sizes. This is due to the mapping accuracy. As the area in one slice of longitude is divided evenly between the number of spots, too large spots can yield a large remainder. The remainder needs to be shared between the number of spots, yielding the respective error. However, with too small spots the error when composing areas increases, as the area of the pieces as mentioned above is discrete. Nevertheless, it is concluded that for the investigated spot sizes, the spot generation is working well with a small error.

The placement of each of the spots depends on the calculation as explained above. In order to ensure that the variations to the placement are insignificant for the results, the positions of the spots are varied. More specifically, the mask is moved 25%, 50% and 75% of the spot size toward down and right. This yields 16 different varied spot placements, including the original one. Figure 2.4 shows that the difference in the results for the 5^{th} percentile are almost negligible for the different investigated spot sizes. The largest difference from the original spot mask is 0.18% of throughput, which is insignificant. Hence, the original spot mask as described above will be used in the following.

Naturally, a real spot deployment differs from this mask. In particular for GEO satellites, the size of each spot increases with the distance from the equator. Nevertheless, this analysis can be used as an estimation of the performance of a specific A2G network, as the aircraft density is the factor which most influences the performance. Moreover, in this study, it is assumed that the capacity in each spot is equally shared among all aircraft in the spot, cf. [P1].

This assumption gives a good first approximation of the capacity per aircraft. Another option is to share the capacity according to the number of users per aircraft. Large aircraft with more passengers have a higher demand than small aircraft. Thus, sharing the capacity with

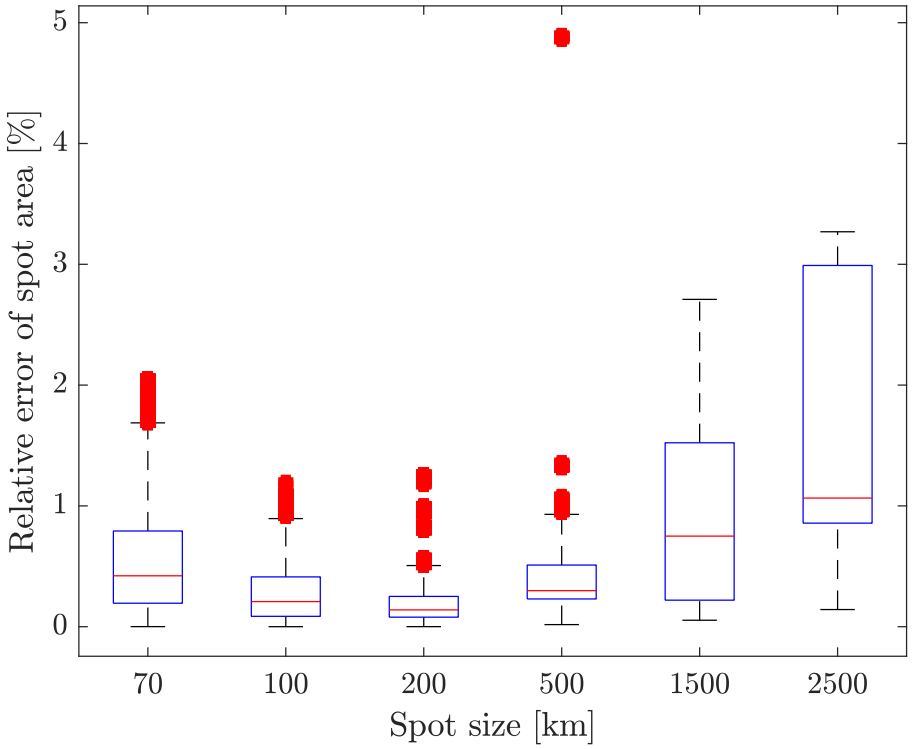

Figure 2.3: Relative error in percent of the spot areas using the mask.

respect to the demand per aircraft would be more fair for each user on the aircraft. This way of distributing the available capacity will be investigated in Chapter 5.

To remain independent of the chosen technology, the throughput is defined as the percentage of the peak capacity. For instance, with two aircraft in one spot, each aircraft obtains 50% throughput. This relation is calculated using Equation (2.1), cf. [P1].

$$\text{throughput} = \frac{100}{\text{number of aircraft in spot}} \quad [\%] \tag{2.1}$$

The throughput ranges from almost zero to 100. To analyze the actual throughput of a specific implementation, the value needs to be multiplied with the peak throughput provided by the implementation. Consequently, the throughput can be used generically for any implementation and eases the comparison. In the example in Figure 2.1, aircraft labeled with A get 50% throughput, whereas aircraft labeled with B receive 100%, cf. [P1].

The results of the analysis are presented in terms of the 5^{th}, 50^{th} and 95^{th} percentiles of the throughput at all time instants. Due to the calculation per time instant, the 5^{th} percentile represents the result for the worst 5% time instants. Moreover, this result was also mapped to every flight, therefore representing the achievable throughput during the flight, cf. [P1].

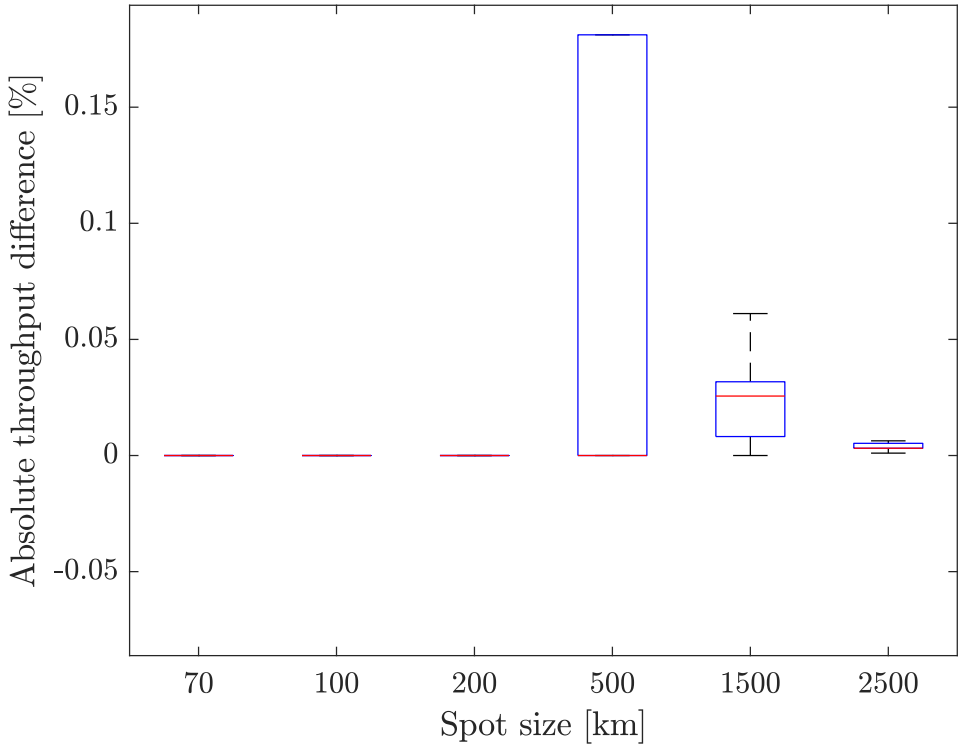

Figure 2.4: Difference of 5^{th} percentile of the throughput for different shifts of the spot mask compared with the original mask.

2.1.2 Results

"Figure 2.5 shows the 5^{th}, 50^{th} and 95^{th} percentile of all time instants of all flights. As expected, the throughput increases with decreasing spot sizes. Moreover, the throughput is highly varying over time. At some instants, aircraft have full capacity, whereas for most of the time the capacity is very low" [P1].

From the results in [P1], it can be seen that "at a spot size of 500 km, 26.89% of the instants achieve 100% throughput whereas the 5^{th} percentile lies at 4.35% of the throughput. This shows that both low density and high density areas exist. Even for the smallest spot size (70 km), highly dense areas occur. In this case, in 5% of all time instants the overall throughput is less than 25%. The reason lies in the fact that busy areas, such as airports, require smaller spots that are capable of delivering more capacity to smaller groups of aircraft. In such areas, a spot size of approximately 12 km would be needed to provide full capacity to all aircraft. At the same time, 69.33% of the time instances achieve full throughput being located in low density areas. An overview of the results can be found in Table 2.2. Since we want to determine the throughput that can be achieved in most of the cases, only the 5^{th} percentile will be used from now on."

"The achievable throughput over flight time for flights with a duration of 5 hours is presented in Figure 2.6. We see that for small spot sizes the throughput in take-off and landing phases is lower than in the middle of the flight. This effect is due to the higher traffic densities in the airport area as well as being over highly populated areas. This effect is not present for larger spot sizes, as a large spot is balancing the available capacity over the large area, resulting in only low throughput. To improve the performance during the beginning and end of a flight, the spot sizes in areas with high traffic density, such as close to airports, have to be substantially smaller than in other areas. In Figure 2.7, we compare the difference between long and short flights as well as flights over ocean and flights over land. Due to higher aircraft density over land and short haul flights flying over busy areas most of the time short flights and flights over land have slightly lower throughput than long flights and flights over the ocean. In general the differences vanish for bigger spots as the throughput is averaged over a large area" [P1].

In [P1] it is shown that "when analyzing flights on different continents, the traffic density varies. For example, North America is the continent with the highest flight density so the maximum number of aircraft stated in Table 2.2 is obtained for flights within North America. As North America, Europe, and Asia have the most continental flights, they also contribute the largest number of inter-continental traffic, with the Europe-North American corridor be-

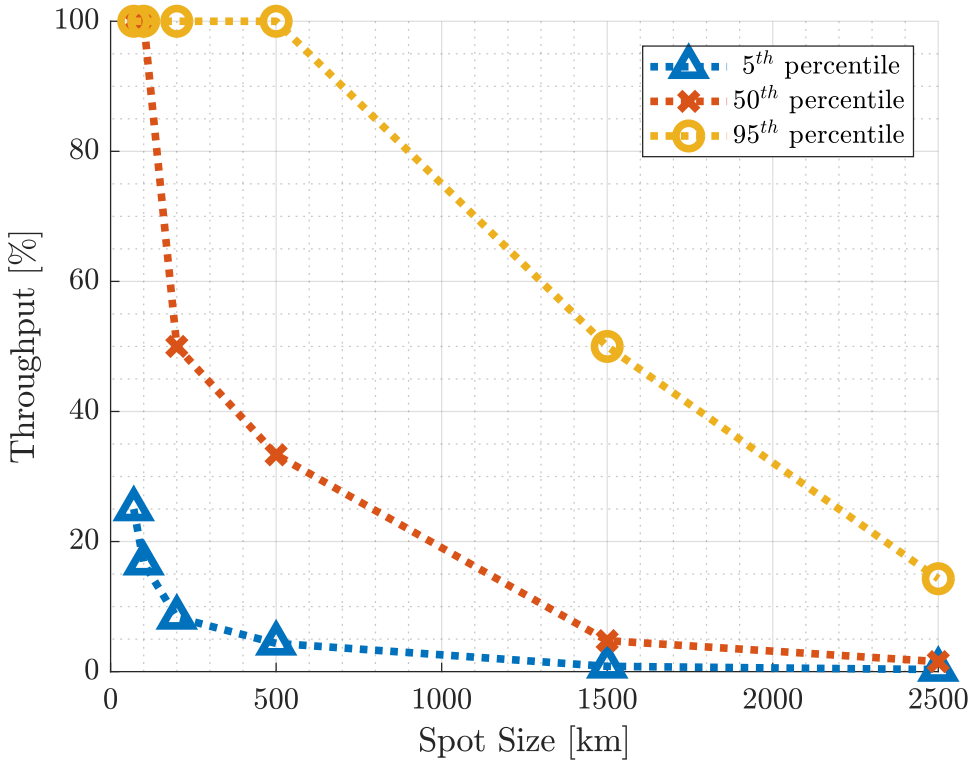

Figure 2.5: Achievable instantaneous throughput per aircraft in terms of the 5^{th}, 50^{th} and 95^{th} percentile [P1] ©2019 IEEE.

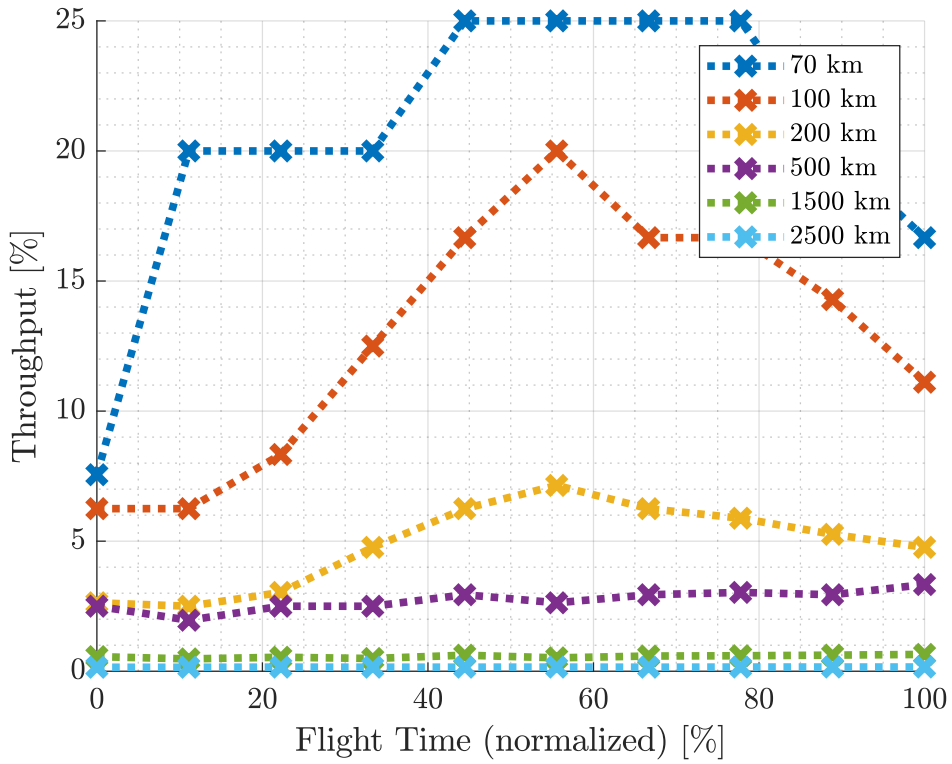

Figure 2.6: Variation of the throughput per aircraft throughout a flight [P1] ©2019 IEEE.

ing the busiest. Therefore the region also has to be taken into account when designing an A2G system."

Figure 2.8 shows the worldwide aircraft density within one week. The number of aircraft at each position within one week is counted. The Figure clearly shows common flight routes and heavily used urban areas. It is also visible that the US and Europe are the busiest areas. Additionally, it becomes evident that there are many areas without any aircraft within one week. Therefore, coverage should be adapted to aircraft routes to provide a high throughput to aircraft.

"As already stated, not all traffic has to be provided by one system, e.g. already multiple GEO satellite operators are available. Therefore, only a part of all aircraft will connect to one system. Figure 2.9 shows the expected throughput in terms of percentage of connected aircraft and spot size. 100% equals today's air traffic. By calculating more than 100% of aircraft connecting to the system, increasing future traffic can be modeled. It can be clearly seen that already a throughput of 100% is only achievable with a very low number of connected aircraft or very small spots. Even with three GEO satellite operators, a spot size of 52 km is needed to achieve 100% throughput. This is unrealistic for GEO satellites due to the high distance

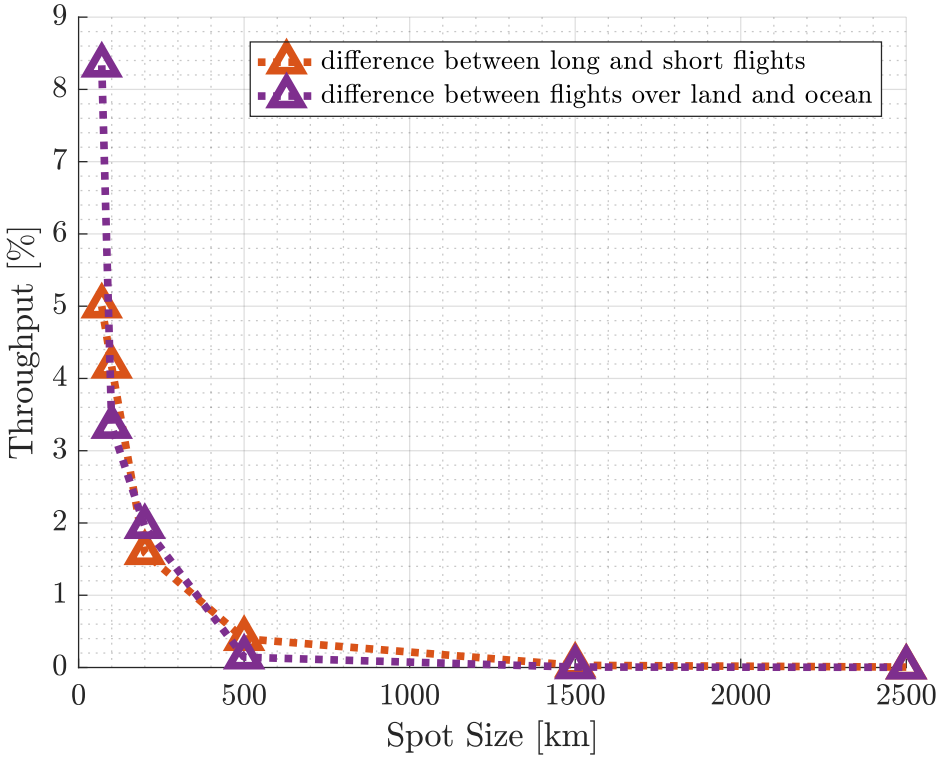

Figure 2.7: Throughput difference between short and long flights and between flights over the land and ocean [P1] ©2019 IEEE.

Table 2.2: Overview of throughput analysis results [P1] ©2019 IEEE.

Spot Size [km]	70	100	200	500	1500	2500
Min. Throughput [%]	2.94	2.44	1	0.93	0.32	0.11
5^{th} Percentile	25	16.67	8.33	4.35	0.81	0.32
50^{th} Percentile	100	100	50	33.33	4.76	1.54
95^{th} Percentile	100	100	100	100	50	14.29
Max. Number of Aircraft	34	41	100	107	316	905
Percentage with 100% Throughput	69.33	62.49	48.27	26.89	2.43	0.97

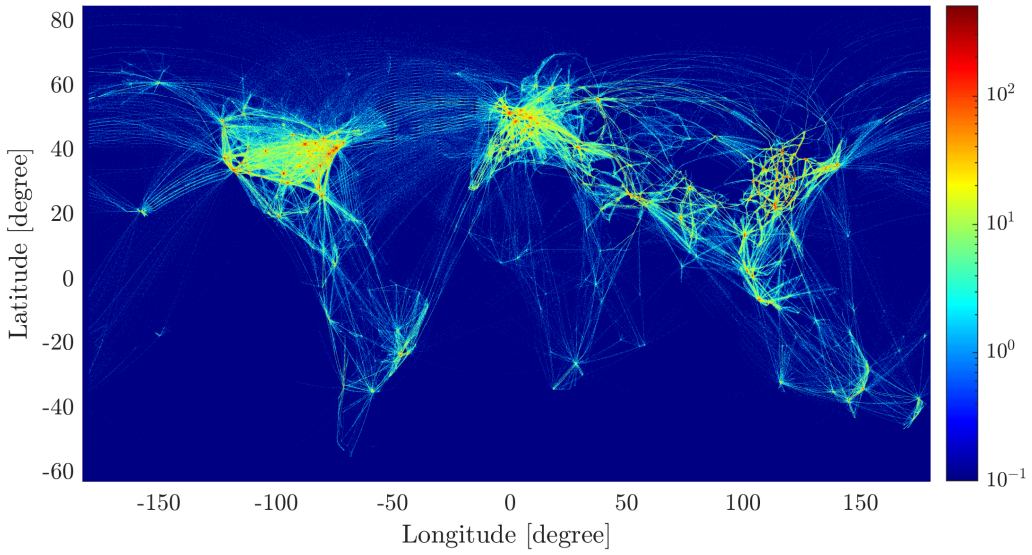

Figure 2.8: Worldwide aircraft traffic density during one week. The color represents the total number of aircraft at the respective position within one week.

from the Earth. A realistic spot size for GEO will not be substantially below 300 km, especially when considering the growth of size with distance from the equator. Using a 300 km spot size, only 17.1% throughput could be achieved with three GEO operators. In order to achieve high throughput, multiple systems with a high peak capacity and small spots have to be used" [P1].

In [P1] it is concluded "that the achievable throughput per aircraft is highly varying. While some aircraft experience full throughput, others have to share the capacity with many other aircraft. This tendency shows that an A2G system has to be specially designed to cope with areas of dense air traffic by introducing smaller spots or using more spectrum for these spots. However, smaller spots introduce the need for frequent handovers. Another option is to have multiple systems, serving only a part of all aircraft."

2.1.3 Application to real systems

As a case study, three already existing or announced A2G communication systems are compared, namely Inmarsat Global Xpress, the EAN and the OneWeb LEO constellation. "Inmarsat Global Xpress provides worldwide GEO Ka-band satellite access using 4 satellites with 89 spots each [8]. As the size of the GEO satellite spots is growing with distance from the equator, we estimate the minimum and maximum sizes to be 1200 - 2000 km. Inmarsat Global XPress offers up to 50 Mbps per aircraft [8]. We take global air traffic into account. We assume three GEO satellite operators; thus each is only serving one third of all aircraft.

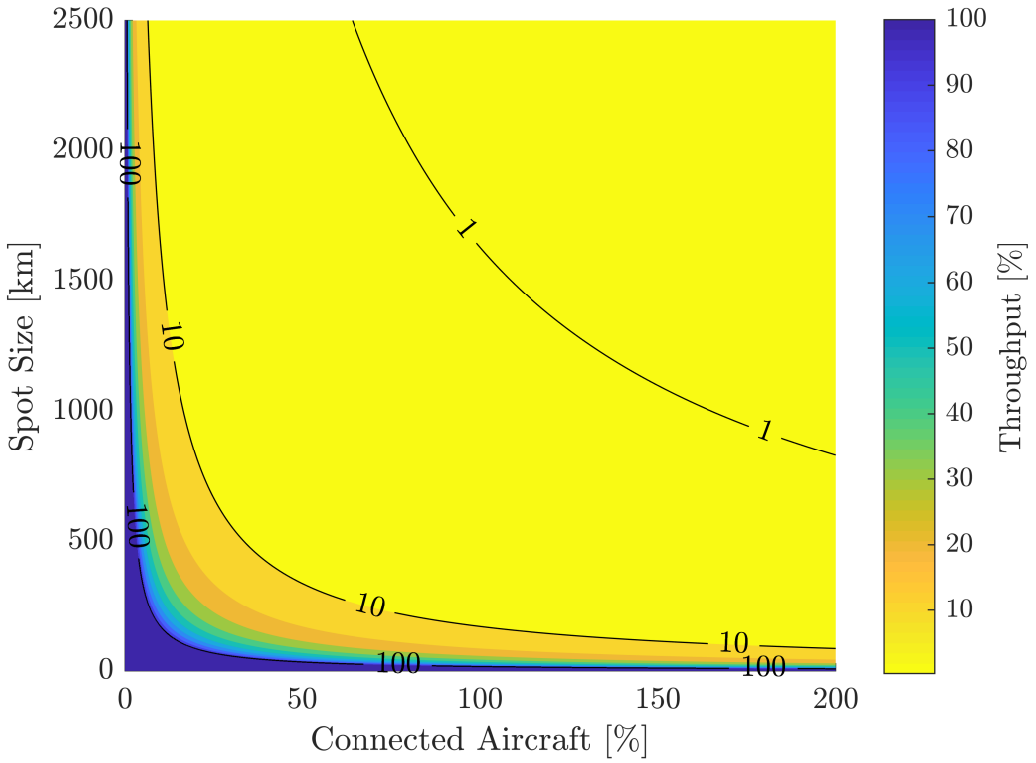

Figure 2.9: Study of the achievable throughput for different spot sizes and percentage of connected aircraft [P1] ©2019 IEEE.

Therefore, the overall traffic has been divided by three. Based on the aircraft traces, this arrangement yields a throughput of 0.69 to 1.83 Mbps, depending on the spot size. As this throughput is in the range of a few Mbps, this is clearly not enough for multiple users on one aircraft. Thus, Inmarsat Global XPress is insufficient for high-throughput applications to all aircraft. Even if it is only used by one third of all aircraft, the throughput has to be increased significantly. Since not all aircraft are equipped with broadband connectivity today, those that are equipped experience higher throughput" [P1].

"The EAN was deployed recently in the European Union. It operates a combined DA2G and GEO system with 75 Mbps per cell. Their network contains 300 ground cell sites with three cells each [34]. Using the area of the European Union and assuming equally sized spots leads to approximately 70 km square area per cell. The combined Inmarsat S-Band Satellite connection consists of three spots in this area. Dividing the area of the European Union by three leads to approximately 1200 km square area per satellite beam. An overview of all values can be found in Table 2.3. For the EAN, only flights within Europe have been considered. Based on the aircraft traces, the achievable throughput for the ground based system with 70 km spot size is 15 Mbps. The satellite segment with 1200 km spot size can provide 0.73 Mbps. The throughput of the DA2G system is not only better than other systems but also the median reaches the full promised capacity of 75 Mbps. However, with several hundred passengers in one aircraft, 15 Mbps appears to be too restrictive. Thus this capacity still has to be improved. Additionally, the throughput provided over satellite is really small compared with the DA2G part" [P1].

OneWeb has been selected as an example for LEO satellite constellations. As already stated in Chapter 1, the full OneWeb constellation will consist of 650 satellites in an orbit with an altitude of 1200 km [14]. Each satellite has 16 spot beams [153] and covers an area of approximately 663300 square miles [154]. Hence, per spot beam 41456 square miles have

Table 2.3: Properties of EAN, Inmarsat Global XPress and OneWeb (extended version of [P1] ©2019 IEEE).

	EAN	Inmarsat Global XPress	OneWeb
Type	DA2G/GEO	GEO	LEO
Peak Throughput [Mbps]	75 [34]	50 [8]	400 [14]
Number of Spots	900 [34]	89 [8]	16 [153]
Spot Size [km] (approx.)	70 / 1200	1200 - 2000	300
Connected Aircraft [%]	100	33.33	100
5^{th} Percentile [Mbps]	15 / 0.73	1.83 - 0.69	30.77
50^{th} Percentile [Mbps]	75 / 2.59	10.71 - 3.85	200
Considered Traffic	Europe	worldwide	worldwide

to be covered, corresponding to approximately 300 km spot size when assuming rectangular spots. The peak throughput of the constellation will be 400 Mbps, which has already been demonstrated in a trial [15]. With these parameters, the calculated achievable throughput per aircraft is 30.77 Mbps. The median throughput even reaches 200 Mbps. These values are significantly higher than the other two examples. However, for several hundreds of users on an aircraft, 30 Mbps is still limiting. Additionally, the peak throughput of 400 Mbps has only been shown in a trial with one user in the network. Hence, in a fully operational network the throughput per user is expected to decrease. Other emerging LEO constellations promise even gigabit speeds, which would be a factor of 2.5 to 25 more than OneWeb. With this speedup, the achievable throughput can reach the necessary order of magnitude. Hence, LEO satellite constellations are very promising for high-throughput connectivity for aircraft. However, as these constellations are not yet fully operational, the performance in a live network still needs to be determined. Furthermore, first deployments will probably be unable to offer the full functionality as envisioned.

2.1.4 Design of A2G networks

"According to International Air Transport Association (IATA), the number of air passengers will double by 2036 [155]. Thus, the number of aircraft offering on-board connectivity will grow accordingly. Hence, using the same modeling as before, 200% of connected aircraft correspond to 2036. Figure 2.9 shows the achievable throughput in terms of the percentage of connected aircraft and spot size. As presented in Section 2.1.2, given the level of air traffic today, it is already difficult to provide sufficient throughput to all aircraft. The effort required to support future air traffic growth will only increase and, thus, this growth must be taken into account when designing A2G networks. In this section, we present the relevant parameters for A2G network design and highlight the need for different spot sizes and multiple A2G systems" [P1].

Design parameters

As presented in [P1], "the throughput analysis demonstrates the need for a meaningful design of the A2G system to provide high throughput to all aircraft during flight. The achievable throughput for an A2G system depends on several parameters. Some are related to the A2G system itself, others depend on the air traffic and the aircraft needs:

Spectrum:
: High capacity cannot be provided without sufficient spectrum. Therefore this parameter is the most important one. Enough spectrum for A2G connectivity has to be ensured by regulation.

Technology:

Advanced technologies can provide high capacity even with small bandwidth. The choice of technology mainly results in higher peak throughput or smaller spots. For example, beamforming can be used to reduce the spot size and to cover single aircraft per beam.

Connectivity:

The available A2G systems provide different connectivity. For example, DA2G can provide smaller spots than satellites but it is unavailable worldwide.

Air Traffic:

The higher the air traffic density, the lower the achievable throughput. This fact is especially relevant for areas with maximum density, as metropolitan areas. The future increase of aircraft density will play an important role.

Aircraft Demand:

Aircraft with a small number of passengers require a lower throughput than large aircraft. Additionally, the requested capacity changes over flight time, leading to a varying demand over time."

Discussion

As discussed in [P1], "to connect several hundred passengers as well as thousands of sensors, the A2G link has to provide extremely high capacity. NGMN estimate the future demand for passengers on aircraft to 1.2 Gbps assuming 20% active passengers at any time with 15 Mbps per passenger [5]. The assumption of only 20% active users already includes over-subscription of the link. As 15 Mbps per user is much more than currently needed, we also recalculate with 3 Mbps per user, which is consumed for video streaming today. In this case, still 240 Mbps would be needed per aircraft. The cumulated capacity of all deployed A2G systems today is some hundreds of Mbps peak throughput. Hence, for 240 Mbps all available systems today would be needed to provide peak throughput at the same time to all aircraft. Reference [143] shows that 1.2 Gbps per aircraft can be reached with DA2G under a certain configuration of bandwidth, transmit power, array size and number of BSs. However, to achieve that, considerably more bandwidth than available today is needed for DA2G. On top of passenger traffic, there is the need to monitor the aircraft in the air, implying sending a significant amount of sensor data to the ground. Hence, in order to provide sufficient throughput to all aircraft, achieving 100% throughput per aircraft is necessary. Therefore, to meet aircraft connectivity demand, A2G communication systems have to be significantly improved."

The performance of A2G networks can be improved in multiple ways. One option is to improve the peak capacity, for instance by optimizing the spectral efficiency or obtaining a higher amount of bandwidth. Moreover, the spots can be optimized to include only one aircraft at each time. To achieve this, the spot size needs to be decreased. DA2G networks could deploy more BSs or implement technologies like beamforming. The same applies for satellites, for instance steerable spot beams can be used to steer the capacity toward hot-spot areas. Nevertheless, as current DA2G spots are significantly smaller than satellite spots, the probability of being able to provide 100% of the traffic to most aircraft is higher for DA2G networks, cf. [P1].

Satellites are able to offer worldwide coverage. Over the continent, they can support DA2G networks where necessary. Over the ocean, satellite connectivity is essential. Increasing satellite capacity is more challenging compared with DA2G networks, due to the large distance and higher number of users to be covered. The large distance to the Earth limits the satellite spot size, in particular for GEO satellites. With a 0.5 degree beamwidth, the spot size is 300 km. Significantly lower spot sizes are unrealistic, as the pointing accuracy and achievable beamwidth is limited. With a 300 km spot size, 6% of the peak throughput can be provided by one GEO satellite. To achieve peak throughput per aircraft, an increase by a factor of 17 is needed. This can be achieved by using multiple GEO operators or improved satellites with increased throughput. While satellite capacities are improving, an increase of 17 times is improbable. Consequently, GEO satellites are unable to provide peak throughput to all aircraft using a spot size of 300 km. Nevertheless, they could be supported by LEO satellites, which can provide smaller spots due to the decreased orbit, cf. [P1].

The analysis in Section 2.1.2 shows two shortcomings of currently deployed A2G networks. Firstly, constant throughput during the flight is not the primary design goal. BSs and satellite spot beams are evenly distributed instead of adjusting the coverage to the flight corridors. Consequently, the spot size needs to be decreased in hot spot areas such as airports while it can be increased in remote areas. Secondly, the throughput provided by one A2G network is inadequate. Therefore, the combination of multiple networks is necessary. One option is to combine multiple systems of the same kind, e.g. having more than one GEO operator. Another option is combining different systems, e.g. DA2G and GEO. However, in both cases the aircraft has to be equipped with both systems, yielding additional cost and weight, cf. [P1].

2.2 A2G connectivity architecture

The A2G network combines many players, different airlines and operators of the networks. Therefore, the A2G connectivity architecture becomes complex. An overview on the A2G

connectivity architecture is presented in Figure 2.10. It combines four different network segments, namely GEO, LEO, HAPS and DA2G, as well as A2A links.

The different network segments are typically handled by different operators. One exception is the EAN, which offers a combined GEO and DA2G network. Depending on the network segment, operators can offer worldwide coverage, which is the case for GEO or LEO satellite operators. DA2G and HAPS operators only cover a specific area. For instance, in Figure 2.10, DA2G operators 1 and 3 serve the same area, whereas DA2G operator 2 covers another region. Besides providing and operating the network infrastructure, challenges for operators include also regulatory aspects. One example is ensuring sufficient spectrum within the coverage region to offer high capacity. For each of the network segments, multiple operators are present, as shown in Figure 2.10. Hence, airlines select one or multiple operators based on their needs, such as coverage area, performance characteristics and cost.

The hardware installed on the aircraft also plays an important role. Besides installation cost, a communication system introduces higher fuel consumption due to increased weight and drag. This effect is greatest for the GEO satellite due to the large distance and respectively high transmission power. Hence, airlines carefully choose the installed communication systems per aircraft. For instance, an aircraft which only covers short range flights over a continent with DA2G coverage, might not need to have a satellite system installed. In addition, each airline selects a different operator for each network segment. Depending on how many aircraft connect to the same operator, the achievable throughput varies. Additionally, different operators might implement different charging policies, e.g. charging per MB or limiting the speed. For A2A, different deployment options exist. As A2A networks are not available today, discussions on the actual implementation are speculative. The main challenges include cooperation between aircraft of different airlines and respective communication protocols. For a detailed analysis, one can refer to the literature introduced in Chapter 1.

Operators, subscription plans and fleet capabilities are business related decisions, which cannot be influenced on a technical level. Hence, in order to focus on the technical challenges, a few simplifications are done. From now, it is assumed that, while there are different operators, aircraft are evenly distributed among operators in relation to the capacity offered by the operator. Hence, similar rates can be assumed per network segment independent of the operator. For airlines, it is assumed that they cooperate to share traffic via A2A links globally or at least on basis of alliances such as Star Alliance. While it is mostly assumed that all aircraft can connect to all network segments, it is also taken into account that there are cases with some aircraft being unable to connect to all network segments. In the model, only one link per network segment and aircraft is allowed except for A2A, as multiple links increase the throughput for one aircraft on the cost of others. Hence, on a global view this is

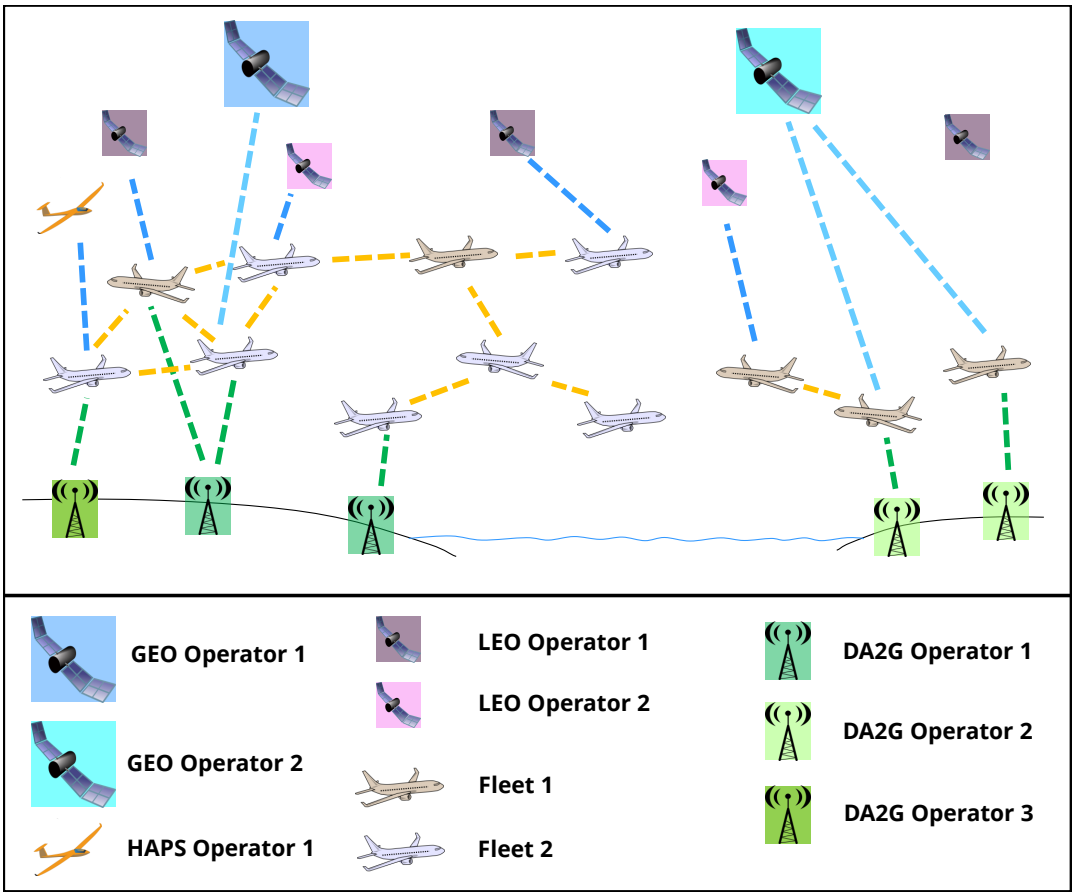

Figure 2.10: Overview on the A2G connectivity architecture.

disadvantageous. The focus lies on the global view to achieve a fair distribution of throughput among aircraft.

The resulting communication link options from the view of an aircraft user are presented in Figure 2.11. There are five types of network elements. The first one is the aircraft itself. The second type are relay nodes, which can be satellites or other aircraft. The third type are ground units, acting as interfaces to the ground networks. The forth type are networks, dividing into ground or cabin networks. Lastly, the fifth type are sinks, which can be servers or other users. Figure 2.11 depicts the UL only, the DL can be defined analogously in the other direction. As shown in Figure 2.11, a user on the aircraft firstly connects to the cabin network. For passengers, this can be either a built-in entertainment system or a wireless communication system using his own device. For other applications such as sensors, it can also be a wired or wireless system. From the aircraft (a/c) router, there are several ways to connect to the respective sink. In case that the content is already stored on the a/c server, an A2G link is unnecessary. If an aircraft is at the airport, it can directly connect to ground networks via a ground access point (GND AP), such as cellular networks or WiFi. The cabin network and infrastructure as well as network connections while the aircraft is on the ground are not part of this work, it is assumed that they are sufficiently dimensioned. While an aircraft is in the air, the options are, as detailed above, DA2G, GEO, LEO, HAPS or another aircraft, given that the respective link is available at the respective point in time. In case the connection is not directed to the ground, it can also redirect to another aircraft. This is the case for multi-hop connectivity, as well as for connecting directly to another aircraft. Examples for the latter are distributed caching or when aircraft exchange operations related information such as weather conditions. Principally, users on aircraft and on ground or users in different aircraft can also directly connect to each other, which works similarly and is therefore grayed out in Figure 2.11.

Within the scope of this work, different parts of the full scenario are investigated. These parts are shown in Figure 2.12. Without loss of generality, on-board aircraft networks and the case of content being on another aircraft are omitted, as explained above. Additionally, HAPS links are omitted, as they are only present in very specific regions and act similar to satellites from the connectivity perspective. Apart from this, Scenario 1, as shown in Figure 2.12a, investigates the full set of options. The goal is to investigate the complete scenario using optimization to develop a benchmark of the achievable throughput. The results are presented in Chapter 4. Scenario 2 is also part of Chapter 4. This specialized scenario aims at investigating the feasibility of connecting aircraft over the ocean without any satellite connectivity, as depicted in Figure 2.12b. This can offer a cheaper solution, since satellite connectivity is more expensive than DA2G and A2A. Scenario 3 is developed from the analysis results of Scenarios 1 and 2. The difference to Scenario 1 is that A2A links are limited to

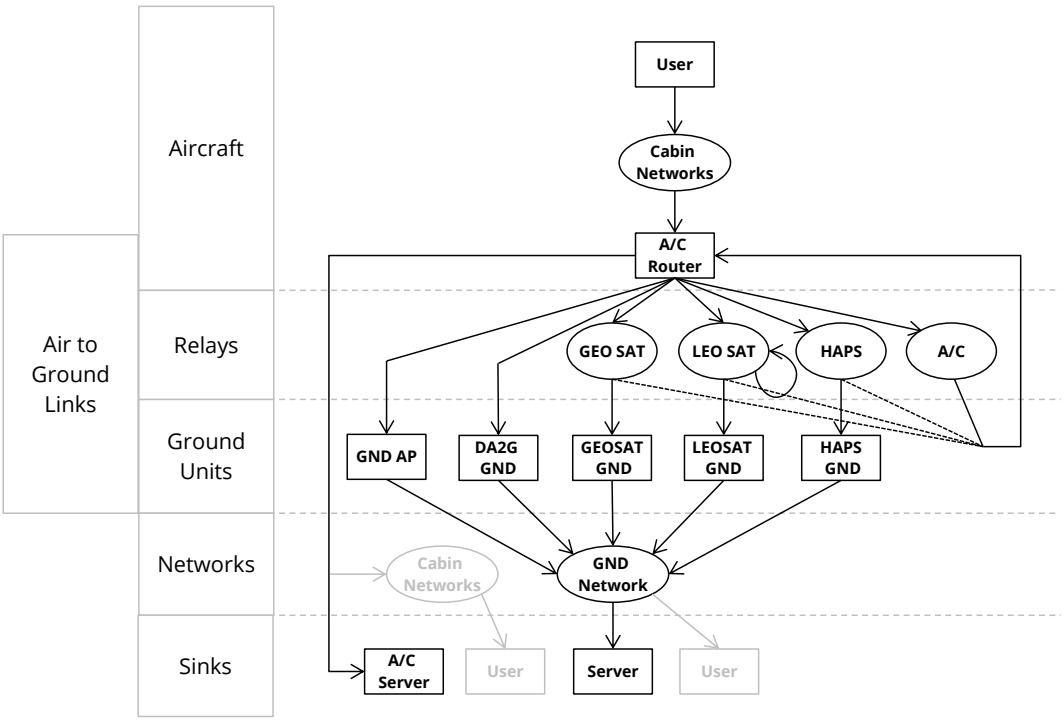

Figure 2.11: A2G network communication links from the perspective of an aircraft user. The Figure shows the UL only, the DL works analogously.

single hop connectivity and used as a backup only in case high throughput via other network segments is unavailable. A distributed throughput allocation for Scenario 3 is developed in Chapter 5. Scenarios 1-3 investigate the absolute throughput that can be achieved per aircraft. However, an aircraft contains up to several hundreds of users. The requirements of user applications also vary. For instance voice connectivity needs a small delay which cannot be provided via GEO satellites. Therefore, Scenario 4 defines the performance on a per-user basis based on the throughput determined in the other scenarios. This is depicted in Figure 2.12d and discussed in Chapters 5 and 6.

2.2.1 Challenges

The A2G connectivity architecture as introduced above yields several challenges. In the following, the most critical challenges are highlighted.

Network integration:

The different network segments of the A2G network are typically separated today. Satellite links have different requirements than for instance a DA2G link due to the higher distance and different frequency bands. Therefore, these networks also use different multiplexing methods and radio access technologies. Nevertheless, to achieve

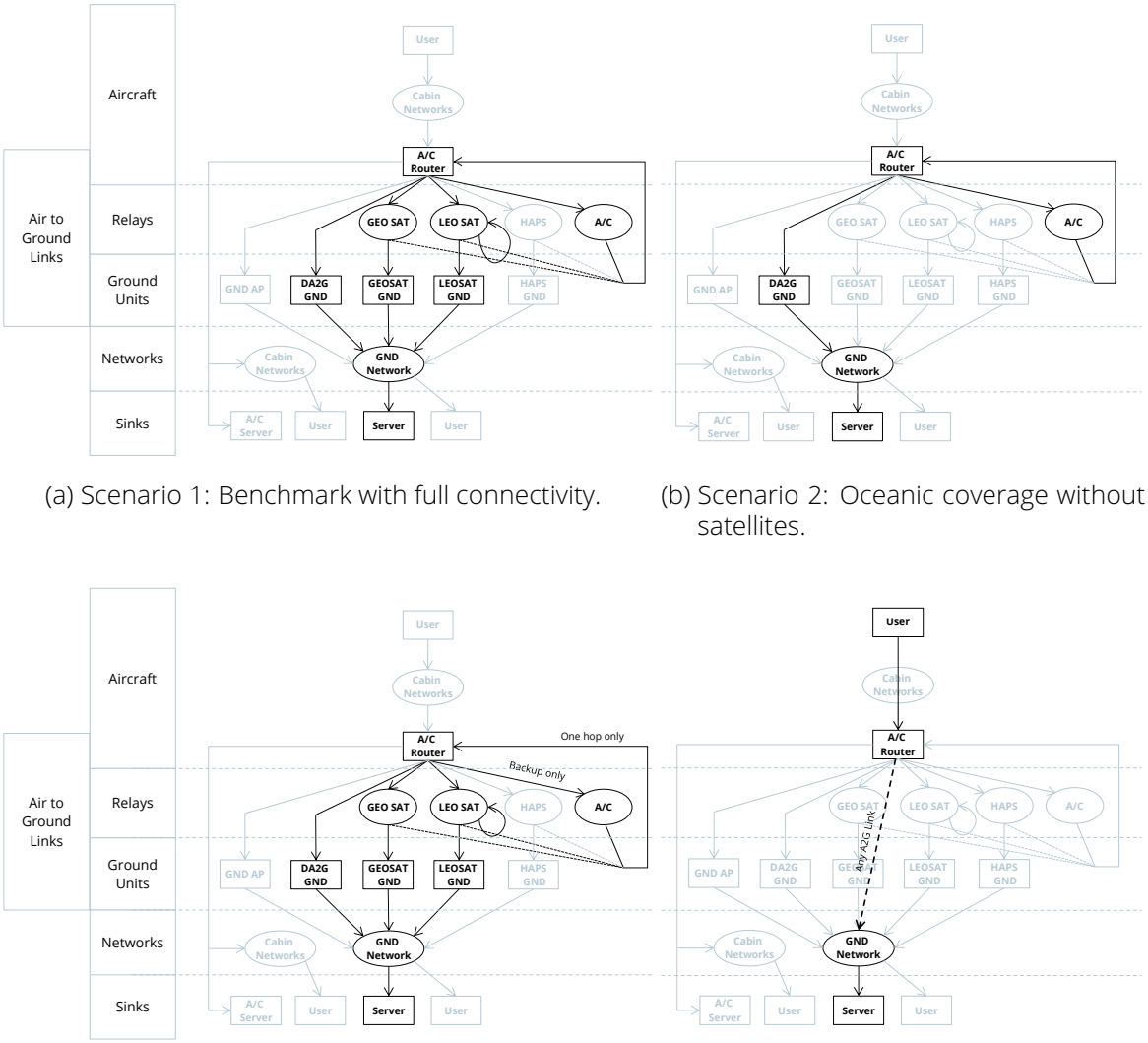

(a) Scenario 1: Benchmark with full connectivity.

(b) Scenario 2: Oceanic coverage without satellites.

(c) Scenario 3: Full connectivity with limited A2A.

(d) Scenario 4: User-centric view.

Figure 2.12: Investigated scenarios.

an efficient high-capacity A2G network, integration of these different networks needs to be enabled.

Multi-link handling:

When users connect to multiple links simultaneously, they need to define how to use these links. There are multiple options, such as preferring one link and using the others for backup only or using specific links for specific traffic types. Different requirements of traffic types, such as delay requirements, complicate the link management even further. While the decision also depends on the type of data, without any management of using multiple links, the overall throughput can even degrade.

Ad-hoc networking:

While many investigations of ad-hoc networks exist in the literature, aircraft ad-hoc networks face a few unique challenges. The distance between aircraft is large compared with other ad-hoc networks. Therefore, one typical approach, which is building on overhearing communication of other nodes, is not applicable. Hence, aircraft ad-hoc networks specifically need to form links between aircraft. Hence, the network needs to decide which links to setup, when to switch links and how to route the traffic. Depending on the data which is being exchanged, security is another aspect to be taken into account.

Fairness:

With different network segments and aircraft having different capabilities to connect to the segments, fairness is an important point. Due to different coverage areas, the achievable throughput of a single aircraft varies during a flight. The throughput can be high over populated areas and degrades over the ocean. To achieve a better user experience, it is beneficial to fairly distribute the traffic among all aircraft.

Aircraft hardware:

The capability to connect to a specific network segment depends on the physical installation of equipment on the aircraft. While especially GEO satellite equipment is expensive and heavy, there has to be a gain of installing equipment for multiple links. Hence, the benefit of multiple links needs to be visible to airlines. Additionally, especially for A2A links, a sufficient amount of aircraft need to be equipped with an A2A system to allow the formation of a network.

Flexibility:

Air traffic and user demand on aircraft are varying over time and geographic position. Additionally, the A2G link is a bottleneck. Hence, the A2G network needs to be able to properly react to changes in demand and redistribute capacity in a flexible way to ensure an efficient use of the available resources.

A2G network design:

For providing a high-capacity A2G network, the system needs to be properly designed. The respective parameters for A2G network design are spectrum, technology, connectivity, air traffic and aircraft demand, as detailed in Section 2.1.4.

2.2.2 Candidate network solution

In existing networks, there are already solutions for some of the challenges identified above. In particular, features introduced in 4G and 5G networks provide solutions to most of the challenges. These features are detailed in the following. A short introduction is also given in [P4].

Non-terrestrial networks:

The support of NTNs within 5G is currently studied by 3rd Generation Partnership Project (3GPP). They define NTNs as a network or network segment which uses an air- or spaceborne platform. This platform can be a satellite or HAPS and can either act as a relay or directly as a Next Generation NodeB (gNB). The potential roles of NTN for 5G are coverage extension for remote areas, service continuity and network scalability, as defined in [156]. NTN coverage can be divided into two types of access networks, broadband access for users on moving platforms and narrow or wide band access to serve 5G devices directly. More specifically, the relevant use case for A2G networks is "passengers on board vessels or aircraft access 5G services and benefit from 50 Mbps+" [156]. The 3GPP studies are partitioned into radio access aspects in [156] and system architecture aspects in [157]. The radio access studies include channel models, antenna patterns, propagation delay, doppler shift studies as well as investigations on necessary modifications to 5G new radio (NR) to support the NTN deployment scenarios. The studies on system architecture focus on ten key issues from mobility management over QoS and multi-connectivity to regulatory issues such as crossing country borders. Hence, active standardization work is ongoing to include satellites into the 5G network to converge to one integrated network.

Access Traffic Steering, Switching and Splitting:

To combine 3GPP and non-3GPP networks, Access Traffic Steering, Switching and Splitting (ATSSS) has been introduced in [158]. ATSSS is only applicable for satellite networks without NTN functionality. If satellites are integrated into 5G using NTN, they are part of the 3GPP network and hence dual connectivity has to be applied instead of ATSSS. Nevertheless, the functionality defined in ATSSS is also relevant in the case of dual connectivity. Dual connectivity for satellites has been identified as a radio access network (RAN) issue in [157]. ATSSS consists of three parts, namely steering, switching and splitting. Access traffic steering is the selection of an access network for a new data flow. Switching is the process of changing the access network of a flow while ensuring the

E2E connection. Lastly, access traffic splitting is the distribution of one flow over multiple networks. The network architectures enabling these functions are defined in [158] and can be based on different known multi-path protocols, such as Multipath Transmission Control Protocol (MP-TCP). According to [158], the different steering modes to select the proper access network are active-standby, priority-based, best-access, redundant and load-balance. This selection is defined per flow, which is recognized by parameters such as IP address or traffic type. Additionally, multiple rules with different priorities can be defined depending on the network state. These mechanisms could be used in the A2G network to select the proper network segment for each flow, for instance the low delay DA2G link for delay sensitive traffic.

Device-to-Device connectivity:

A part of the 4G standard is device-to-device (D2D) connectivity, defined as Proximity Services [159]. A detailed overview on D2D connectivity in the 3GPP standards is given in [160]. The 3GPP D2D use cases have a focus on public safety applications, but also include other areas, such as vehicle-to-everything (V2X), Internet of Things (IoT) and data offloading. Network architectures to enable the respective use cases have been defined in [159]. In general, the definition of D2D within 3GPP includes many features and options. However, it is not yet widely used. The defined D2D functionality can be used to enable A2A connectivity.

Self-organized networks:

To enable the network to react to changes and to ensure an optimized network operation, self organized network (SON) features have been introduced in the 4G standard. One of the SON features is mobility load balancing [161]. This includes load reporting between evolved NodeBs (eNBs), load balancing actions and adapting the handover configuration. Hence, eNBs can exchange their load status and adjust handovers to balance the load between neighbor eNBs. This feature is useful to ensure evenly distributed load within the A2G network, for instance if a DA2G cell at an airport is overloaded.

When comparing the 4G and 5G features above to the challenges stated in Section 2.2.1, most of the challenges can already be solved by using a 5G network. NTN is a candidate solution for network integration and multi-link handling can be implemented using ATSSS and dual connectivity. The 3GPP D2D procedures are an option for ad-hoc networking between aircraft and SON can provide the needed flexibility. Additionally, the A2G design parameters are similar to design parameters of 5G networks. Hence, using a 5G A2G network, the remaining challenges are fairness and aircraft hardware. As hardware installation decisions are not a technical issue, in the remainder of this work, the focus lies on the fair throughput distribution among aircraft.

2.3 Conclusion

The results of the analysis show that one A2G network will be unable to provide sufficient throughput to connect all aircraft. With a spot size of 200 km, 8.33% of the maximum throughput is available per aircraft for 95% of the time. With the high-throughput demand of aircraft, this is insufficient. To achieve a sufficient throughput to aircraft, each aircraft needs to receive the peak capacity. For instance, this can be achieved by improving the A2G network, such as providing higher peak throughput, decreasing the spot sizes or increasing the available bandwidth. However, due to limitations in coverage and minimum spot size, a sufficient throughput to all aircraft can only be provided by multiple A2G networks, assuming that the bandwidth cannot be easily increased. While DA2G coverage is limited to the continent, the minimum spot size of satellites is limited by their distance to the Earth and the deployable antenna size. In particular, the spot size available for GEO satellites is insufficient to provide peak throughput to aircraft over the ocean. Consequently, A2G networks need to be combined to achieve a peak throughput for each aircraft worldwide, cf. [P1].

Additionally, the integrated A2G connectivity architecture is presented and discussed. The A2G architecture includes different technical and non-technical components, such as link types or operators. After a detailed discussion, the A2G architecture is reduced to cover technical components. Four scenarios are identified, which are further investigated in the following chapters. The challenges in implementing a fully integrated A2G architecture are also highlighted. 5G is introduced as a candidate network solution, as it already includes features which overcome most of the identified challenges. The remaining challenge focuses on fairness between aircraft, to achieve a fairly distributed throughput per aircraft independent of position and time. This will be investigated in the remainder of this work, cf. [P4].

3 Air-to-ground network model

This section introduces the A2G network model, which is used as a basis for the subsequent chapters. The model contains properties of all A2G links as well as characteristics of the complete network. Physical system parameters as well as network properties are introduced and discussed. Lastly, the problem formulation is stated, which models the A2G network as a mixed integer linear program (MILP).

Parts of the content in this chapter have been published by the author in the following papers:

- "Combined Optimal Topology Formation and Rate Allocation for Aircraft to Aircraft Communications" [P2]
- "Optimal Throughput Allocation in Air-to-Ground Networks" [P3]

3.1 Model

The basis for formulating the A2G network are the network and system parameters. Firstly, physical link parameters, such as link budget as well as hardware limitations are defined and maximum link distance and capacity are calculated. Subsequently, the A2G network model is specified. This also covers network changes over time by utilizing time snapshots.

3.1.1 Link capacity

The A2G network contains four different types of links, DA2G, A2A, satellite and ground links. For each of these types, a respective link capacity is defined. In reality, the capacity varies with different operators and implementations, as described in Section 1.3. Hence, the link capacity is modeled in a simple and adaptable way, such that it can be replaced by implementation specific properties if needed. For the ground link, the capacity is assumed to be

unlimited, as the ground network is properly dimensioned to handle A2G traffic.

The DA2G network is a cellular network which is specifically built to offer aircraft connectivity. Hence, it is assumed that the network is capable of providing optimal signal quality to the aircraft, for instance by using antennas and parameter settings optimized for the DA2G use case. Therefore, it is assumed that a 4G A2G network can offer maximum 4G capacity. One limitation of the peak capacity of a DA2G network compared with a terrestrial network is the capability of using MIMO. MIMO relies on using multiple transmit and receive antennas to transmit data in parallel over multiple spatial streams. Hence, with two receive and transmit antennas, the capacity can be doubled. This scales linearly with the number of antennas, and thus is one of the main drivers for multi gigabit capacities. However, MIMO is relying on multi-path signal propagation, which is present in terrestrial networks but unavailable for the DA2G or A2A links. Therefore, the MIMO concept cannot be easily adapted to A2G networks. Nevertheless, instead of relying on multi-path transmission, MIMO can also be based on using the signal polarization. So by using dual polarization MIMO, the capacity can be doubled. Hence, a MIMO gain of two is assumed for DA2G and A2A links. Additionally, instead of multiplying the data rate for one user, multiple antennas can also be used to create separate beams for different users. This allows each user to receive the maximum available capacity without the need to share the capacity with other users. For DA2G, both cases are implemented. In the first case, users need to share the capacity without using beamforming. In the following, this is called limited backhaul. In the second case, beamforming is implemented. This is referred to as unlimited backhaul, cf. [P3]. For calculating the maximum capacity, a bandwidth of 20 MHz is used as a reference. The respective parameters will be detailed in Section 3.1.3.

As A2A networks are not yet deployed, reference implementations are unavailable. The A2G network is limited by the DA2G and satellite links, as discussed in Chapter 2. Therefore, A2A links do not benefit from higher capacities than DA2G and satellite links. Hence, the assumed A2A link capacity is based on the same 4G properties as used for the DA2G links. Additionally, to adjust to the specific properties of the A2A links, two more parameters are taken into account. The first parameter is interference between A2A links. The details of the interference model can be found in Section 3.1.5. The second parameter is an adaptive modulation scheme to adjust the capacity to the quality of the received signal. The modulation scheme is based on 4G parameters as well. Hence, in case of interference and high distances, the A2A link capacity decreases, cf. [P2].

The calculation of the link capacities for DA2G and A2A based on 4G is conducted in the following. In general, the capacity of a single link depends on different aspects. The most important parameter is the received signal-to-interference-plus-noise ratio (SINR). For DA2G

and A2A links, the SINR mainly depends on the distance between transmitter and receiver. In 4G, the modulation format can vary from quadrature phase shift keying (QPSK) to 256-quadrature amplitude modulation (QAM), depending on the channel quality and transmitter and receiver capabilities. The respective symbol efficiency *SE*, depending on the modulation format, is defined in Table 7.2.3 in 3GPP TS 36.213 [162]. Table 3.1 shows the symbol efficiency with the respective SINR limits from [163]. By defining the number of subcarriers N_{sub}, the number of OFDMA symbols per subcarrier N_{ofdma} and the number of slots per second N_{slots} as well as the bandwidth, the 4G capacity can be calculated. The first step is to obtain the number of symbols $N_{symbols}$, which can be transmitted per second, as defined in Equation 3.1. Standard 4G parameters are $N_{sub} = 12$, $N_{ofdma} = 7$ and $N_{slots} = 2 \times 10^3$ [164]. This leads to $N_{symbols} = 168000$ symbols/second.

$$N_{symbols} = N_{sub} \cdot N_{ofdma} \cdot N_{slots} \quad \text{[symbols/second]} \tag{3.1}$$

Furthermore, the capacity depends on the bandwidth, a higher bandwidth results in a higher number of physical resource blocks N_{PRB}. For 20 MHz, N_{PRB} is equal to 100. Another factor is the number of layers v_{layers}, which is the number of streams introduced by MIMO. Lastly, not all data can be used for payload data. The overhead of control signals in 4G is typically $OH = 25\%$. With this information, the 4G capacity R_{4G} can be calculated as follows:

$$R_{4G} = OH \cdot N_{PRB} \cdot N_{symbols} \cdot SE \cdot v_{layers} \quad \text{[Mbps]} \tag{3.2}$$

With the values introduced above and the maximum symbol efficiency for 256-QAM modulation, $SE = 7.4063$ bps/symbol, the maximum 4G data rate is $R_{4G} = 186.6388$ Mbps. The capacities for the other modulation formats and symbol efficiencies can be found in Table 3.1, cf. [P2].

In [P8], the same maximum capacity is used as an early estimation of the 5G capacity. With maturing 5G, the expected capacity can be estimated more precisely. The formula for the 5G capacity is defined in 3GPP TS 38.306 [165]. To be comparable to the 4G calculations above, similar parameters are used. This means, one component carrier, a maximum coding rate of 948/1024, two layers and 256-QAM. To cope with the various use cases, 5G implements a multitude of custom settings on the physical layer. The highest capacity can be reached with a scaling factor of one and a numerology of zero, which corresponds to 15 kHz subcarrier spacing and 106 resource blocks for 20 MHz of bandwidth. This leads to a maximum 5G capacity of 226.85 Mbps, according to the formula in [165]. This capacity is approximately 20% higher than with 4G and similar settings. Nevertheless, for this study, the calculated 4G link capacities as presented in Table 3.1 are used. Firstly, this is due to the maximum 4G capacity of 168.6388 Mbps being significantly higher than achievable capacities of deployed systems today. Secondly, for 4G, exact values for symbol efficiencies and SINR limits are available.

Table 3.1: Capacity in terms of SINR (extended version of [P2] ©2019 IEEE).

SINR	Modulation	Symbol Efficiency [bps/symbol]	Capacity [Mbps]
(-∞, -9.478)	Weak Signal	0	0
[-9.478, -3)	QPSK	0.1523	3.8380
[-3, -0.2)	QPSK	0.377	9.5004
[-0.2, 4.9)	QPSK	0.877	22.1004
[4.9, 7)	16-QAM	1.4766	37.2103
[7, 8.8)	16-QAM	1.9141	48.2353
[8.8, 10.5)	16-QAM	2.4063	60.6388
[10.5, 13)	64-QAM	2.7305	68.8086
[13, 14.5)	64-QAM	3.3223	83.7220
[14.5, 16.2)	64-QAM	3.9023	98.3380
[16.2, 18.8)	64-QAM	4.5234	113.9897
[18.8, 20.5)	64-QAM	5.1152	128.9030
[20.5, 22)	256-QAM	5.5547	139.9784
[22, 23.7)	256-QAM	6.2266	156.9103
[23.7, 27.3)	256-QAM	6.9141	174.2353
[27.3,+∞)	256-QAM	7.4063	186.6388

Still, the study can easily be extended with different link capacities, and the effect of varying the link capacity is studied in Section 4.2.2.

For the satellite link capacity, a different approach is used. The capacity of a satellite link depends on two factors, the total capacity of the satellite and the capacity and number of active users in a respective spot beam. These two factors depend on the type of the satellite. GEO satellites have a large footprint, therefore, the coverage area is divided into small spot beams to allow frequency reuse. The size and shape of the spot beams differ with the geographic position. At the equator, spot beams are small and circular. With increasing distance to the equator, the spot beams grow and become elliptical. Traditionally, the spot beams are stationary, but recently beam steering and even smaller beam sizes have been implemented. LEO satellites also implement spot beams, but due to the lower orbit they have a smaller footprint and are equally shaped and sized.

As these parameters highly depend on the specific satellite design and orbit, a simplified model ist used. Satellites are modeled in terms of the capacity they can provide to a specific area, representing a spot beam. For GEO satellites, a 1000x1000 km area is assumed. This is the approximate size of a typical spot beam in a latitude corresponding to Europe or North America. For LEO satellites, the assumed area is 300x300 km, which approximately corresponds to the spot beam size of the proposed OneWeb constellation [153]. The respective peak capacity per area is assumed to be 100 Mbps. This corresponds to the maximum peak

capacity promised by operators today as presented in Section 1.3. This ensures comparability to the DA2G capacity. Moreover, it is assumed that multiple satellite operators are present, hence, each aircraft connects to exactly one of the available operators. The number of operators is assumed to be six for GEO and three for LEO. Additionally, for further simplification, satellite movements are omitted. It is assumed that each satellite operator is capable of providing connectivity to all areas at all times. Handovers between spot beams and satellites are properly handled by the operator and therefore not modeled here. For a short description of the satellite link model, cf. [P3].

As a conclusion, for DA2G links, a maximum capacity of 186.6388 Mbps is used. Additionally, DA2G includes the option of using beamforming. For A2A, the same maximum link capacity is assumed. Additionally, a flexible modulation scheme is implemented, which adapts the data rate depending on aircraft distance and interference with other links. For satellite links, it is assumed that a 100 Mbps peak capacity can be provided for a 1000x1000 km area for GEO satellites and 300x300 km area for LEO satellites.

3.1.2 Maximum A2A and DA2G range

The maximum range of DA2G and A2A links is an important parameter to design the link parameters. As there are no obstacles in the air, a direct LOS between two aircraft or an aircraft and a BS can be assumed. There are two approaches to determine the maximum distance between two aircraft or between and aircraft and a BS. These two approaches are illustrated in Figure 3.1. The simple approach is based on geometric considerations. The maximum link range is limited by the curvature of the Earth. From a geometric perspective, this is the case, if if the line between two aircraft is parallel to the Earth's surface, as shown in Figure 3.1a. With alt_1 and alt_2 being the altitudes of aircraft 1 and 2 and R_{earth} as the radius of the Earth, the distance can be calculated as follows:

$$\begin{aligned} d_{max} = d_1 + d_2 &= \sqrt{(\text{alt}_1 + R_{earth})^2 - {R_{earth}}^2} + \sqrt{(\text{alt}_2 + R_{earth})^2 - {R_{earth}}^2} \\ &= \sqrt{{\text{alt}_1}^2 + 2\text{alt}_1 R_{earth}} + \sqrt{{\text{alt}_2}^2 + 2\text{alt}_2 R_{earth}} \end{aligned} \tag{3.3}$$

Using Equation (3.3), $R_{earth} = 6371$ km, and an altitude $\text{alt}_1 = \text{alt}_2 = 10$ km, the maximum A2A range is $d_{max} = 714.2$ km. For DA2G and $\text{alt}_1 = \text{alt}_2$, the range is half of the A2A range, which is 357.1 km. In reality, the maximum range increases due to refraction of the signal in the atmosphere. This is shown in Figure 3.1b. In this case, the maximum range can still be calculated using Equation (3.3), but with an Earth radius scaled by a factor of $\frac{4}{3}$ [166]. This approximation yields a maximum DA2G range of $d_{max} = 824.6$ km. Hence, as a conservative approximation, the assumed A2A range is 700 km and the DA2G range is 350 km, cf. [167,P2].

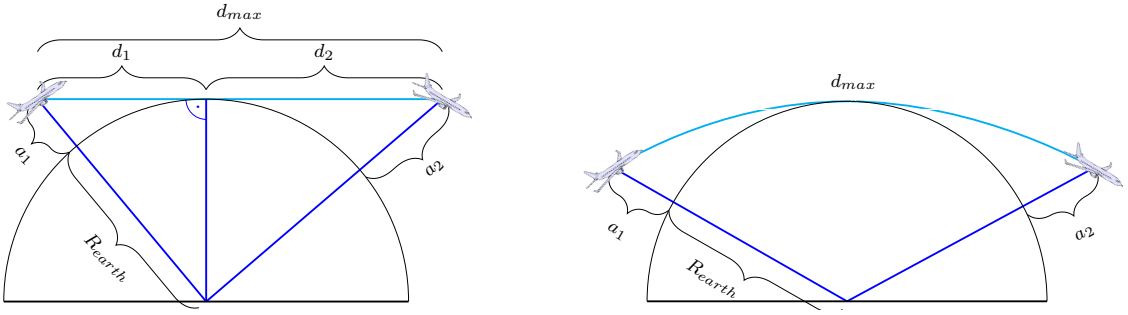

(a) Maximum link distance without atmospheric refraction.

(b) Maximum link distance with atmospheric refraction.

Figure 3.1: Maximum link distance with and without atmospheric refraction.

3.1.3 Link budget

The link between two aircraft and between an aircraft and a BS can be characterized by a LOS connection, as stated in Section 3.1.2. The main attenuation is due to the link distance, as other attenuations are significantly smaller. Hence, Friis transmission equation [168] can be applied. With P_{RX} as the receive power, P_{TX} as transmit power, G_{TX} and G_{RX} the gains of transmit and receive antennas, the speed of light c, frequency f and distance d_{TX-RX}, the Friis equation can be written as follows using decibel:

$$P_{RX} = P_{TX} + G_{TX} + G_{RX} + 20 \log_{10} \frac{c}{4\pi f d_{TX-RX}} \tag{3.4}$$

The SINR needs to lie above a margin, such that the receiver can detect the signal. In order to use the modulation schemes as shown in Table 3.1, the respective SINR threshold s_{thresh} needs to exceed the limits stated in the first column. Hence, the relation can be stated as follows:

$$P_{RX} - P_N \geq s_{thresh} \tag{3.5}$$

For calculating the best case, it is assumed that there is no interference, so P_N only consists of thermal noise N_0. If interference is present, the data rate decreases accordingly. Hence, the best case can only be reached without interference. The thermal noise can be calculated as follows:

$$P_N = N_0 = 10 \log_{10}(k_B \cdot BW \cdot T) \quad [dB] \tag{3.6}$$

The Boltzmann constant is $k_B = 1.380649 \times 10^{-23} \frac{\text{Ws}}{\text{K}}$. BW is the bandwidth in Hz and T the temperature in Kelvin. At cruising altitude, the temperature is $T = 223.25$ K [169]. To take into account additional losses, such as hardware related losses, $L_{other} = 10$ dB is assumed.

Combining equations (3.4), (3.5) and (3.6) yields:

$$s_{thresh} + N_0 + L_{other} \leq P_{TX} + G_{TX} + G_{RX} + 20\log_{10}\frac{c}{4\pi} - 20\log_{10} d_{TX-RX} - 20\log_{10} f \tag{3.7}$$

Antenna gain, diameter and beamwidth are directly related. While the calculation differs for each antenna type, Equations (3.8) and (3.9) can be used as an approximation [170] with a typical value of the efficiency $\eta = 0.7$.

$$G = \left(\frac{\pi D f}{c}\right)^2 \eta \tag{3.8}$$

$$\psi = \frac{70c}{Df} \tag{3.9}$$

To calculate the link parameters using the equations above, input parameters need to be defined. As implementations depend on regulatory as well as hardware limitations, the input parameters stated here are just one possible example, while other options will be highlighted as well. For all input parameters, exemplary reference values will be stated for the reference scenario, cf. [167, P2].

The frequency band is a parameter which mostly depends on regulations. For DA2G in Europe, two frequency bands have been defined in [171], namely 1.9 GHz and 5.8 GHz. The 5.8 GHz band with 20 MHz of bandwidth is chosen here. For A2A, implementations are still unavailable, hence, there is no dedicated frequency band. Frequency bands with wavelengths in the millimeter range offer highly directive and small phased antenna arrays and are currently researched for ground applications. Therefore, 31 GHz is used as a reference here, as this frequency has local minimum for the atmospheric attenuation in the millimeter wave spectrum. The bandwidth is set to 20 MHz, to be comparable to DA2G and as much higher A2A capacities than DA2G or satellite links are not improving the A2G capacity due to the A2G bottleneck, cf. [167, P2].

For the A2A antennas, 50 dBm transmit power and 33 dBi antenna gain are assumed. This yields an Equivalent Isotropically Radiated Power (EIRP) of approximately the range of current satellite antennas [172]. These gain and transmit power values could also be generated by an array of many small antennas, adding up gain and transmit power of the single elements. To proof that the maximum capacity can be reached using these values, the margin of the link budget stated in Equation (3.7) is calculated. The margin is the difference between the right and the left side of Equation (3.7). With the A2A frequency of 31 GHz, a maximum distance of 700 km, the maximum value for $s_{thresh} = 27.3$ dB from Table 3.1 and $N_0 = -132.1$ dB for 20 MHz bandwidth, the margin of Equation 3.7 is 1.638 dB. For the DA2G link, the range is

reduced to 350 km. With the frequency of 5.8 GHz and a gain of 30 dBi at the BS and 15 dBi at the aircraft, this yields a margin of 1.208 dB. As both margins are positive, the setup is feasible. The respective antenna size and beamwidth can be calculated using Equations (3.8) and (3.9). For 33 dBi gain and 31 GHz, the approximate diameter $D = 0.16$ m. With this diameter, the beamwidth is $\psi = 4.1$ degree. The size and beamwidth for DA2G is similar. The size of the antennas is feasible for an aircraft. As smaller gain antennas have higher beamwidth and the antenna is a parameter that can be varied, a more conservative beamwidth of 10 degree is assumed in the reference scenario. Hence, for both links, the assumed parameters are feasible, cf. [167, P2].

As already mentioned, other combinations of parameter settings are also feasible. The parameters which can be varied are transmit power, antenna gains, communication range, maximum capacity or s_{thresh}, bandwidth and frequency. As the above assumed transmit power and antenna gains are rather ambitious in terms of size and weight of the needed equipment, some examples with reduced transmit power and antenna gains are calculated in the following. This would yield a reduced weight and thus can be advantageous for the implementation. Nevertheless, other parameters need to be adjusted to achieve this. Three relaxation options are calculated. The first and the second option use the same antenna gains, but the transmit power is decreased to 40 dBm. This leads to a reduction of $\Delta dB = -10\ dB$. For the third option, the transmit power and antenna gains are decreased even further. The assumed transmit power is 40 dBm and the antenna gains are decreased to 15 dBi. This corresponds to a reduction of $\Delta dB = -46\ dB$. For each option, the resulting parameter changes are detailed in Figure 3.2. They have been calculated using the equations introduced above. As a conclusion, the options with relaxed antenna parameters can also be achieved by reducing link distance, increasing the bandwidth or reducing the frequency.

As a conclusion, the link budget for the A2A and DA2G links has been calculated. The antenna parameters have been chosen to be able to achieve the maximum capacity from Table 3.1. While these antenna parameters are ambitious, alternatives to reach the same capacity have also been presented.

3.1.4 Hardware limitations

The communication performance can be significantly influenced by the hardware installation on the aircraft. The aircraft structure can obstruct the LOS connection. Additionally, weight and drag of the equipment plays an important role, as it relates to operation cost. Hence, the antennas and communication equipment need to be placed on the aircraft intelligently. The relevant parameters are discussed in the following.

For satellite and DA2G connectivity, the antenna placement is simple. To be able to com-

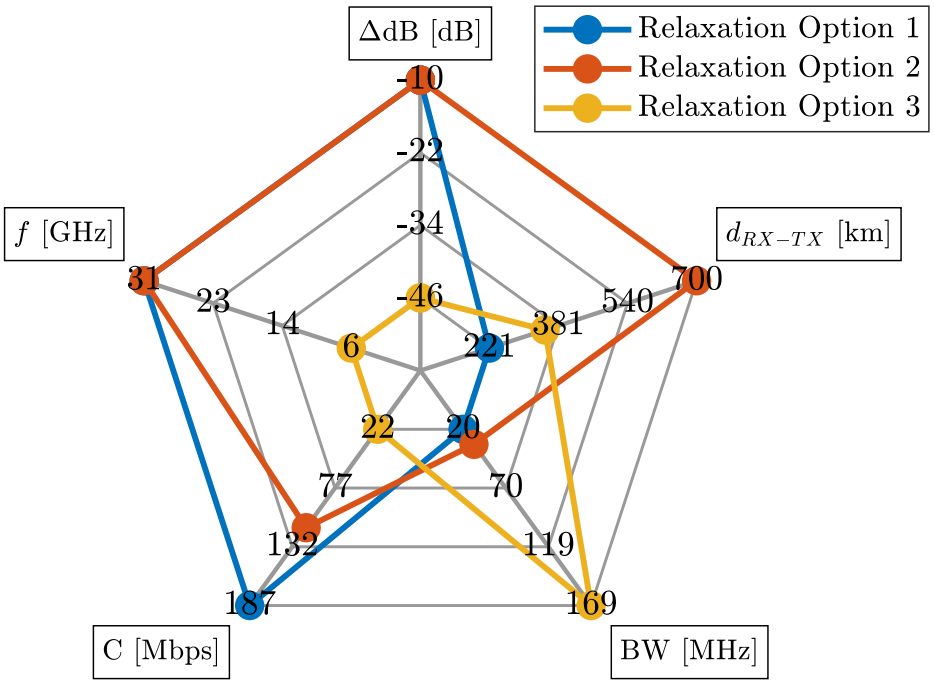

Figure 3.2: Possible alternative link budget parameter settings.

municate with the satellite, the antenna needs to be installed on the top of the aircraft. As the DA2G BS is below, the antenna is placed below the aircraft body. For A2A connectivity the placement is more challenging. Other aircraft can be present in any direction, hence, antennas need to be placed to cover these angles to the largest possible extent. Additionally, aircraft should be able to connect to more than one other aircraft at the same time. This can either be realized by utilizing multiple antennas for multiple links or by implementing multiplexing between multiple links, e.g. on basis of time division. The installation and position of an antenna on the aircraft depend on multiple factors. For instance, these can be optimal LOS conditions, aerodynamics, cabling and equipment placement or interworking with existing equipment. As these factors are very specific to the aircraft type and configuration, a simplified model is introduced in the following.

The model contains two parameters, the number of possible connections D_n and the steering angle θ. D_n states how many aircraft can be connected to one aircraft simultaneously. This is an important constraint for A2A, as a limited number of links need to be selected from the available ones. D_n combines the number of deployed antennas and the number of aircraft per antenna. To align with the capacity calculation in Section 3.1.1, the first case is assumed without loss of generality. The steering angle θ is modelling the angles that allow an A2A connection between two aircraft. This combines antenna steering angles and visibility range due to shadowing of the aircraft. θ is implemented with respect to the heading of the aircraft. $\theta = 90$ degree corresponds to steering the antenna by 90 degrees to the right

and to the left with respect to the heading. This is applicable for looking forward as well as backward. Hence, a steering angle of 90 degrees indicates that all angles can be covered. For $\theta = 45$ degree, only a sector of 90 degrees to the front and to the back can be used for A2A links, therefore communication to the side is impossible. The steering angle is modeled as a two-dimensional parameter, as it assumed that the distance between two aircraft is significantly larger than the difference in altitude. Additionally, altitude differences are small during cruise flight, which represents the largest part of the flight. For satellite and DA2G, only D_n is modeled, which is assumed to be 1. As it is assumed that satellite and DA2G antennas are properly dimensioned to connect to their respective satellite or ground station, θ is unnecessary for satellite and DA2G, cf. [P2, P3].

3.1.5 Interference model

Interference is modeled for the A2A link. For satellite and DA2G links, only one link to each aircraft is present as presented in Section 3.1.4 and separate frequencies are used. Therefore, interference does not need to be modeled in these cases. Interference could be avoided also in the A2A case, e.g. by using multiple channels if enough bandwidth is available. However, this adds additional complexity, as aircraft need to coordinate which channel to use at which time and position. Therefore, the approach including interference is pursued here.

From a geometric perspective, interference occurs, if two aircraft are within each others beam. More specifically, the receiving aircraft has to be present within the beam of the interfering aircraft. This must also hold for the other direction. For example, in Figure 3.3, two links (1,2) and (3,4) are depicted. Aircraft 4 receives interference from aircraft 1, as the angle between aircraft 2-1-4 is smaller than half of the beamwidth. This also holds for the opposite direction. Aircraft 2 does not receive interference from aircraft 3, as it is not within the beam of aircraft 3. In the model, interference is stated as binary parameter, which is one if link (i,j) receives interference by link (k,l), cf. [P2].

3.1.6 Network model

The A2G network architecture has been introduced in Section 2.2. Figure 3.4 depicts the model of the A2G network architecture. The model contains four different types of nodes, i.e. aircraft, satellites, BSs and a source node. The source node represents the ground network including satellite gateways on ground. As the capacity bottleneck lies within the A2G network, it is assumed that the ground network, i.e. the source node, is properly dimensioned to support the capacities required by the A2G network. The model presented here is defined for the DL, which is the link from the ground to the aircraft. The same is applicable for the UL as well, cf. [P3].

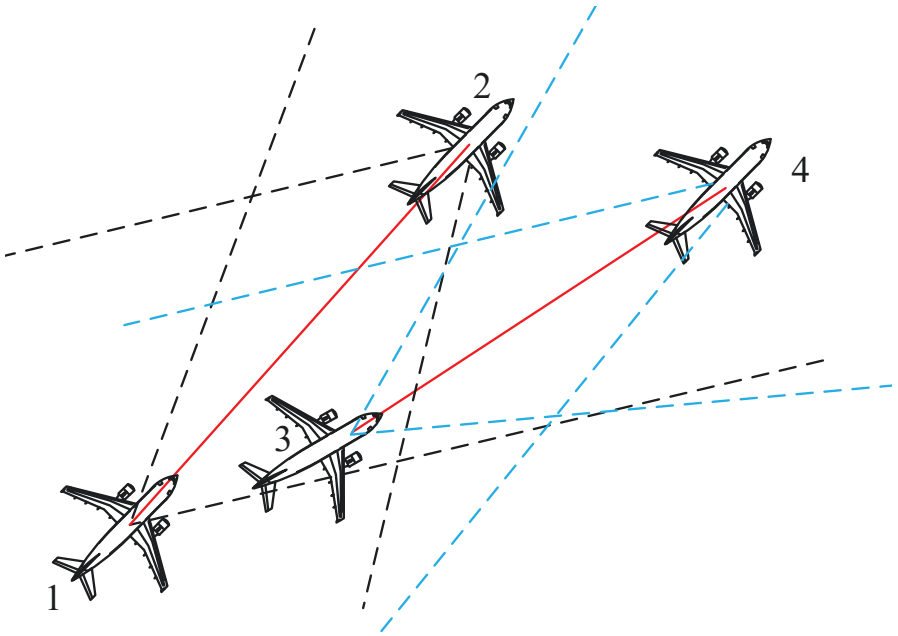

Figure 3.3: Illustration of interference calculation [P2] ©2019 IEEE.

There are three options for an aircraft to connect to another node, either via satellite, a BS or another aircraft, as depicted in Figure 3.4. The capacity for the satellite and DA2G links is modeled in terms of the capacity from the source to the respective node. This is only the case for limited backhaul for DA2G. In case of unlimited backhaul, the maximum capacity on the DA2G link is limited by the link between the BS and each aircraft. For A2A, the maximum capacity is a function of the interference by other links as detailed in Section 3.1.1, cf. [P3].

This analysis is performed on the basis of time snapshots, as also shown in Figure 3.4. Hence, time is modeled as a discrete variable using snapshots in 15 minutes intervals. This is adequate for the throughput allocation in Chapter 4, as the topology changes only slowly and the main goal is to evaluate the a benchmark capacity at different times of the day. However, to implement routing mechanisms and track specific links over time, a shorter time interval has to be selected. Therefore the interval between snapshots is reduced to one minute in Chapter 5. Due to practical link setup, changes in the chosen links between two time instants should be minimized. Therefore, this is taken into account for the heuristic algorithm, for the benchmark calculation it can be omitted, cf. [P3].

Lastly, a model containing all aircraft worldwide is infeasible due to the high number of aircraft in the air at any time instant. Hence, the Earth is divided into representative geographic scenarios. The size of the scenarios is selected such that the number of aircraft does not exceed the maximum size for the optimization. Scenarios are defined in terms of their latitude

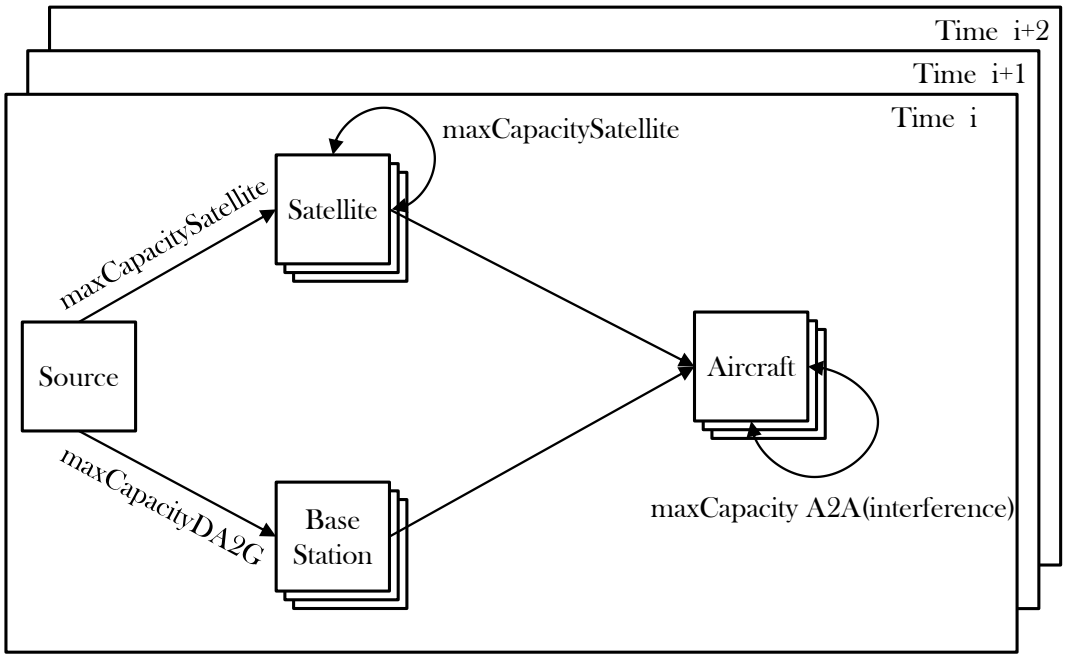

Figure 3.4: Model for the A2G network architecture including time snapshots [P3] ©2020 IEEE.

and longitude. To cover different situations, the scenarios are selected to cover different areas, such as oceanic regions or regions with a high aircraft density. The selected scenarios are described in Section 4.1.4 and Section 5.4.3, cf. [P3].

3.2 Problem formulation

The A2G capacity optimization is stated in this section. Different versions of this problem formulation have been described in [P2] and [P3]. The formulation presented here updates and combines the two versions.

As described in [P3], "the A2G network is modeled in a set of vertices V and edges E. The set of edges E consists of multiple sub-sets, namely E_{AIR} for A2A edges, E_{DA2G} for DA2G edges, E_{GEO} and E_{LEO} for edges to GEO and LEO satellites, E_{ISL} for inter-satellite links between GEO and LEO and E_{GND} for edges from satellites and BSs to the source. A2A and inter-satellite links are bidirectional, whereas the other links are modeled unidirectional from the source to all aircraft. The set of data rates per aircraft is denoted as Λ and the variable $\lambda_{s,t} \in \mathbb{R}_{\geq}0$ is the throughput from the source s to destination aircraft t. The traffic flow on each edge (i,j) from source s to destination t is modeled by the variable $f_{i,j}^{\lambda_{s,t}} \in \mathbb{R}_{\geq}0$. It is measured in the unit of the capacity of the link. Aircraft are constraint on the number of DA2G, satellite and A2A links they can use simultaneously as explained in Section 3.1.4. The maximum nodal degree values are defined by D_{air}, D_{sat} and D_{da2g} respectively and are sufficiently large

for the source, satellites and BSs. For enforcing the degree constraint, we model the binary topology variable $z_{i,j} \in \{0,1\}$, which becomes 1 if (i,j) is selected in the optimized topology. For modeling interference between A2A links, the received power is defined as $P_{i,j}$ at aircraft j from aircraft i. The received interference of link (i,j) by link (k,l) is denoted $I_{i,j}^{k,l}$ as defined in Section 3.1.5. It is a binary parameter, which is one if (i,j) receives interference by link (k,l). N_0 denotes the noise power. While the capacity of A2A is depending on the level of interference as a function $\Phi(s_{i,j})$ of the SINR variable $s_{i,j}$ with a maximum capacity c_{maxAir}, the capacities for (inter-) satellite and DA2G links c_{GEO}, c_{LEO} and c_{DA2G} are a fixed input parameter. $\Phi(s_{i,j})$ is a step function based on the modulation format with capacity values in Table 3.1."

The SINR at aircraft j by link (i,j) is defined as

$$\text{SINR}_{i,j} = \frac{P_{i,j}}{N_0 + I_{i,j}^{k,l} P_{k,j} z_{k,j}} \tag{3.10}$$

From the SINR limits in Table 3.1, the applicable maximum capacity can be deducted in terms of a step function for each modulation. Equation (3.10) is non-linear. To linearize the equation, the capacity limits are redefined in terms of upper 1/*SINR* limits. Table 3.2 shows the modified capacity limits v_{step} in terms of the 1/*SINR* limits l_{step}. To model the modified step function, additional binary variables $h_{i,j,step}$ are introduced per step. These variables must be one if $s_{i,j}$ exceeds the respective limit l_{step}. n_s defines the number of steps, which is 17 in this case. To satisfy constraint (3.22), the additional 17^{th} step needs to be present, cf. [P3].

The analysis in Chapter 4 investigates two different objectives. The first objective is maximizing the minimum capacity of all aircraft as defined in Equation (3.11). This objective ensures an equal distribution of capacity among all aircraft. If aircraft weights are introduced, the minimum capacity needs to be divided by the respective weight. Additionally, a second objective is necessary in a second step as stated in Equation (3.12). The objective minimizes

Table 3.2: Capacity step function parameters [P3] ©2020 IEEE.

Step	l_{step}	v_{step}	Step	l_{step}	v_{step}
1	0	186.6388	10	0.0891	60.6388
2	0.0019	174.2353	11	0.1318	48.2353
3	0.0043	156.9103	12	0.1995	37.2103
4	0.0063	139.9784	13	0.3236	22.1004
5	0.0089	128.9030	14	1.0471	9.5004
6	0.0132	113.9897	15	1.9953	3.8380
7	0.0240	98.3380	16	8.8675	0
8	0.0355	83.7220	17	10e9	0
9	0.0501	68.8086			

the sum of flows with the given objective throughput. Hence, this removes loops within the final topology, cf. [P3].

$$\text{maximize} \quad \min \lambda_{s,t} \tag{3.11}$$

$$\text{minimize} \quad \sum_{(i,j)\in E, \lambda_{s,t}\in\Lambda} f_{i,j}^{\lambda_{s,t}} \tag{3.12}$$

The second objective covers a different perspective. An equal distribution of capacity among all aircraft might lead to a low overall throughput. Hence, a threshold can ensure a certain minimum performance, while disconnecting some aircraft at a certain time. Hence, the objective is maximizing the number of aircraft that receive a throughput exceeding a threshold β. Therefore, the binary variable $A_{\lambda_{s,t}}$ is introduced, which is one if β is exceeded for demand $\lambda_{s,t}$. With these definitions, the second objective can be defined as in Equation (3.13), cf. [P2].

$$\text{maximize} \quad \sum_{\lambda_{s,t}\in\Lambda} A_{\lambda_{s,t}} \tag{3.13}$$

subject to

$$\sum_{(v,j)\in E} f_{v,j}^{\lambda_{s,t}} - \sum_{(j,v)\in E} f_{j,v}^{\lambda_{s,t}} = \begin{cases} \lambda_{s,t} & \text{if } v = s \\ -\lambda_{s,t} & \text{if } v = t \\ 0 & \text{otherwise} \end{cases} \qquad \forall \lambda_{s,t} \in \Lambda \quad \forall v \in V \tag{3.14}$$

$$\sum_{\lambda_{s,t}\in\Lambda} f_{i,j}^{\lambda_{s,t}} \leq \begin{cases} z_{i,j} \cdot c_{maxAir} & \forall (i,j) \in E_{AIR} \\ z_{i,j} \cdot c_{GEO} & \forall (i,j) \in E_{GEO} \\ z_{i,j} \cdot c_{LEO} & \forall (i,j) \in E_{LEO} \\ z_{i,j} \cdot c_{DA2G} & \forall (i,j) \in E_{DA2G} \end{cases} \tag{3.15}$$

$$z_{i,j} = z_{j,i}, \quad \forall (i,j) \in E_{AIR} \cup E_{ISL} \tag{3.16}$$

$$z_{i,j} = 1, \quad \forall (i,j) \in E_{GND} \tag{3.17}$$

$$\sum_{(i,v)\in E_{AIR}} z_{i,v} \leq D_{air}, \quad \forall v \in V \tag{3.18a}$$

$$\sum_{(i,v)\in E_{GEO}\cup E_{LEO}\cup E_{ISL}} z_{i,v} \leq D_{sat}, \quad \forall v \in V \tag{3.18b}$$

$$\sum_{(i,v)\in E_{DA2G}} z_{i,v} \leq D_{da2g}, \quad \forall v \in V \tag{3.18c}$$

$$P_{i,j} \cdot s_{i,j} \geq N_0 + \sum_{(k,l)\in E} l_{i,j}^{k,l} P_{k,j} z_{k,l}, \quad \forall (i,j) \in E_{AIR} \tag{3.19}$$

$$\begin{aligned} \sum_{\lambda_{s,t}\in\Lambda} f_{i,j}^{\lambda_{s,t}} &\leq \Phi(s_{i,j}) \quad \forall (i,j) \in E_{AIR} \\ \Phi(s_{i,j}) &= v_1 h_{i,j,1} + \sum_{step=2}^{n_s-1} (v_{step} - v_{step-1}) h_{i,j,step} \end{aligned} \tag{3.20}$$

$$h_{i,j,step} \leq h_{i,j,step-1} \quad \forall (i,j) \in E_{AIR} \quad \forall s \in (2..n_s) \tag{3.21}$$

$$s_{i,j} \leq l_1 + \sum_{step=1}^{n_s} (l_{step+1} - l_{step}) h_{i,j,step} \quad \forall (i,j) \in E_{AIR} \tag{3.22}$$

The conservation of the flows is stated by Constraint (3.14). Constraint (3.15) limits the sum of all flows to the capacity of the link and ensures that flows can only be placed on the chosen sub-topology. Constraint (3.16) states that the chosen sub-topology needs to be symmetric for A2A and inter-satellite links (ISL) links. Ground links should always be part of the sub-topology which is defined by Constraint (3.17). The nodal degree limitations for each link type are defined in Constraints (3.18a)-(3.18c). The relation of A2A link capacity, the SINR and the sub-topology is modeled in Constraint 3.19. The respective step function, as stated in Table 3.2, is modeled in Constraints (3.20)-(3.22), cf. [P3].

For the second objective two additional constraints are needed. With Constraint (3.23), $A_{\lambda_{s,t}}$ is forced to zero if $\lambda_{s,t}$ is unable to meet the threshold β. Constraint (3.24) ensures that only aircraft meeting the threshold β are forwarding capacity to other aircraft, cf. [P2].

$$\lambda_{s,t} \geq A_{\lambda_{s,t}} \cdot \beta \quad \forall \lambda_{s,t} \in \Lambda \tag{3.23}$$

$$\sum_{(t,j)\in E} \sum_{\lambda_{s,t}\in\Lambda} f_{t,j}^{s,t} \leq A_{\lambda_{s,t}} \cdot M \quad \forall \lambda_{s,t} \in \Lambda \tag{3.24}$$

To investigate the importance of different types of links for the A2G network, a penalty $\pi_{i,j}$

can be added to all links. This case is investigated in Section 4.2.2. The default value for $\pi_{i,j}$ is one. A higher penalty value reduces the probability of choosing the respective link type. In case a penalty $\pi_{i,j}$ is introduced, Constraint (3.15) is replaced by Constraint (3.25).

$$\sum_{\lambda_{s,t} \in \Lambda} f_{i,j}^{\lambda_{s,t}} \leq \begin{cases} \frac{z_{i,j} \cdot c_{maxAir}}{\pi_{i,j}} & \forall (i,j) \in E_{AIR} \\ \frac{z_{i,j} \cdot c_{GEO}}{\pi_{i,j}} & \forall (i,j) \in E_{GEO} \\ \frac{z_{i,j} \cdot c_{LEO}}{\pi_{i,j}} & \forall (i,j) \in E_{LEO} \\ \frac{z_{i,j} \cdot c_{DA2G}}{\pi_{i,j}} & \forall (i,j) \in E_{DA2G} \end{cases} \tag{3.25}$$

3.3 Conclusion

In this chapter, the A2G network model is introduced. It includes basic connectivity parameters, such as the maximum link capacity and the maximum range for DA2G and A2A links. Moreover, the link budget is calculated to determine transmission parameters, such as transmit powers and antenna gains. It is shown that the maximum link distances can be reached. As there are degrees of freedom in choosing the transmission parameters, different viable setups are presented. While the presented alternatives are designed for maximum link distance and maximum link capacity, these parameters can be relaxed, if a smaller link distance or lower capacity is sufficient. This is studied in the next chapters. Additionally, the model implements time snapshots and geographic scenarios. This allows to study the network at different times of the day and regions of the Earth. The mathematical problem formulation is also provided, which is the basis of solving the problem optimally. As a conclusion, the presented A2G network model enables to study the network under different parameter constellations and to determine the best throughput allocation to aircraft.

4 Optimal aircraft throughput allocation

In this chapter, the optimal throughput allocation is investigated. To achieve this, the problem formulation as introduced in Section 3.2 is implemented and the problem is solved using the Gurobi solver. The focus lies on the achievable throughput in different parameter configurations. The basic configuration is a combined A2G network. Other configurations such as a DA2G and A2A network or a satellite network are investigated as well. An extensive variation of multiple parameters is conducted to gain insight on the effect of each parameter on the achievable throughput per aircraft. Firstly, the reference values for all parameters are introduced. Then the results for the throughput allocation are presented. The main contribution of this chapter is to provide a benchmark on the optimal achievable throughput per aircraft under different conditions.

Parts of the content in this chapter have been published by the author in the following papers:

- "Combined Optimal Topology Formation and Rate Allocation for Aircraft to Aircraft Communications" [P2]
- "Optimal Throughput Allocation in Air-to-Ground Networks" [P3]

4.1 Implementation and parameter setup

This section introduces all parameters which are necessary for the optimization. This includes the model implementation, the aircraft flight traces and BS positions. Additionally, the chosen geographic scenarios are introduced and all parameters of the reference setup are stated.

4.1.1 Model implementation

The A2G network model, as introduced in Chapter 3, is implemented using MATLAB, AMPL and Gurobi. The workflow is illustrated in Figure 4.1. Firstly, MATLAB processes the raw input, such as flight traces, BS positions and parameter settings. The full list of parameters is summarized in Section 4.1.5. The MATLAB scripts calculate the resulting full topology as well as additional input parameters, such as interference and received power between aircraft. As an output, MATLAB writes one folder per time instant and parameter setting. The files in each folder contain the calculated input parameters in a format which is readable by AMPL. With this input, the MILP is solved using the AMPL modelling language and the Gurobi solver. It is executed on an Intel(R) Xeon(R) E5-2557 CPU with 24 cores and 265 GB RAM. The results contain the optimized topology including the optimal allocation of flows on the optimized topology. The results are then evaluated using MATLAB to generate statistics and figures.

4.1.2 Flight traces

The information about the position and heading of aircraft is extracted from flight traces from FlightRadar24 [152]. The traces are based on ADS-B data, which is used for air traffic control. When using ADS-B, aircraft are constantly broadcasting their position. Besides the position, the data contains also other identifying data, such as flight number or aircraft type. A full list of parameters is shown in Table 4.1. Within this work, two different traces are used. The first data set is called week data set. It contains flight traces of one week between 2017/11/03, 9:30 UTC to 2017/11/10, 9:30 UTC, in time intervals of 15 minutes. The second data set is called day data set and contains 24 hours of data on February 9, 2018. This data set has a higher resolution in time, as the time intervals are in the order of a few seconds.

The number of aircraft worldwide over the different days of the week is illustrated in Figure 4.2. It can be seen that all days follow a similar pattern. This is due to the time of day in different places of the world, as most flights are starting or landing during the day. The small differences between different days of the week can be considered as insignificant. In the connectivity analysis is Chapter 2, the full week data set is utilized. For the throughput allocation in Chapter 4 and 5, the time span is reduced to 24 hours as this sufficiently covers the pattern described above. Additionally, the season influences the number of aircraft in the air, as destinations are varying in winter and summer. Comparing one day of the week

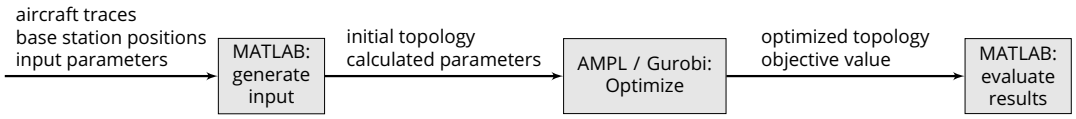

Figure 4.1: Implementation workflow.

Table 4.1: Full list of parameters of the flight traces.

Registration	MODE-S Code	Latitude (deg)
Longitude (deg)	Heading (deg)	Altitude (ft)
Speed (kt)	Squawk (4-digit ID of Transponder)	Radar ID
Aircraft Type	Tail Number (Aircraft Registration)	Timestamp
Departure Airport	Destination Airport	Flight Number (short)
Vertical Speed (ft/m)	Flight Number (long)	

data set to one day of the day data set shows that the maximum calculated throughput values are identical, while the median differs by 7.3%, which is 1.6 Mbps. This small difference is due to the different time of the year. When comparing each time instant separately, the shapes of the curves are similar and differences stay within slight variations. Hence, the selected aircraft traces are utilized as representative examples.

As a summary, the week data set is used in Chapter 2 and 4, whereas the day data set is used in Chapter 5. This is due to the higher time resolution which is needed for the heuristic algorithm. The detailed points in time are specified in Table 4.2. The reduced time span for the North Atlantic scenario is due to the high number of aircraft compared with the other scenarios.

The time resolution of the week data set is 15 minutes, as already mentioned. Hence, the analysis is conducted in time steps of 15 minutes. This is sufficient, as the topology is changing slowly and the benchmark calculation is independent from the last time step. Hence, a high time resolution is unnecessary. However, in Chapter 5, the link status of the last time step is taken into account for the calculation of the current time step. Hence, a smaller interval of 1 minute is used. Before usage, the data sets need to be cleaned in order to only contain the desired data. In the raw data, some aircraft appear twice in the same time instant, for instance if they have been received by multiple ground stations. Moreover, for aircraft over the ocean, the position cannot always be received on the ground. Hence, the missing positions need to be interpolated. Additionally, ADS-B is also used by different types of aircraft, such as small private airplanes or helicopters. To exclude these, all aircraft without a

Table 4.2: Flight traces data set overview.

Chapter	Data set	Time and date
2	week	2017/11/03 9:30 UTC - 2017/11/10 9:30 UTC
4	week	North Atlantic: 2017/11/05 22:30 - 23:45 UTC
4	week	Other scenarios: 2017/11/04 23:30 UTC- 2017/11/05 23:45 UTC
5	day	2018/02/09 00:00 UTC - 23:59 UTC

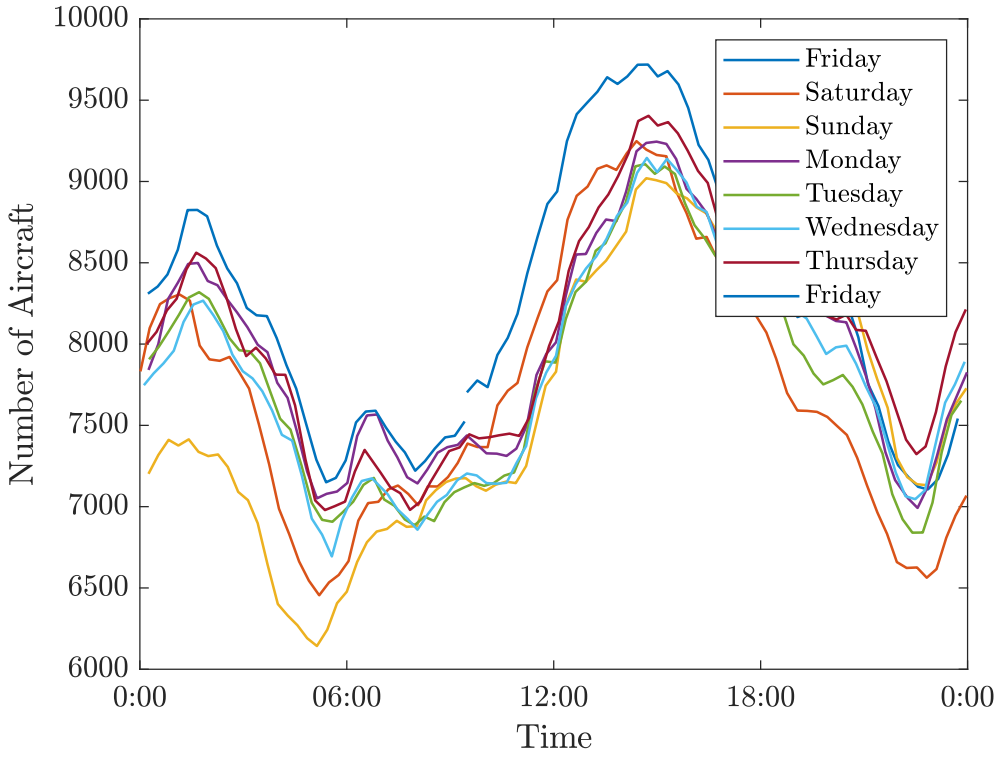

Figure 4.2: Number of aircraft over time for different days of the week.

flight number are removed. Lastly, some aircraft keep broadcasting their position while they are on the ground, hence aircraft on ground are also excluded.

4.1.3 BS positions and satellite operators

The positions of the BSs is relevant to determine aircraft with DA2G connection. Today, A2G BSs are specifically positioned for the aircraft use case. In the EU and the US networks are already deployed. Therefore, the BS positions of the EAN are used for Europe and the ones of the GoGo network for the US. They have been approximated from [173] and [174], respectively. These networks are designed to cover aircraft which fly over the continent. For the North Atlantic use case, these BSs are insufficient. Hence, in this case additional BSs at the US coast and on Greenland and Iceland are assumed. The positions have been chosen to maximize the coverage area. A high number of BSs is beneficial, as for the oceanic A2A network, the capacity of an aircraft in the middle of the ocean depends on the available DA2G capacity. Figure 4.3 shows the positions of all BSs. It can be seen that the BS density of the EAN is higher than in the GoGo network, cf. [P3].

For the satellite links, two different deployments are assumed. As already stated in Sec-

tion 3.1.1, the capacity is assumed per spot beam area. The varied parameter is the availability of a LEO network. The setup without LEO satellites includes six GEO operators. In the setup with LEO satellites, three additional LEO operators are present. The capacity scales with the number of operators. It is assumed that aircraft are equally distributed among operators, cf. [P3].

4.1.4 Geographic scenario setup

More than 6000 aircraft are in the air worldwide at any point in time. This number is too high to be solved optimally using a MILP. Therefore, a geographic scenario based approach is taken. Seven representative scenarios are chosen. They represent different configurations of aircraft density ρ_{AC} and BS density ρ_{BS}, as well as continental, oceanic and mixed setups. An overview of the selected scenarios can be found in Table 4.3. The geographic range of the scenarios is visualized in Figure 4.4, cf. [P3].

The scenarios are defined to contain a similar maximum number of aircraft within the respective area. Thus, the size of the area differs with aircraft density. The only exception is the North Atlantic, as it does not make sense to analyze only a part of the North Atlantic corridor. Hence, in this scenario the area and the maximum number of aircraft is larger. The scenario is used to evaluate the feasibility of a DA2G and A2A network without satellites in an area without DA2G coverage. Additionally, it is the only oceanic scenario. To investigate the impact of large areas of water, two other scenarios have also been designed with partial ocean and land. The first one is called Iberia, which includes the north-western part of the Iberian Peninsula, extended towards the Atlantic ocean. The other scenario is Italy, including the Tyrrhenian Sea in between Sardinia and the Mainland of Italy. The continental scenarios can be divided in terms of the BS density. As stated above, the BS density of the EAN in Europe

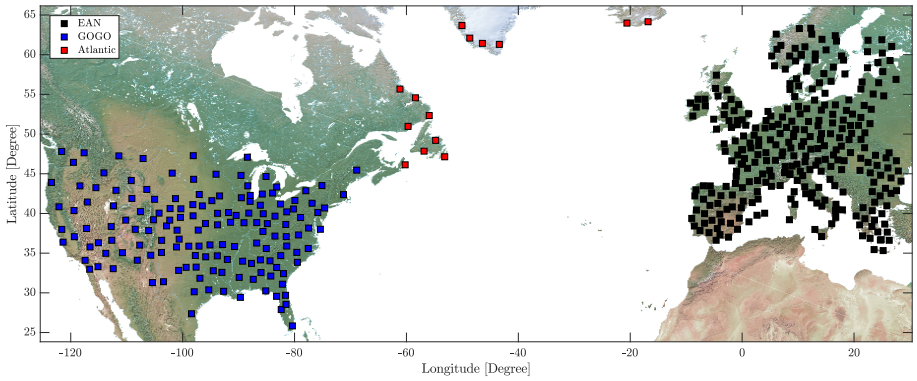

Figure 4.3: BS locations of the EAN (black), GoGo network (blue), as well as additionally assumed locations in the North Atlantic (red).

Table 4.3: Overview on scenario parameters (extended version from [P3] ©2020 IEEE).

Scenario	Latitude [Deg]	Longitude [Deg]	Area [km^2]	ρ_{AC}	ρ_{BS}
Rural US	41 - 48	-107.5 - (-100.5)	458000	low	low
Urban US	41 - 44	-72.5 - (-69.5)	84000	medium	low
Rural Europe	49 - 52	10.7 - 14	81000	medium	high
Urban Europe	48.5 - 51	7.5 - 10	51000	high	high
Italy	37 - 42	7 - 17	494000	low	medium
Iberia	40 - 44	-22 - (-3.5)	701000	medium	medium
North Atlantic	40 - (-65)	-60 - (-10)	11715000	low	low

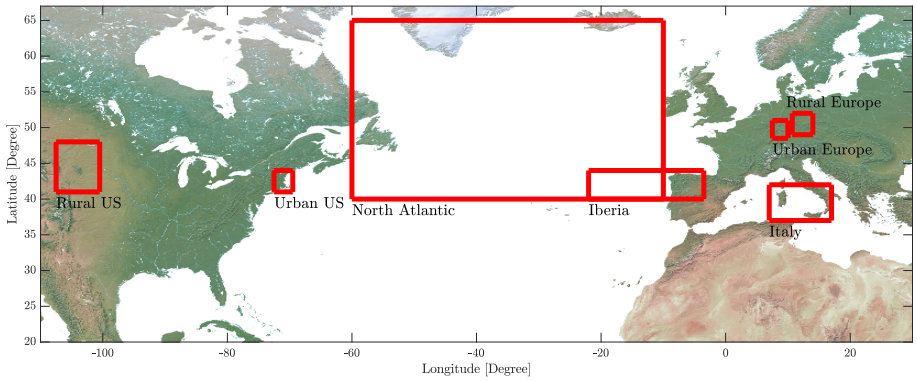

Figure 4.4: Overview on the geographic scenarios.

and the GoGo network in the US differs. Hence, these two areas are taken as representatives for low to medium and medium to high DA2G density, respectively. The two European scenarios have been partitioned into rural and urban. The urban scenario is positioned in the area of Frankfurt, Germany, which is a large airport. The rural scenario is placed toward the east, covering the eastern part of Germany and parts of the Czech Republic, leading to a lower aircraft density than the urban scenario. The US serves as example for medium DA2G BS density. Again, it is divided into urban scenario covering the area around Boston and a rural scenario in the area located north of Denver.

4.1.5 Reference parameters setup

The A2G network contains many different parameters as highlighted in the previous sections. To ensure comparability of the results, a reference setup is used. The parameter values of the reference setup are summarized in Table 4.4. The conducted parameter variations are described in Section 4.2, cf. [P3].

The available link options per aircraft depend on multiple factors. Three setups are modeled exemplarily. The first setup includes all possible links on all aircraft, hence A2A, DA2G and satellite links. This is the reference setup, as it provides most information for the benchmark. The second setup is DA2G and A2A only, without satellite availability. This allows a cost efficient solution, as the satellite equipment is heavy and costly. Hence, if sufficient connectivity can be achieved without the satellite, the cost would be reduced. The third setup is with satellite links only. This setup is a reference to the current situation, where most aircraft have only satellite connectivity. This improves the understanding of the achievable benchmark.

The MILP is solved optimally with a maximum gap of 1% as a default to limit the computation time. Only in case of the parameter variation, a maximum gap of 5% is allowed for the second objective, i.e. the removal of loops. In this case the gap for loop removal is higher, as it is a secondary objective only and therefore not influencing the benchmark. Additionally, a time limit of 24 hours is implemented to limit computation time. However, this is only exceeded in 3.6% of the runs with a median gap of 9%.

4.2 Throughput allocation results

The results of the throughput optimization are presented in this section. Three link setups and two different objectives are studied, as introduced in Section 4.1. The full A2G network is studied first, including an extensive parameter study. Then, the DA2G and A2A setup is

Table 4.4: Reference parameters setup overview.

Parameter	Value
scenario	Urban Europe
link distance	A2A: 700 km, DA2G: 350 km, satellite: n/a
link capacity	A2A: 187 Mbps, DA2G: 187 Mbps, satellite: 100 Mbps, 6 operators
link setup	A2A: on, DA2G: on, satellite: GEO on, LEO off
equipped aircraft	all aircraft, all available links
weights	all aircraft equal weights
penalty	A2A: 1, DA2G: 1, satellite: 1
interference	on
BS diversity	off
limited backhaul	on
nodal degree D_n	A2A: 3, DA2G: 1, satellite: 1
steering angle θ	A2A: 90, DA2G: n/a, satellite: n/a
beamwidth ψ	A2A: 10, DA2G: n/a, satellite: n/a

investigated. Lastly, satellite only case is investigated.

4.2.1 Combined A2G connectivity

The full A2G network is investigated in this section. The focus lies on the max-min throughput which can be achieved per aircraft. This can be used as a benchmark on how much throughput can be provided per aircraft. The partition of throughput on the different link types is studied to understand the importance of each single link. Additionally, the influence of parameters such as limited backhaul, LEO satellites, A2A links and BS diversity is investigated. Additionally, the number of needed A2A hops is studied. Aircraft capabilities are also taken into account, to study the case that not all aircraft can connect to all links. Finally, the minimum achievable throughput for the different geographic regions is presented.

In [P3], "we compare the max-min throughput to the mean throughput. The mean throughput is determined as the total available capacity from DA2G and satellites divided by the number of aircraft. The comparison is depicted in Figure 4.5. We observe that for times with more than 20 aircraft, the max-min throughput equals the mean throughput. This means that all capacity can be perfectly shared between all aircraft. Also for less aircraft, the difference between max-min and mean throughput is small. This difference comes from the lack of available links to reduce the effect of multiple aircraft being close to each other. Additionally, Figure 4.5 shows that removing A2A links has a minor effect on the max-min throughput. In general we can conclude that the bottleneck for achieving higher throughput is the capacity on the A2G links, meaning satellite and DA2G links. The available throughput can easily be divided between all aircraft."

As shown in [P3], "in Figure 4.6, we analyze the relation of throughput per aircraft originating from the different types of links. For this example, we show the results with LEO satellites as the GEO satellite contribution is small compared with the DA2G throughput per aircraft. In general, we can observe that the throughput on all links is heavily decreasing with a rising number of aircraft. During peak-aircraft-density times, the achieved throughput is very low. The mean DA2G throughput per aircraft varies around 20 Mbps, the satellite throughput per aircraft around 4 Mbps. We can also observe that the A2A throughput is decreasing in high-aircraft-density cases. The reason is that there is already a sufficient degree of freedom to achieve the optimal max-min throughput, hence A2A is dispensable. In the case of low-aircraft-density, the need for A2A is higher. Nevertheless, in this case the absolute data rates are also much higher. A similar behavior can also be observed in the other scenarios. Hence, we conclude that the experienced throughput mostly depends on the time of day. When flying during the day, the throughput is much lower than during night. The offer needs to be provisioned for the demand during the day. Even with perfect sharing, the achievable throughput during night will be higher."

"To further evaluate the role of A2A links, we investigate the maximum number of hops that connects an aircraft to the ground. Table 4.5 shows the maximum number of hops with A2A for the different parameters. We see that in all setups more than 98.2% of aircraft are connected to zero or one hop. Hence, in the investigated continental scenario, multi-hop A2A connections are unnecessary to share the capacity between aircraft" [P3].

As presented in [P3], "in the reference scenario, we restrict aircraft to connect to the closest DA2G BS only. In Figure 4.7, we investigate the effect of BS diversity on the max-min throughput. Figure 4.7 shows the optimal max-min throughput for four different setups enabling and disabling BS diversity and A2A links. This has been calculated for different time instants with different number of aircraft. We can observe that without BS diversity and without A2A links, the performance degrades quite significantly. This effect increases with lower number of aircraft. This is again due to reduced link options when multiple aircraft are close to each other. Nevertheless, in all the other three cases the difference vanishes for more

Table 4.5: Maximum number of hops per aircraft in different setups (percentage of all aircraft) [P3] ©2020 IEEE.

Hopcount	0	1	2	3-4
Unlimited backhaul, with LEO	84.84%	13.83%	1.24%	0.08%
Unlimited backhaul, without LEO	94.58%	4.97%	0.39%	0.07%
Limited backhaul, with LEO	83.47%	15.84%	0.69%	0%
Limited backhaul, without LEO	76.77%	21.46%	1.50%	0.10%

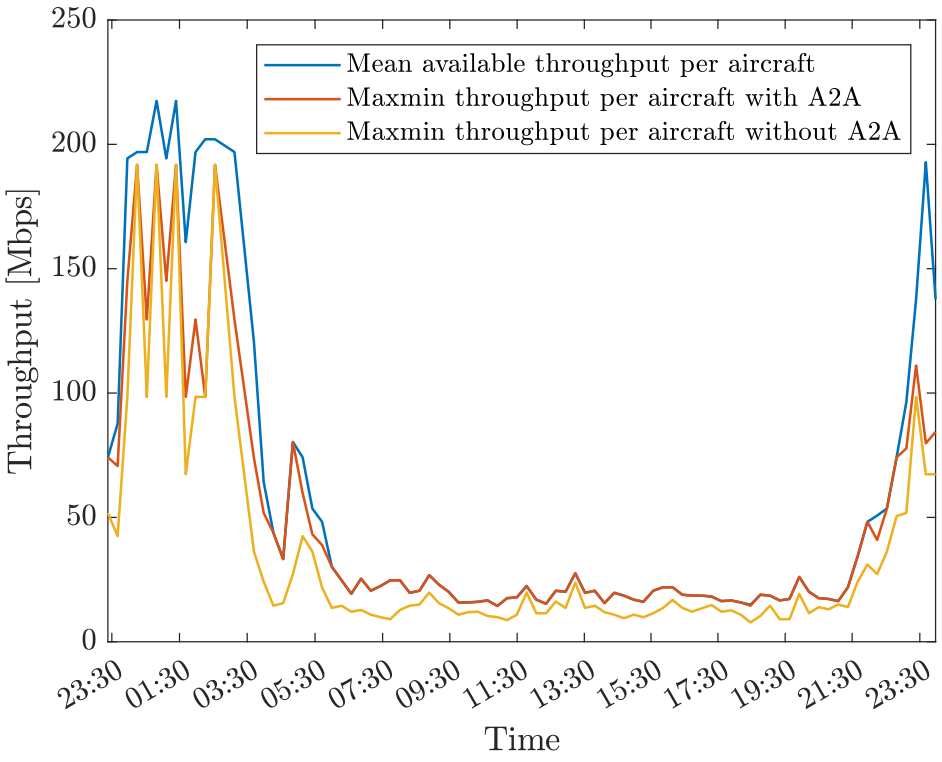

Figure 4.5: Mean and max-min available throughput during one day in the reference setup, with and without A2A links [P3] ©2020 IEEE.

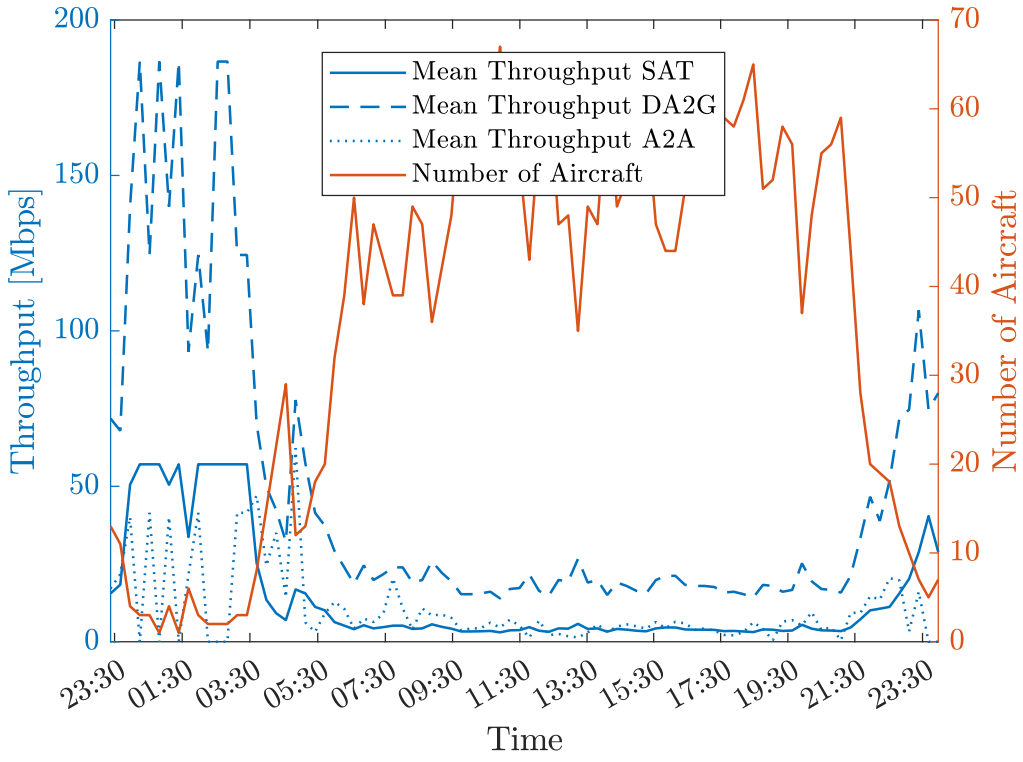

Figure 4.6: Mean throughput on satellite, DA2G and A2A links in the reference setup including LEO [P3] ©2020 IEEE.

than ten aircraft. Especially, when comparing the case with BS diversity and without A2A depicted in blue with the opposite setup depicted in green, the difference is insignificant. Hence, we conclude if we enable the aircraft to choose between different BSs in reach, we do not need A2A connectivity when being in reach of DA2G stations."

"The result of the variation of the other parameters is shown in Tables 4.6 and 4.7. Both tables show the minimum throughput of all time instants for the respective parameters. In Table 4.6, we vary the different scenarios. We observe that both urban scenarios lead to the lowest capacities. This is due to the higher aircraft density in urban regions. The highest throughput is achieved in the Italy scenario, as the relation between the number of BSs and the number of aircraft is higher than in the other scenarios. From Table 4.6, we also see that the achieved throughput highly depends on the scenario. Hence, to ensure more smooth throughput sharing between aircraft, sharing needs to be done within larger areas. Throughput sharing in large regions will be tackled in our future work, as the optimization problem is limited to a small number of aircraft. The remaining parameter variation for backhaul, LEO and A2A is shown in Table 4.7. Obviously, unlimited backhaul has the biggest influence on the minimum throughput. The reason is that in this case each aircraft receives the peak capacity of 187 Mbps from its connected BS, irrespective of the number of other aircraft connected to the same BS. The effect of adding LEO is smaller, as the additional LEO capacity still needs to be shared between aircraft. In general, to achieve a very high throughput per aircraft, advanced techniques like beamforming are needed. This enables each aircraft to receive the peak capacity from the BS." [P3].

"Lastly, in a realistic network not all aircraft might be able to connect to all types of links. Hence, we also investigate the effect when some aircraft have only access to some link options. In Figure 4.8, we modified the aircraft capabilities such that one third of the aircraft can only connect to DA2G, one third can only connect to satellite and the last third can connect to all links. For Figure 4.8, we selected the scenario Urban US. We can observe that even though two third of all aircraft cannot connect to all types of links, the capacity can still be

Table 4.6: Minimum daily throughput for different geographic scenarios (extended version from [P3].) ©2020 IEEE

Scenario	Minimum throughput
Rural US	18.58 Mbps
Urban US	4.74 Mbps
Rural Europe	22.21 Mbps
Urban Europe	14.39 Mbps
Italy	34.25 Mbps
Iberia	21.52 Mbps

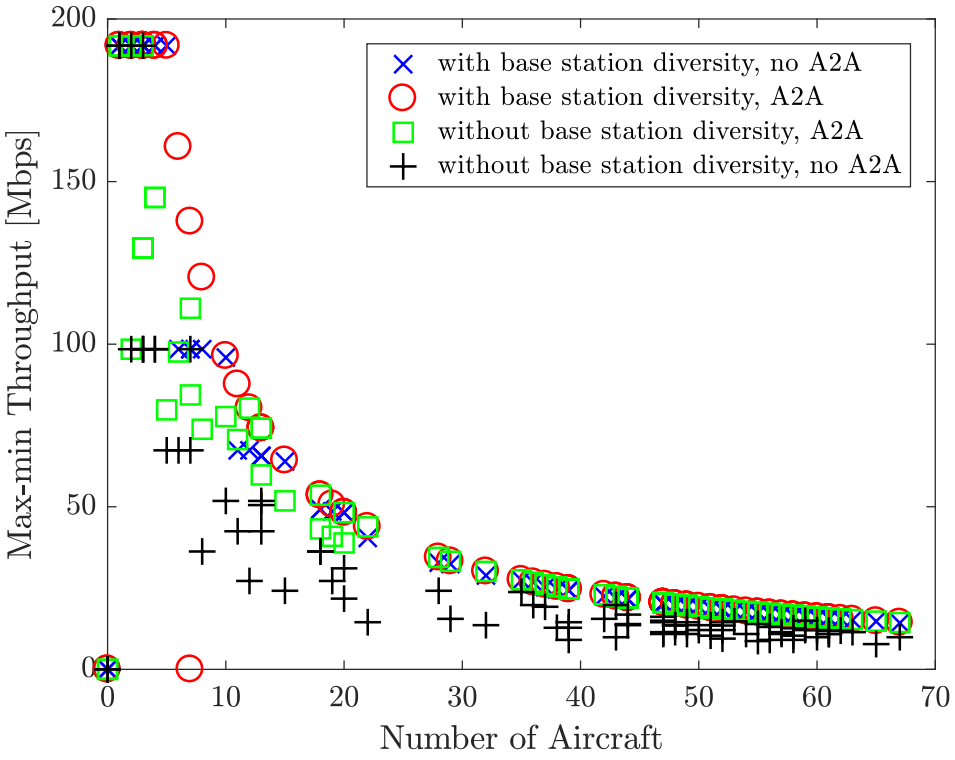

Figure 4.7: Max-min throughput in terms of BS diversity and enabled or disabled A2A links (extended version from [P3] ©2020 IEEE).

Table 4.7: Minimum daily throughput for different parameter variations [P3] ©2020 IEEE.

Scenario UrbanEurope	A2A	no A2A
limited backhaul, no LEO	14.39 Mbps	7.77 Mbps
limited backhaul, LEO	16.94 Mbps	12.79 Mbps
unlimited backhaul, no LEO	186.90 Mbps	186.64 Mbps
unlimited backhaul, LEO	189.65 Mbps	189.65 Mbps

perfectly shared with more than approximately 20 aircraft. In low-aircraft-density cases a difference occurs, which is even significant at 7:30. We conclude that there is a high degree of freedom in choosing the links to achieve the same throughput." [P3].

Additionally, the threshold objective has also been analyzed for the reference scenario. The threshold is varied from 10 to 150 Mbps. The resulting percentage of connected aircraft is presented in Figure 4.9. With a threshold of 10 Mbps, all aircraft can be connected. However, if 50 Mbps have to be provided, only approximately 40% of the aircraft can be connected. For 100 and 150 Mbps, this percentage decreases to less than 20% of all aircraft. Hence, the threshold objective can be used to provide a minimum throughput to a part of all aircraft. The application determines which of the two objectives is more suitable.

4.2.2 Parameter variation

The aircraft throughput allocation problem contains many different parameters. The parameters are antenna parameters, available links overall and per aircraft, maximum link distance, penalty and capacity per link. Each parameter influences the achievable throughput per aircraft. To quantify this influence, the parameters are varied. One parameter is varied at a time, while the other parameters are based on the reference scenario. In this way, the influence of each parameter can be determined. The variations are conducted for two representative time instants, one with low aircraft density at 4:45 and the other with high aircraft density at 10:15. Additionally, two different geographic scenarios are studied, namely Urban Europe and Iberia. To compare the influence of different parameter values, the throughput is always presented in terms of percentage of the maximum throughput of the varied parameter set.

Antenna parameters

The antenna parameters include the steering angle, maximum nodal degree and beamwidth. They influence the interference between links and the options for choosing links for the optimal topology. For the high aircraft density case, the impact of the antenna parameters is marginal. For the low aircraft density case, the results are presented in Table 4.8. The highest impact on the throughput is introduced by variation of the steering angle θ. The throughput can drop up to 28% with reduced steering angle. Additionally, a small beamwidth is beneficial. Hence, during low-aircraft-density times, the steering angle is the most critical antenna parameter. The absolute value of 72% of the maximum throughput during low-aircraft-density times is 70 Mbps, which is higher than the absolute maximum value of 36.3 Mbps in high density times. Hence, the antenna parameters are rather uncritical.

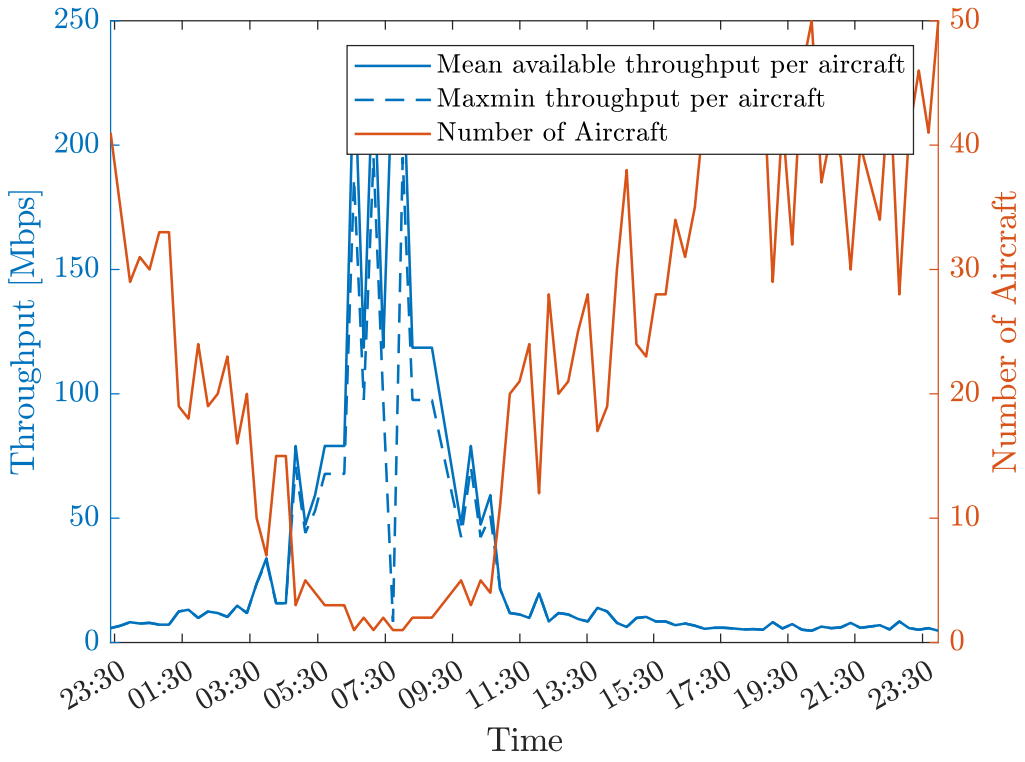

Figure 4.8: Achievable throughput over time with reduced capabilities in the Urban US scenario (one third DA2G only, one third satellite only, one third all links) [P3] ©2020 IEEE.

Table 4.8: Achievable throughput for different antenna parameters for two scenarios at low aircraft density in percent of the maximum throughput.

θ	D_n	ψ	Iberia	Urban Europe
45	3	10	100%	96.8%
90	3	10	100%	100%
45	10	10	100%	100%
90	10	10	100%	100%
45	3	40	72%	83.8%
90	3	40	100%	100%
45	10	40	100%	83.8%
90	10	40	99.9%	100%

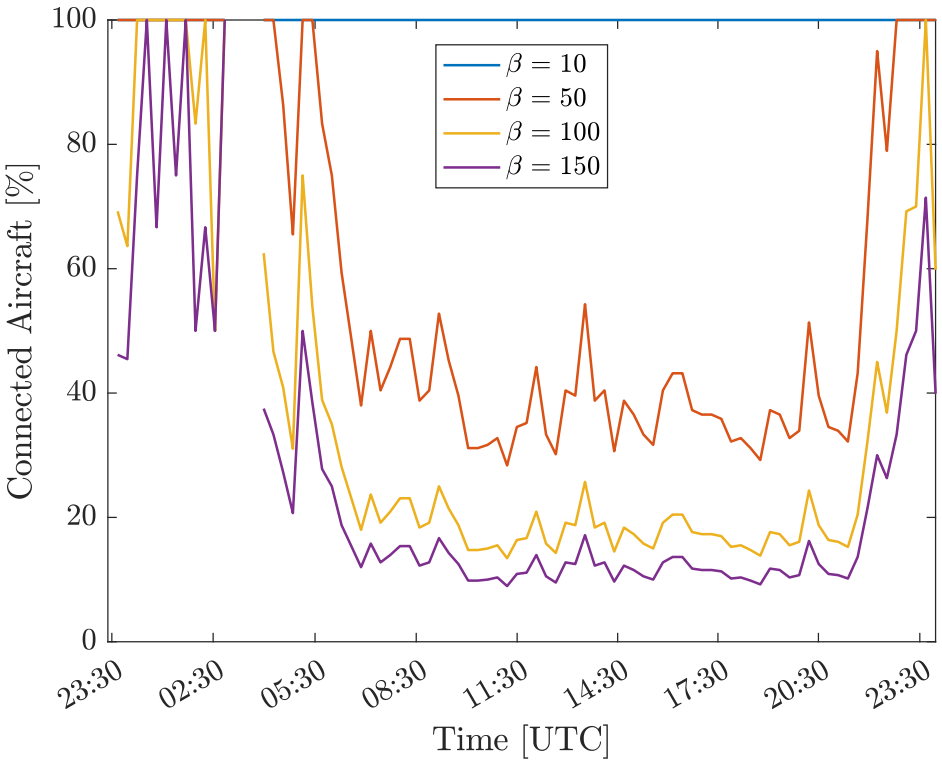

Figure 4.9: Percentage of connected aircraft in terms of different thresholds for the reference scenario.

Links

The available A2G links considerably impact the throughput. Therefore, the availability of the different connectivity options is varied. The results are presented in Figure 4.10. The figure shows that the least throughput is present in the cases without DA2G links. In the Iberia scenario, the case with only DA2G limits the throughput additionally, since aircraft over the ocean are unable to connect. In general, disabling links impacts low-aircraft-density times more, as fewer alternative link options exist. In the Urban Europe scenario, disabling only the satellite has a low impact, hence, the largest part of the throughput is provided by DA2G. In the Iberia scenario, however, DA2G has a higher influence, due to lower aircraft density and incomplete DA2G coverage. As a conclusion, more links can provide higher throughput, but the influence of each link depends on the scenario.

Aircraft capabilities

As aircraft need to be equipped with hardware for each link, some aircraft are unable to connect to all links. While some aircraft might only be able to connect to a satellite, others might be unable to connect to DA2G or A2A. This constraint is modeled by the aircraft capability. While many different combinations exist, three representative setups are compared, namely Mode 1 to 3. Mode 1 is the standard setup used in the reference scenario, hence, all links are available at all aircraft. In Mode 2, aircraft are partitioned into three groups. One third of all aircraft can connect to all links, one third lacks satellite connectivity and one third does not have DA2G equipment. These groups are chosen randomly. While in Mode 2, each aircraft has A2A capabilities, these are limited in Mode 3. Therefore, in Mode 3 aircraft are partitioned similar to Mode 2, but additionally, only one third of all aircraft can connect to A2A. The aircraft having A2A capabilities are also chosen randomly.

The results are presented in Table 4.9. In high-aircraft-density times, Mode 1 and 2 can provide the maximum throughput. However, with Mode 3, the achievable throughput reduces by 84% in the Urban Europe scenario and by 100% in the Iberia scenario. This is due to the massively reduced link options with many aircraft being only able to connect to satellite or DA2G. In this case, if one satellite beam or DA2G cell is congested, additional traffic cannot be provided via other links. In the case of Iberia, the achievable throughput is zero due to aircraft with only DA2G option outside the coverage of a BS. In the low density scenario, this is even more critical, as there are already fewer options available. As a conclusion, reduced aircraft capabilities limit the available link options and therefore the achievable throughput. Hence, for an effective throughput allocation, a sufficient number of link options needs to be available.

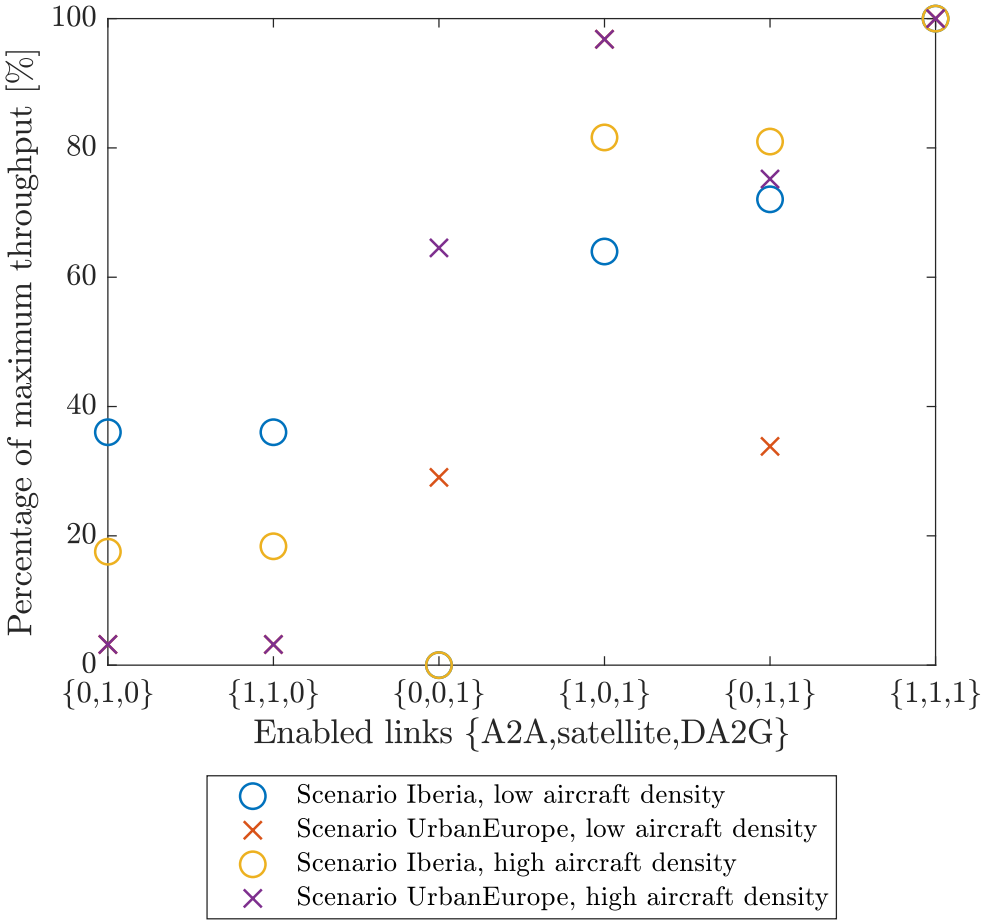

Figure 4.10: Different link options for high and low aircraft density in Urban Europe and Iberia scenarios.

Table 4.9: Achievable throughput for different aircraft capabilities for two scenarios at low and high aircraft density in percent of the maximum throughput.

Density	Capability mode	Iberia	Urban Europe
low	1	100%	100%
low	2	68%	41.9%
low	3	56.7%	6.4%
high	1	100%	100%
high	2	100%	100%
high	3	0%	16%

Distance

The maximum link distance for A2A and DA2G influences the available link options. With a high link distance many link options are enabled but achieving a high throughput is challenging from the physical layer and hardware perspective. Therefore, the link distance should be as small as possible to ease practical implementation. In this setup, the link distance is varied from 50 km to 350 km for DA2G and 100 km to 700 km for A2A. The results are presented in Figure 4.11. From the figure it becomes evident that in the high-aircraft-density case, the link distance has only a marginal impact on the throughput. However, during low-aircraft-density times, distance matters. The achievable throughput decreases by 30% or more. Hence, if only high-density-times need to be covered, small link distances are sufficient. This relaxes the physical layer and hardware requirements. Hence, a tradeoff between connectivity at low and high-aircraft-density times is necessary. Nevertheless, the absolute capacity in the low-aircraft-density case for Iberia is 52.5 Mbps, which is significantly higher than the absolute capacity of 36.3 Mbps in the high-aircraft-density case. Therefore, the link distances, as defined in the reference scenario, can be relaxed.

Link penalty

The penalty of a link determines the probability that the link is chosen in the optimal topology. A higher penalty decreases this probability. The penalty of DA2G, satellite and A2A links is varied from the default of 1 to 1.01, 1.1 and 2. The results for the values of 1 and 1.01 and low aircraft density are presented in Table 4.10. The other values show a similar behavior. It can be seen that increasing DA2G penalty impacts the throughput most while A2A penalty has no impact. For the Iberia scenario, the satellite link penalty has a higher impact compared with the Urban Europe scenario.

As A2A penalty does not show any influence for penalty of up to two, the study is extended for penalty up to 100. The results for low aircraft density are presented in Table 4.11. The results for high aircraft density are similar. It is evident that there is no influence for A2A penalty equal or smaller than five. As the penalty is implemented by restricting the available

Table 4.10: Achievable throughput for different link penalties for two scenarios at low aircraft density in percent of the maximum throughput.

DA2G penalty	A2A penalty	SAT penalty	Iberia	Urban Europe
1	1	1	100%	100%
1.01	1	1	99.2%	99%
1	1.01	1	100%	100%
1	1	1.01	99.8%	99.9%

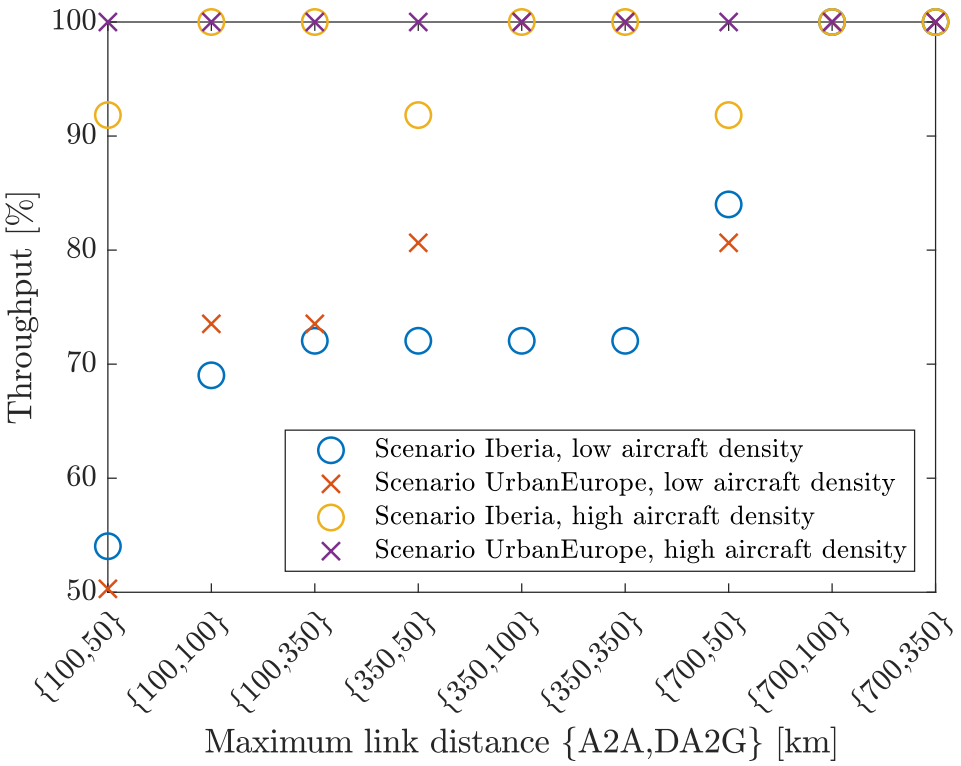

Figure 4.11: Different link distances for high and low aircraft density in Urban Europe and Iberia scenarios.

capacity, this result shows that one fifth of the A2A capacity is sufficient. This is the case, as only a part of the DA2G and satellite capacity is forwarded via A2A links. Therefore, a lower capacity compared with DA2G and satellite is sufficient for A2A links. Hence, the link budget for A2A links can be relaxed.

Interference

Interference can occur between multiple A2A links and decreases the available capacity. To study the influence, interference is enabled and disabled. In the two studied scenarios, no difference is observed with or without interference. This is in alignment with the result of the A2A penalty variation. Even if interference occurs, enough A2A capacity is available. The difference between enabling and disabling interference is the link choice for the final topology. When disabling interference, any link can be chosen. Additionally, due to the large node distance compared with connectivity on the ground, interference is not the limiting factor. Nevertheless, with more limited A2A capacity, interference might play a role depending on the specific case.

Capacity

The capacity of the DA2G and satellite links is the most important factor for the achievable throughput per aircraft. The influence of the link capacity is studied with capacity values of 100 Mbps, 500 Mbps and 1000 Mbps for both, DA2G and satellite links. The results for high aircraft density are presented in Table 4.12. The capacity scales directly, if both, DA2G and satellite capacities are increased by the same amount. The scaling is indirect if only one link capacity is increased. The reason is that the achievable throughput is the sum of the individual link throughput. Therefore, only this part is increased, while the other part is stable. In both scenarios, an increase of the DA2G capacity has a higher increase on the achievable throughput than the same increase of the satellite capacity. This is due to a larger part of the

Table 4.11: Achievable throughput for different A2A link penalties for two scenarios at low aircraft density in percent of the maximum throughput.

A2A penalty	Iberia	Urban Europe
1	100%	100%
2	100%	100%
5	100%	100%
10	91.2%	68.7%
25	79.7%	47.8%
100	74%	37.3%

throughput coming from DA2G. As a conclusion, more capacity on the DA2G and satellite links can successfully be distributed to the aircraft.

4.2.3 DA2G and A2A link only

This section studies the special setup with DA2G and A2A links but without the satellite. This setup is investigated for the North Atlantic scenario. The goal is to study to which extent oceanic regions can be supported without the satellite link. This would potentially enable cheap high-throughput connectivity. In this section, the primary objective is the threshold objective. This objective ensures that a certain throughput can be guaranteed. Therefore, even with many aircraft and a limited overall capacity, all connected aircraft receive a minimum performance which would not be the case for the max-min objective. Hence, an aircraft might be disconnected at a certain time, but receives the minimum performance once it is able to reconnect. Therefore, the main metric is the percentage of connected aircraft given a threshold throughput. Nevertheless, to provide a comparison with the complete A2G setup, the max-min objective is determined as well. As the overall DA2G capacity is crucial in this case, the backhaul is considered unlimited in this section, in contrast to the defined reference scenario.

As presented in [P2], different parameters variations are investigated. "This includes the maximum number of connections per aircraft, i.e. the nodal degree $D_n = (3, 10)$, the beamwidth $\psi = (10°, 40°)$ and the maximum steering angle $\theta = (45°, 90°)$ as defined in Section 3.1.4. Additionally, being the most interesting parameter, we evaluate the variation of the threshold β between 50 Mbps and 150 Mbps with respect to the maximum capacity of a single beam in a BS of 187 Mbps as defined in Section 3.1.1. We define the reference scenario with $D_n = 3$, $\psi = 10°$ and $\theta = 90°$. The results of this optimization problem provide a benchmark of the achievable throughput for A2A."

Table 4.12: Achievable throughput for different link capacities for two scenarios at high aircraft density in percent of the maximum throughput.

DA2G capacity	SAT capacity	Iberia	Urban Europe
100 Mbps	100 Mbps	10%	10%
500 Mbps	100 Mbps	35.7%	47.7%
1000 Mbps	100 Mbps	58%	94.3%
100 Mbps	500 Mbps	21.8%	12.3%
500 Mbps	500 Mbps	50%	50%
1000 Mbps	500 Mbps	85.2%	97.1%
100 Mbps	1000 Mbps	36.6%	15.2%
500 Mbps	1000 Mbps	40.1%	52.9%
1000 Mbps	1000 Mbps	100%	100%

"In order to understand the impact of different threshold values, we analyze the calculated optimal topologies. Figure 4.12 shows them for the reference scenario for the snapshot at 22:30 UTC. The full topology, taking into account all possible connections between aircraft based on LOS distance, is depicted in Figure 4.12a. It can be seen that at this time instant significantly more aircraft are located close to the American side. The reason lies in the time difference between Europe and America, as in America it is 18:30 EDT. Nevertheless, we can observe that connectivity between America and Europe via aircraft is in principle feasible at this snapshot" [P2].

"As the number of maximum connections per aircraft is limited, this topology has to be reduced to meet the maximum nodal degree. Figure 4.12b - 4.12d shows the resulting topologies after algorithm execution. Due to the threshold constraint, not all aircraft are able to connect depending on their achievable data rate. These aircraft are represented by red dots, whereas connected aircraft are depicted in green. Even in this low density snapshot, the network spans from America to Iceland in the 50 and 100 Mbps case. For high density time instances, we expect an even more distributed topology. Furthermore, we observe that with increasing threshold the number of aircraft being able to connect decreases. In the 150 Mbps case, most of the aircraft without DA2G connection cannot be served" [P2].

As shown in [P2], "this can also be observed in Figure 4.13. It shows the distance distribution from the closest BS for all connected aircraft in all snapshots. In the case of 150 Mbps threshold, the distance is mostly below 350 km, which is within the reach of DA2G. With a threshold of 50 Mbps, the maximum distance increases to 1600 km, which corresponds to an aircraft close to the middle of the ocean. However, it should be noted that in the low density cases investigated here, many aircraft are located close to the mainland as seen in Figure 4.12. Therefore, the median distance from BSs is rather low and is expected to increase for higher density snapshots. Hence, the limitation for the distance from the BSs here is the snapshot topology."

"Depending on the defined threshold, the percentage of aircraft able to connect is varying. This can be seen in Figure 4.14 which shows the percentage of connected aircraft for different thresholds for all snapshots. It should be noted that the connection can change over time for a specific aircraft, e.g. when leaving the continent. With a threshold of 50 Mbps, however, most aircraft can be connected. The connectivity decreases with increasing threshold. With more aircraft having to share the same throughput provided by the ground network, the percentage of connected aircraft will decrease as less capacity is available in the network. Hence, for higher density snapshots we expect these values to decrease" [P2].

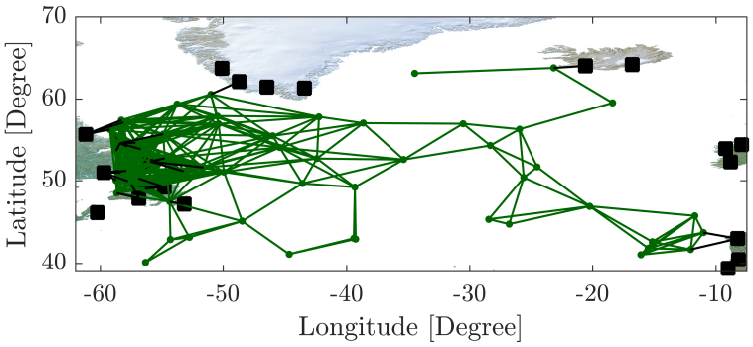

(a) Initial topology

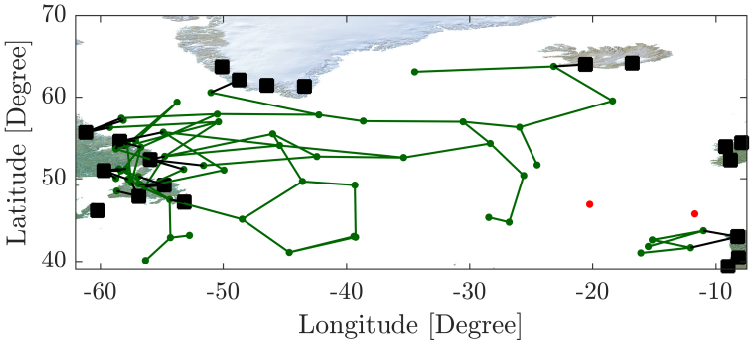

(b) $\beta = 50$ Mbps

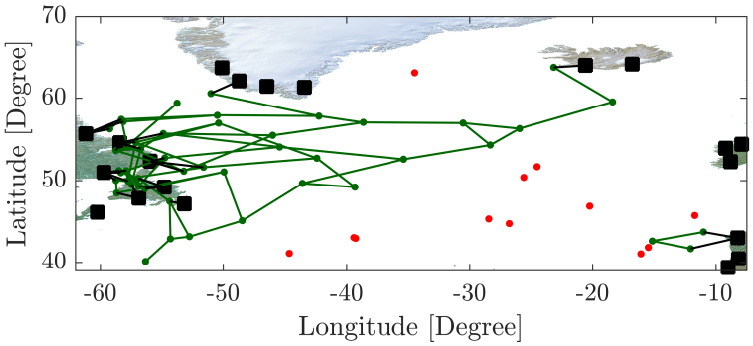

(c) $\beta = 100$ Mbps

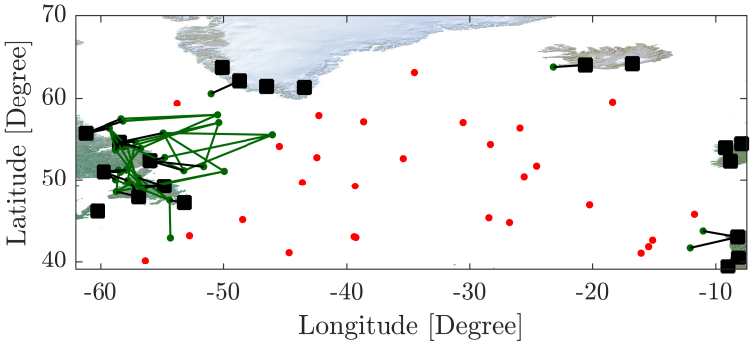

(d) $\beta = 150$ Mbps

Figure 4.12: Optimal aircraft topologies in the North Atlantic scenario for one time snapshot. Green aircraft are connected, red aircraft are unconnected [P2] ©2019 IEEE.

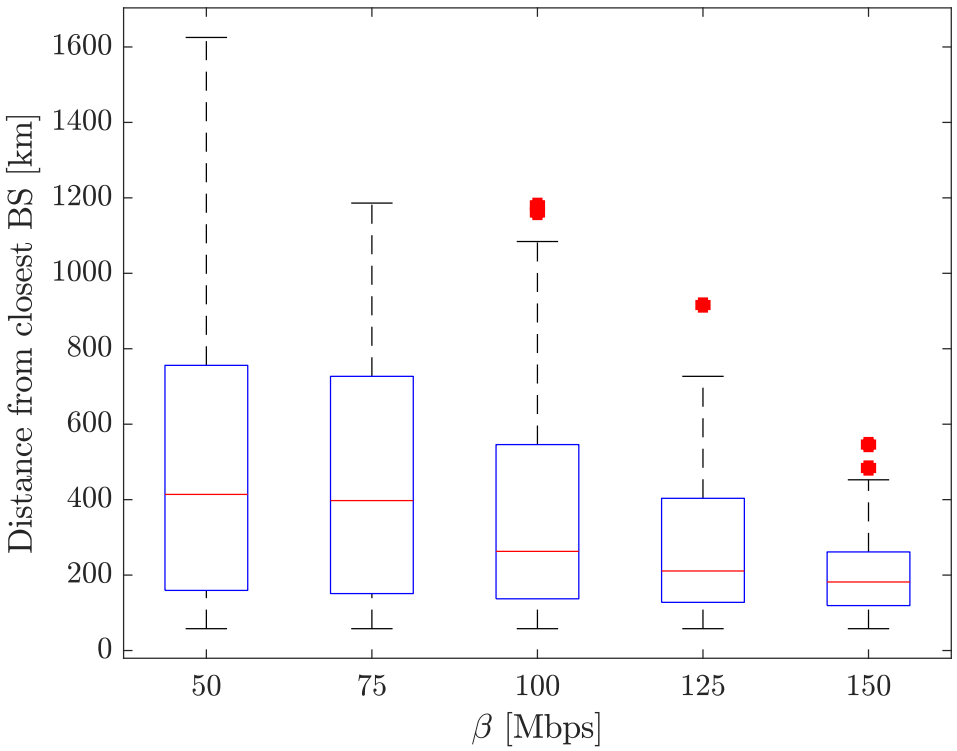

Figure 4.13: Distance between connected aircraft and the nearest BS [P2] ©2019 IEEE.

In [P2], "we analyze the impact of parameter changes with respect to their impact on the percentage of connected aircraft. In Figure 4.15, we can clearly distinguish between scenarios with $\theta = 90°$ and $\theta = 45°$. The parameter with the second highest impact is the maximum number of connections, as higher nodal degree leads to higher connectivity. Hence, the antenna placement and capabilities show the biggest impact on the possible network connectivity. With proper antenna placement, the percentage of connected aircraft can improve significantly. The same applies to the number of antennas, defining the maximum nodal degree. The beamwidth is the least important parameter. In general the impact of different parameters decreases with threshold value increasing to 150 Mbps. This is due to more DA2G connectivity as shown above."

To compare the two objectives, the reference scenario has also been analyzed using the max-min objective. The scenario settings are chosen similar to the other objective. In order to further analyze the effect of parameters limiting the overall capacity, limited backhaul and BS diversity are varied as well. The result is presented in Figure 4.16. Firstly, it is visible that at 23:00, the max-min throughput is zero. This is due to one aircraft not being able to connect to neither A2A nor DA2G. In general, the case of unlimited backhaul provides a higher throughput as aircraft connected to the same BS do not need to share their capacity. There

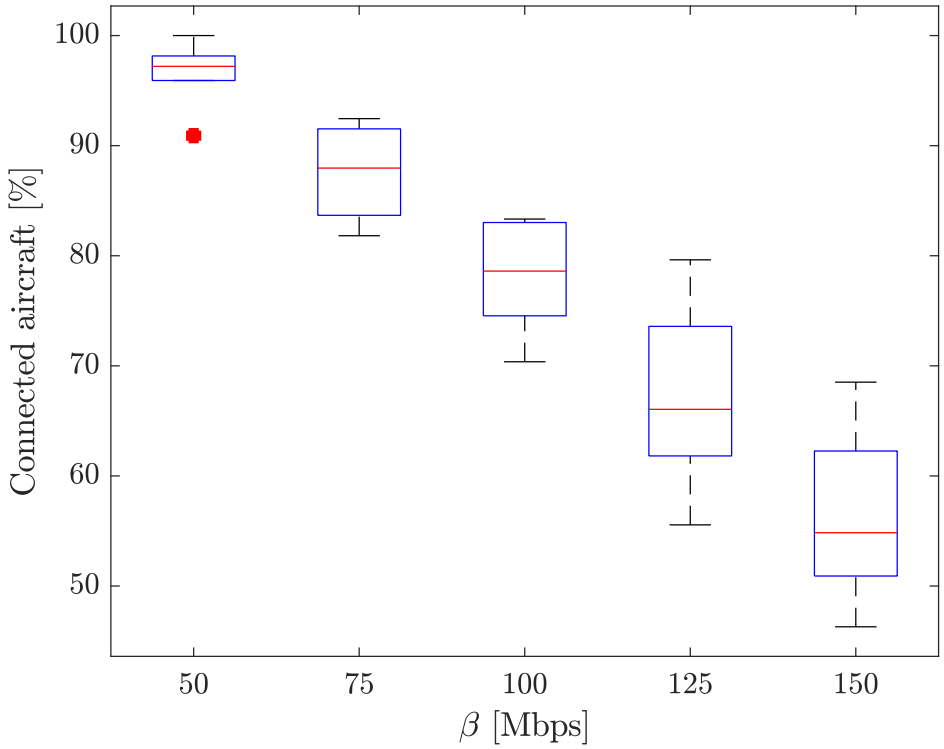

Figure 4.14: Relation between the percentage of connected aircraft and the threshold β [P2] ©2019 IEEE.

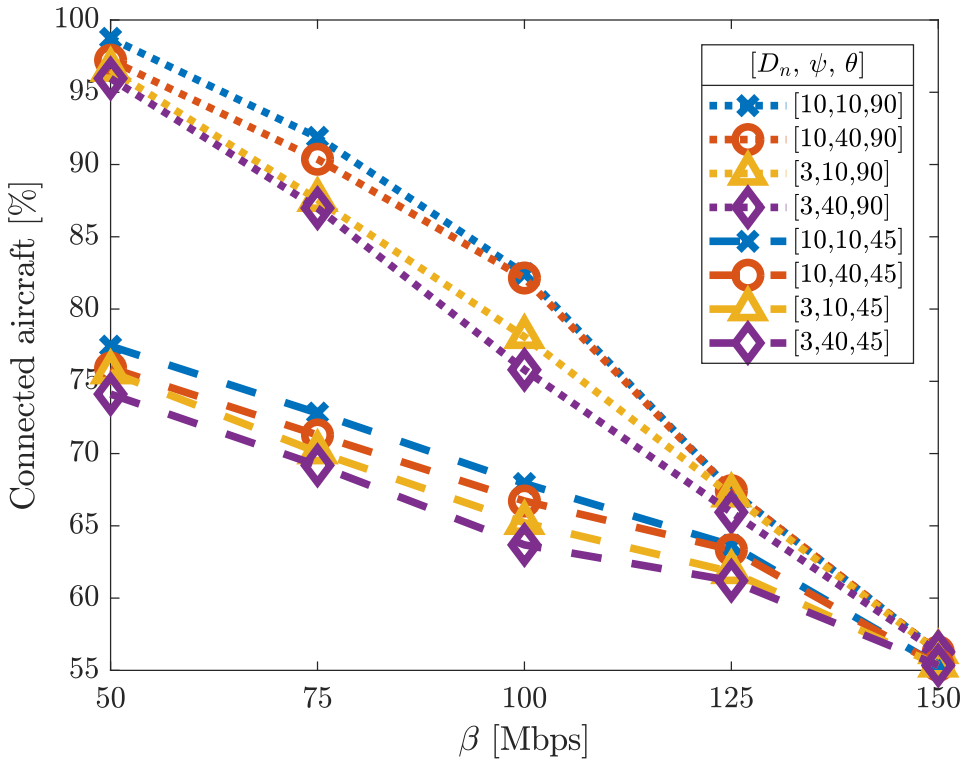

Figure 4.15: Influence of nodal degree D_n, beamwidth ψ, steering angle θ and threshold β on the percentage of connected aircraft. [P2] ©2019 IEEE.

is no improvement at time 23:15 as in this case all aircraft are already connected to different BSs. This is expected to change for higher aircraft densities. At the other time instants, the throughput decreases significantly with limited backhaul. If the backhaul is limited, BS diversity is beneficial, as it allows a better distribution of aircraft among BSs.

4.2.4 Satellite link only

Today, in-flight internet connectivity mostly depends on satellite, especially for long-haul flights, where DA2G is unavailable. Hence, the satellite link only setup can be used as a reference for single link performance today. In this case, solving the optimization problem is simplified. The optimal throughput can be determined by distributing the aircraft among the available satellite operators. Hence, the capacity directly depends on the number of aircraft. Figure 4.17 shows the throughput over time for the different scenarios. The North Atlantic scenario has a higher throughput than the other scenarios. This is due to the low aircraft density over the ocean compared with the continent. With a low aircraft density, fewer aircraft have to share the capacity within one satellite beam. Additionally, the shape of the throughput over time differs in the North Atlantic scenario. Due to limitations to start and land at night, there are two peaks of aircraft over the Atlantic, flying from Europe to the US and in the opposite direction. The shape of the other scenarios is determined by night and day, as during night the number of aircraft decreases. In terms of the throughput, Iberia and Italy show very similar values due to their similarity in terms of aircraft density as they include a part of the ocean. Rural US also has a similar aircraft density, and therefore throughput, but the maximum values are shifted due to the time shift. The aircraft density for the other three scenarios is higher, therefore the throughput is smaller. The minimum throughput per scenario can be found in Table 4.13. In case of additional LEO satellite links as introduced in Section 3.1.1, this throughput increases by a factor of 5 – 7, depending on the scenario. Even in this case, the resulting throughput for most scenarios is low compared with the combined A2G network. In general the throughput for the satellite only case is low due to the limited satellite capacity compared with the number of aircraft per area, but future satellites might provide a significantly higher capacity.

4.3 Conclusion

The optimal throughput allocation for A2G networks is studied. The results show that the combined A2G network, consisting of DA2G, A2A and satellite links, is able to provide a high throughput to all aircraft by using the different types of links. The combination of the networks provides an improved performance compared with the separate networks. The study

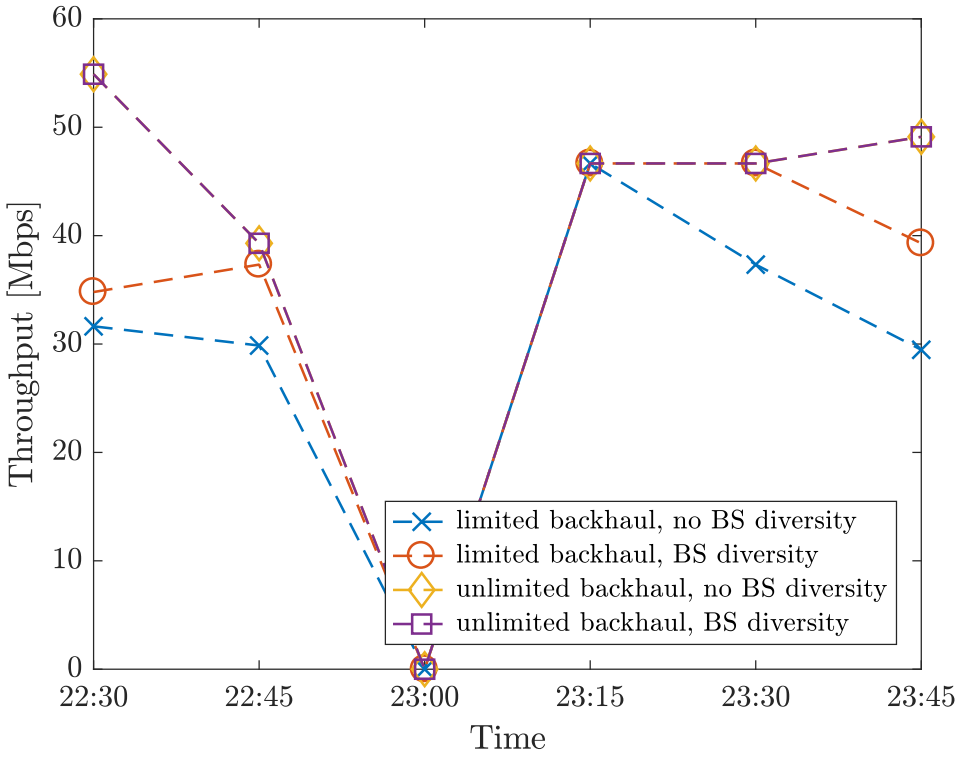

Figure 4.16: Max-min throughput for the North Atlantic scenario with variation of backhaul and BS diversity.

Table 4.13: Minimum throughput during one day for different scenarios with satellite links only.

Scenario	Minimum Throughput [Mbps]
Rural US	4.1636
Urban US	0.9346
Rural Europe	0.7325
Urban Europe	0.4281
Italy	4.1158
Iberia	4.3789
North Atlantic	24.926

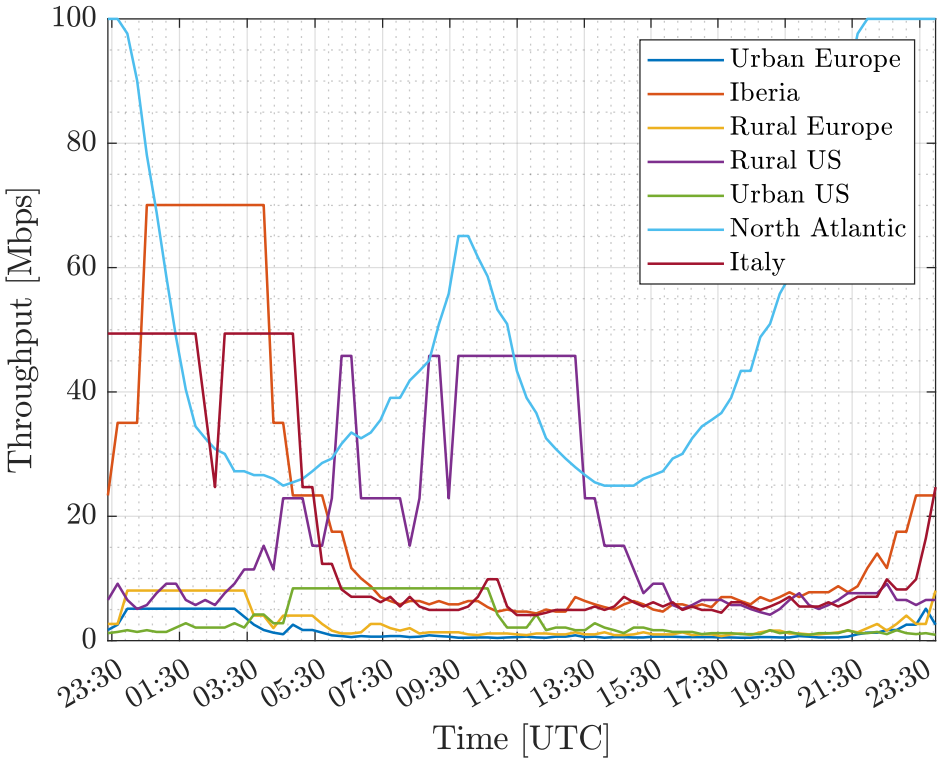

Figure 4.17: Throughput over time with satellite links only for different scenarios.

is conducted for six representative geographic areas, including continental and oceanic areas as well as high and low aircraft density. It is shown that the limitation of the achievable aircraft throughput lies in the capacity of the DA2G and satellite links. The DA2G network can provide 20 Mbps during high aircraft density in the reference scenario including LEO, while the capacity provided by the satellites is limited to 4 Mbps, cf. [P3]. DA2G can provide a higher throughput than the satellite due to the smaller DA2G cells compared with the satellite beams. Therefore, to improve the capacity, it is essential to reuse the available frequency to a large extent. One option is using separate beams per aircraft. This is modeled as unlimited backhaul and improves the minimum throughput by a factor of 13 in the reference scenario. Moreover, it is shown that the capacity can be distributed optimally to all aircraft as long as the network contains a sufficient number of aircraft. Additionally, there is a degree of freedom in how to achieve the optimal throughput. Even if some aircraft are unable to connect to DA2G or satellite, the optimal throughput can still be achieved. It is also shown that A2A links are least relevant when DA2G coverage is available, especially if the aircraft is able to connect to multiple BSs. In this case, single-hop A2A connectivity is sufficient. This simplifies the network architecture, as traffic can be restricted to single-hop relaying. Nevertheless, in areas without DA2G coverage, A2A can play a considerable role. Another relevant parameter influencing the throughput is the time of the flight. While the lowest through-

put in the reference scenario is 14.39 Mbps during high aircraft density, it increases up to 191.78 Mbps during low aircraft density, cf. [P3]. As the number of aircraft in the air cannot be influenced, it is critical to improve the throughput per aircraft during high-aircraft-density times. The comparison of the two objectives shows that they offer two different angles to the problem. While the max-min objective aims at connecting all aircraft, the throughput objective guarantees a minimum performance instead. Both objectives work well while being more suitable to specific types of scenarios.

Besides the unlimited backhaul, many other parameters influence the achievable throughput per aircraft. This includes antenna parameters, available links per aircraft and in general, maximum link distance, link penalty and link capacity. To quantify the influence on the throughput by each of these parameters, a parameter variation is conducted. It is shown that the assumed hardware parameters can be relaxed by using a reduced A2A capacity and A2A and DA2G link distance. It is shown that one fifth of the A2A capacity is still sufficient in the reference scenario. The maximum A2A and DA2G link distance can also be relaxed when focusing on the high-aircraft-density times. This is a tradeoff with the connectivity in low-aircraft-density times, but the absolute throughput during low-aircraft-density times is still higher. With this relaxation in A2A capacity, the link budget, as stated in Section 3.1.3, can be relaxed by 20 dB. If the A2A link distance is reduced from 700 km to 221 km, another 10 dB can be reduced. This can be reflected in the antenna power and gain, leading to lower cost and smaller hardware. The variation of aircraft capabilities showed that it is crucial to have a sufficient number of link options per aircraft. Some aircraft without specific link types can easily be covered. However, if the number of aircraft limited by only one link option is too high, an even distribution of capacity becomes infeasible.

The geographic area highly influences the air traffic. Continental airspaces are highly occupied and aircraft are passing in many different directions. Over the ocean, there are fewer aircraft following specific routes. Additionally, the ocean is lacking DA2G coverage. Therefore, the oceanic scenario is investigated separately. Additionally, this study investigates, if oceanic connectivity can also be provided without satellite connectivity using only A2A relay from DA2G. The investigated geographic scenario is the north Atlantic corridor, which is the busiest oceanic airspace. The analysis is restricted to low-aircraft-density times due the number of aircraft at peak times is larger than the optimization is able to solve. It is shown that even without the satellite, a high throughput can be provided to aircraft. The threshold objective is best applicable to this scenario, as some aircraft will are unable to connect to any link due to the very low aircraft density. Therefore, the max-min objective results in zero throughput, while the threshold objective guarantees a minimum throughput to connected aircraft. The analysis shows that most aircraft can be connected with a threshold of 50 Mbps, cf. [P2]. This throughput is high, given that no satellite is used. However, it relies on unlim-

ited backhaul of the DA2G network. Additionally, the percentage of connected aircraft with 50 Mbps is assumed to drop during high density times. In this setup, even aircraft far away from the coastline can be connected with high throughput. In this special case, however, high A2A capacity is needed, in contrast to the result described above. Hence, A2A and DA2G can be an alternative for connecting aircraft over the ocean, especially if aircraft follow the same tracks with a small distance. However, DA2G capacity needs to be high, as many aircraft will be connected. Satellites can provide additional capacity. Especially, LEO constellations become interesting for this case due to their reduced beam size and high promised capacities compared with GEO satellites.

To understand the role of satellites in the A2G network, the satellite only scenario is also investigated. The result shows that the satellite only throughput is low, as many aircraft need to share the capacity in large spot beams. Hence, satellite spot beam sizes need to be reduced and become more flexible, which is an ongoing effort by the satellite operators. Nevertheless, GEO satellites are limited by the huge distance from the Earth, so small spot beams can only be supported by LEO constellations. Therefore, there is limited capacity per satellite for all aircraft today, but as only a part of all aircraft are connected today, the achievable throughput is acceptable. With an increase in satellite capacity, more aircraft can be supported, but for an optimal throughput, the full A2G network needs to be used.

As a conclusion, for a high achievable throughput per aircraft, it is important to include high-throughput satellites and DA2G networks into the A2G network. These networks need to provide a high throughput per aircraft, ideally without needing to share capacity between aircraft. The achievable throughput per aircraft is far below the 1.2 Gbps per aircraft as stated by [5]. This can only be achieved with highly improved DA2G and satellite networks. Most importantly, the networks need to have more spectrum available, as high spectral efficiencies are hard to achieve over the long distances present in A2G networks. Additionally, the achievable throughput during the flight mostly depends on the time of day, and therefore the achievable throughput during high-aircraft-density times needs to be improved primarily. Optimal parameters depend on the specific scenario. Nevertheless, it is critical that enough aircraft have multi-link connectivity to ensure a sufficient number of link options. If there is flexibility, as for instance by beam steering by the satellite, areas with high and low aircraft density can balance their throughput. To study this, larger geographic areas need to be taken into account. As this is infeasible for an optimal solver, a heuristic algorithm is developed in Chapter 5.

5 Distributed aircraft throughput allocation

To enable A2G throughput allocation in large areas, a heuristic algorithm is developed. As a centralized solution is infeasible for the large A2G network, the heuristic algorithm is executed distributedly. Additionally, weighted throughput allocation is introduced. This enables an improved throughput allocation depending on the aircraft demands. Firstly, the distributed A2G load balancing concept is introduced as well as the distributed A2G network model. Then, the procedures of the heuristic algorithm are detailed. Subsequently, the implementation and parameter setup is stated. Finally, the results of the distributed A2G throughput allocation are analyzed.

Parts of the content in this chapter have been published by the author in the following paper:

- "Distributed Resource Allocation and Load Balancing in Air-to-Ground Networks" [P4]

5.1 Distributed A2G load balancing concept

The optimal throughput allocation, as presented in Chapter 4, provides a benchmark on the optimal throughput that can be achieved per aircraft. However, the optimal solution is limited by the number of aircraft per scenario, which allows small scenarios only. Furthermore, the optimal solution relies on a centralized execution. This means that the throughput allocation needs to be performed by a central entity with full knowledge of the A2G network. This is unrealistic as the A2G network is large. Therefore, a distributed heuristic algorithm is developed to overcome these shortcomings of the optimal throughput allocation. The goal of the algorithm remains unchanged, which is to fairly distribute the throughput among all aircraft and to achieve a smoother throughput during the flight. As the distributed through-

put allocation primarily needs to balance the load between different BSs, it is also called load balancing algorithm.

In addition, the fairness measure for throughput allocation is refined. In Chapter 4, the same throughput is allocated for each aircraft. However, small aircraft with a low number of passengers have a different demand compared with large aircraft. Therefore, an additional weight w_a is defined per aircraft. The weight defines, how the throughput should be partitioned among different aircraft. This factor can be defined based on different parameters, such as number of passengers, number of active flows or size of the aircraft. This allows a fair throughput allocation based on the needs of all users, cf. [P4].

The A2G architecture has been presented in Section 2.2. Figure 5.1 refines the A2G architecture in terms of placement of the load balancing execution and the interconnections between BSs and core. For the distributed load balancing, a 5G network is assumed. The candidate network solutions as discussed in Section 2.2.2 are assumed to be implemented in this network. Hence, as presented in Figure 5.1, the satellite network is integrated into the 5G core network via non-3GPP access. Moreover, the BSs can connect to their neighbor BSs. The results in Chapter 4 show that for continental scenarios, one-hop A2A links are sufficient. Therefore, the number of A2A hops is limited to one. This can be implemented via D2D user equipment (UE) to network relay. To achieve the maximum throughput for all aircraft, all available links are utilized. Additionally, ATSSS can be used to control the available throughput over different links such that the throughput becomes usable. As presented in Figure 5.1, two different load balancing mechanisms are executed for satellites and DA2G. This is due to the different coverage areas. A BS covers a specific area with a small overlap to neighboring BSs. A satellite, however, covers a large area, including many BSs at once. Therefore, a different setup for the load balancing algorithms is necessary, cf. [P4].

DA2G load balancing is primarily based on the comparison of the loads of neighboring BSs and the own load. If the own load is higher than the neighbor loads, load balancing is triggered. The algorithm determines an aircraft a_h which needs to be handed over to a neighbor BS b_h. Then a handover request is sent to the other BS. In order to find the optimal aircraft and BS for handover, a few additional parameters need to be available at the BS. These parameters are position, heading and weight of each connected aircraft, positions of neighboring BSs and the current load data of all neighboring BSs, cf. [P4].

The load of the neighbor BSs can be obtained via the interfaces defined by 3GPP [161]. To find the best aircraft for handover, besides load information, the geographical position of the aircraft and neighbor BS is consulted as well. An aircraft is only handed over to a BS in the direction of its heading. This reduces the number of handovers, as it minimizes

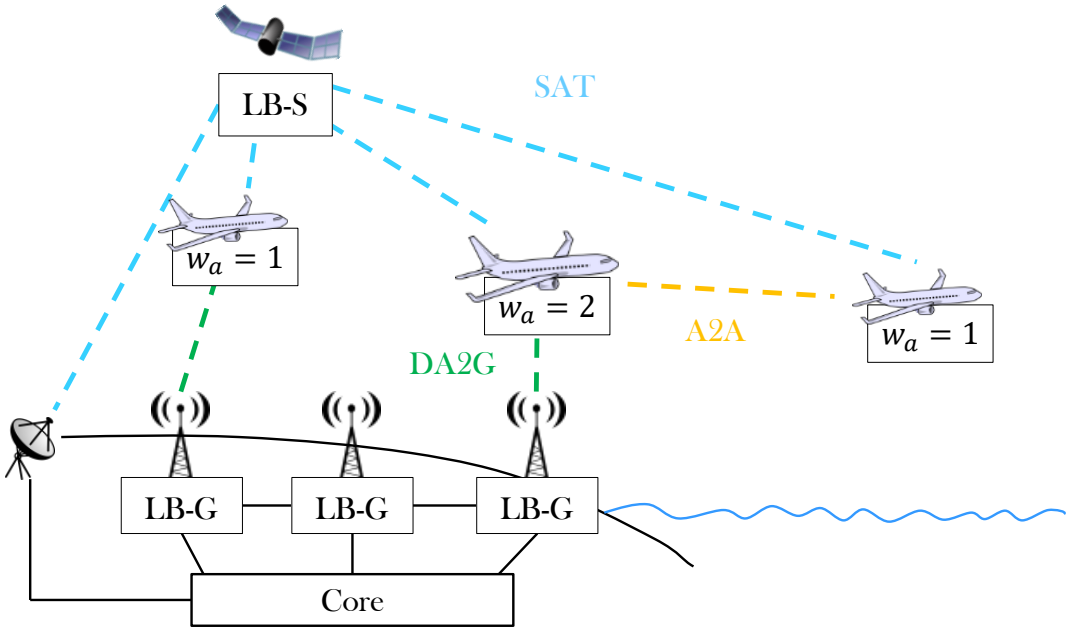

Figure 5.1: A2G load balancing architecture with load balancing ground (LB-G) algorithm at the BSs and load balancing satellite (LB-S) algorithm at the satellite [P4].

the probability that the aircraft flies out of coverage of the new BS in a short time. Positions and heading of users are normally unknown to the BS. For aircraft, multiple options to retrieve the positions and heading exist. The first option is to use ADS-B data, which the aircraft broadcasts regularly. An ADS-B receiver could be integrated into each BS to obtain the positions and heading of aircraft in reach. Another option is to use the signal information for positioning the UE. Different available positioning protocols are available in cellular networks [175]. These protocols can be based on cellular network parameters as well as on separate systems such as global navigation satellite system (GNSS). Lastly, the aircraft weight is needed. Different implementations are possible, depending on the parameter the weight is based on. Aircraft size information can also be retrieved from the ADS-B data. The number of active users could be estimated from the number of flows on the link. The load balancing algorithm is executed separately on each BS. Due to a low number of link changes within one minute, as shown in Section 5.5, it can be executed in intervals of one minute. If one BS receives multiple simultaneous handover requests, only the first one will be processed, cf. [P4].

The satellite load balancing is based on the throughput of all aircraft in the coverage area of the satellite. Aircraft with a low throughput receive a higher share of the satellite capacity than aircraft with a high throughput. The information about the current throughput per aircraft is obtained by querying all connected aircraft. This is done separately by each operator, as different operators are unable to balance load among them. As aircraft are distributed over different satellite operators, with more aircraft connecting to operators with higher capacity, it is assumed that the load is automatically balanced among operators, cf. [P4].

5.2 Distributed A2G model

The distributed A2G model is based on the A2G model presented in Chapter 3. The problem formulation is identical. However, to model the distributed heuristic algorithms, the model needs to be adjusted.

The heuristic algorithms define the load of a BS and a satellite. Load can be characterized in multiple ways. Depending on the physical layer implementation, load can be defined in terms of resource blocks, time slots, or similar. The A2G model is defined independently from specific implementations. Therefore, the model defines load in terms of the maximum capacity that can be provided by a BS or satellite. For instance, a satellite which can provide up to 100 Mbps to all users, is half loaded with 50 Mbps, cf. [P4].

Multiple satellite operators offer services to aircraft. An airline connects to one of the available operators. Since, different satellite networks are operated separately, load balancing among them is infeasible. Hence, it is assumed that each operator is executing the load balancing separately. It is also assumed that aircraft will be distributed among the operators, hence a balanced load is feasible even under multi-operator conditions. Therefore, the model includes only one satellite which offers the combined overall capacity of all operators. Only one combined satellite operator is modeled in contrast to six separate operators as defined in Chapter 3. Additionally, it is assumed that all aircraft with satellite capabilities are always connected to the satellite, even though they receive no capacity at a specific point in time. This allows aircraft to be queried for their current load status as described in Section 5.1, cf. [P4].

5.3 Heuristic algorithm

Algorithms 1 and 2 state the procedures for DA2G and satellite load balancing, respectively. As presented in Figure 5.1, Algorithm 1 describes the DA2G load balancing LB-G executed at each BS and Algorithm 2 defines satellite load balancing LB-S executed at the satellite. At each time instant, both algorithms are executed. The computational complexity is $O(N^2)$, with N being the number of aircraft. However, the complexity is limited by the number of aircraft flying within the coverage area, cf. [P4].

Algorithm 1 starts with updating the load information of the neighbor BSs l_b. This function uses 4G-based procedures defined in [161] and is denoted as *updateNeighborLoads*. In the next step, the difference between the own load and the neighbor loads Δl is calculated.

Algorithm 1 load balancing ground (LB-G) [P4].

Input:
connected aircraft $a \in A$ including p_a, h_a, w_a
neighbor BSs $b \in B$ including p_b, l_b
own parameters l_o, d_o
for $t \in T$ **do**
  l_b = updateNeighborLoads(b)
  $\Delta l = l_o - l_b$
  w_{min} = min(w_a)
  while max(Δl) $> 2 \cdot w_{min}$ **and** ($d \neq \overrightarrow{0}$ **or** first iteration) **do**
    for $a_i \in A$ **do**
      for $b_j \in B$ **do**
        if a_i can connect to b_j **then**
          $d_{a_i b_j}$ = calculateDirections(p_{a_i}, h_{a_i}, p_{b_j})
          remove $d_{a_i b_j}$ with $d_{a_i b_j} > d_o$
          $d = d \cup d_{a_i b_j}$
          $l_{e_{ij}} = |\Delta l_j - 2 \cdot w_a|$ with $a_i, b_j \in d$
          $l_e = l_e \cup l_{e_{ij}}$
        end if
      end for
    end for
    if $d \neq \overrightarrow{0}$ **then**
      r_l, r_d= rank(l_e, d)
      a_h, b_h = selectHandover(min(r_l+r_d))
      initiateHandover(a_h, b_h)
      update Δl, w_{min}
    end if
  end while
end for

Algorithm 2 load balancing satellite (LB-S) [P4].

Input:
connected aircraft $a \in A$ including l_a, w_a
own parameters l_o, c_o
for $t \in T$ **do**
  l_a, w_a = updateAircraftThroughput(a)
  $l_{des} = (\sum(l_a) + c_o) / \sum(w_a)$
  $l_e = l_{des} \cdot w_a - l_a$
  while min(l_e)< 0 **do**
    fix $l_e(l_e < 0) = 0$
    $l_{des} = (\sum(l_a) + c_o) / \sum(w_a) \quad \forall a$ where $l_e \neq 0$
    $l_e = l_{des} \cdot w_a - l_a \quad \forall a$ where $l_e \neq 0$
  end while
  implementLoadDistribution(l_e)
end for

Furthermore, the minimum weight of all connected aircraft, w_{min}, is determined. The next step is to determine the necessity of load balancing. The condition is that the maximum load difference to a neighbor BS, max(Δl)), exceeds twice the smallest aircraft weight. This means, that at least one aircraft with the smallest weight can be moved to another BS, while the new load of the other BS remains smaller or equal than the new load of the current BS. The factor of two originates from the absolute difference of removing an aircraft at one BS and adding it to another one. As the load balancing condition can be true for multiple aircraft and BS combinations, the preferred combination needs to be determined. This functionality is provided by *calculateDirections*. For this, the heading of the aircraft with respect to the neighbor BS is taken into account. The variable d is calculated for all aircraft and BS combinations and denotes the difference between the heading of the aircraft and the direction toward the neighbor BS. This angle ranges from 0 to 180 degrees, with 180 degrees corresponding to an aircraft flying away from a BS. Aircraft should only be moved to BSs with a smaller angle than the current BS, to avoid frequent reconnection. Therefore, aircraft and BS combinations with a larger angle than the current one are removed from d. Besides the angle, the aircraft weight is also taken into consideration. The effect of moving an aircraft with a large weight compared with a small weight is different. It should be avoided to move aircraft with large weights if the load difference between two BSs is small. Therefore, the estimated new load difference l_e for each aircraft-BS combination is calculated. To decide, which aircraft to move, directions d and estimated load l_e variables are ranked. The best, i.e. smallest, rank is given for the smallest angle and smallest estimated new load difference, respectively. The function *selectHandover* selects the aircraft-BS combination to be moved, which corresponds to the smallest sum of both ranks r_l and r_d. After moving the selected aircraft, the load difference Δl and the minimum weight w_{min} are updated. The procedure is repeated until no more aircraft can be moved according to the load balancing condition, cf. [P4].

The satellite load balancing procedure as described in Algorithm 2 follows a different approach. This is due to the large satellite footprint, covering multiple BSs simultaneously. The first step is to update the current throughput of all connected aircraft l_a. This function is called *updateAircraftThroughput*. Subsequently, the satellite calculates the desired throughput per aircraft l_{des}, which is the sum of the throughput of the connected aircraft l_a and the satellite capacity c_o divided by the sum of aircraft weights. The next step is to determine the estimated difference between the current aircraft throughput and the ideal throughput l_{des} per aircraft, l_e. The variable l_e is smaller than zero, if aircraft already receive a higher throughput than desired. Hence, these aircraft will not receive any satellite throughput. Instead, the remaining capacity is distributed to the other aircraft. After the satellite load distribution l_e is fixed for each aircraft, the satellite implements the desired distribution in *implementLoadDistribution*, cf. [P4].

5.4 Implementation and parameter setup

In this section, the implementation setup and the selected parameters are described. This includes model implementation, flight traces, geographic scenario setup and the reference parameters setup.

5.4.1 Model implementation

The algorithms have been implemented in Matlab and executed on an Intel(R) Xeon(R) Gold 6134 CPU with 16 cores and 265 GB RAM. The input files are prepared in the same way as in the optimal case. Hence, the same input files can be used for the optimal solver as well as for the heuristic algorithm. Due to implementation reasons, the load balancing on each BS is implemented subsequently in contrary to the definition in the model. Nevertheless, the evaluation of the number of aircraft change requests per BS and time instant shows that the number of requests is low. The probability of zero or one change request per BS and time instant is 93.7%, as presented in Table 5.1. Hence, the probability of a collision of change requests is low. In case of a collision, only the first request would be processed. Therefore, a subsequent implementation is feasible, cf. [P4].

5.4.2 Flight traces, base station positions and satellite operators

The flight trace used in this chapter is the day dataset with one minute intervals as described in Section 4.1.2. The BS positions are equal to the optimal setup described in Section 4.1.3. Hence, the positions of EAN BSs are used in Europe and the GoGo network is assumed for north America. The satellite operators are combined to one substitute operator as described in Section 5.2, cf. [P4].

5.4.3 Geographic scenario setup

As the heuristic algorithm enables larger geographic scenarios than the optimal solution, two new scenarios are defined. Their geographic boundaries are shown in Figure 5.2. The first scenario is Central Europe, which includes the central part of Europe as well as a part of

Table 5.1: Number of aircraft change requests at each BS and time instant.

Number Requests	0	1	2	3	>3
Percentage	84.8%	8.9%	1.9%	1.3%	3.1%

the Atlantic ocean. The second scenario is Continental US, which covers north America. The parameters of both scenarios are presented in Table 5.2. Additionally, the Urban Europe scenario as defined in Section 4.1.4 is used to compare the optimal and heuristic solution, cf. [P4].

5.4.4 Weights

While the reference scenario includes equal weights per aircraft, a weighted scenario is also investigated. There are many options to implement weights as discussed in Section 5.1, therefore, one example implementation is investigated here to prove the effectiveness of the concept. The implemented weights are based on the wake turbulence category of the aircraft. The wake turbulence category is defined by the ICAO and is based on the maximum take-off weight of the aircraft. Four categories are defined, which are light, medium, heavy and super. This criteria is used here, as it scales with the size of the aircraft and provides a higher throughput to large aircraft. The resulting weights, i.e. the share of the throughput with weights, are defined to 0.05 for light aircraft, 1 for medium aircraft, 2 for heavy aircraft and 3 for super aircraft. While the weights are chosen to reflect the number of passengers in each category, this is solely an exemplary parameter setup, cf. [P4].

5.4.5 Reference parameters setup

The reference scenario is similar to the optimal reference scenario presented in Section 4.1.5 with three exceptions. Firstly, for the geographic scenario, Central Europe is used as a reference, reflecting the larger area that can be covered. Secondly, the satellite capacity is 6×100 Mbps, which represents the combined satellite operator. Thirdly, interference is disabled, as by limiting the number of A2A hops to one, the probability of interference is low. The resulting reference parameters setup is specified in Table 5.3, cf. [P4].

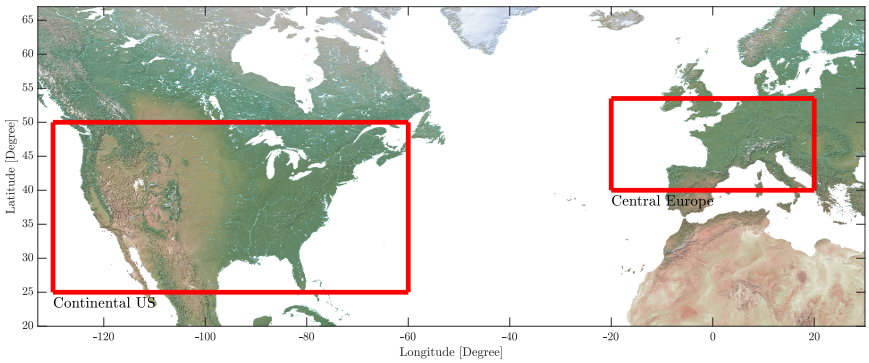

Figure 5.2: Geographic area of the heuristic scenarios.

Table 5.2: Overview on heuristic geographic scenario parameters.

Scenario	Latitude [Deg]	Longitude [Deg]	Area [km^2]
Central Europe	40 - 53.5	-20 - 20	5082000
Continental US	25 - 50	-130 - (-60)	19361000

5.5 Results

This section presents the results of the distributed A2G load balancing implementation. Firstly, the two geographic scenarios are studied. This includes the number of changes per BS, the number of aircraft as well as weight distribution and execution time. Subsequently, the result of the heuristic is compared with the optimal solution as described in Chapter 4. Lastly, the load balancing results for the two scenarios are evaluated.

5.5.1 Scenario analysis

As aircraft are moving, multiple handovers between DA2G BSs are necessary during a flight. As introduced in Section 5.2, the load balancing algorithms are executed once per minute. To validate this time interval, the number of link changes between two time instants is analyzed. The cumulative distribution function of this relation for both geographic scenarios is presented in Figure 5.3. Link changes are defined as aircraft entering or leaving the scenario area or handovers between BSs due to aircraft movement. For the Central Europe scenario in 95.6% of all time instants there is up to one change per BS and time instant, as depicted in Figure 5.3. In the Continental US scenario, this number decreases slightly to 87%. The difference is due to the different aircraft and BS density. In the Continental US scenario, more aircraft are distributed among fewer BSs. Hence, the probability of two aircraft leaving the BS at the same time increases. Nevertheless, the number of changes per time instant is low in both scenarios. Hence, one minute time intervals are feasible, cf. [P4].

The number of aircraft in each scenario is depicted in Figure 5.4. The number of aircraft in the Central Europe scenario varies between 53 aircraft during the night and 1388 aircraft during the day. In the Continental US scenario, more aircraft are present, i.e. 398 aircraft during the night and 2816 aircraft during the day. The increased number of aircraft in the Continental US scenario is due to the larger geographic area. Additionally, Figure 5.4 clearly shows the time shift between the two continents, as the minimum values are shifted by approximately eight hours, cf. [P4].

Table 5.3: Reference parameters setup heuristic.

Parameter	Value
scenario	Central Europe
link distance	A2A: 700 km, DA2G: 350 km, satellite: n/a
link capacity	A2A: 187 Mbps, DA2G: 187 Mbps, satellite: 6×100 Mbps
link setup	A2A: on, DA2G: on, satellite: GEO on, LEO off
equipped aircraft	all aircraft, all available links
weights	all aircraft equal weights
penalty	A2A: 1, DA2G: 1, satellite: 1
interference	off
BS diversity	on
limited backhaul	on
nodal degree D_n	A2A: 3, DA2G: 1, satellite: 1
steering angle θ	A2A: 90, DA2G: n/a, satellite: n/a
beamwidth ψ	A2A: 10, DA2G: n/a, satellite: n/a

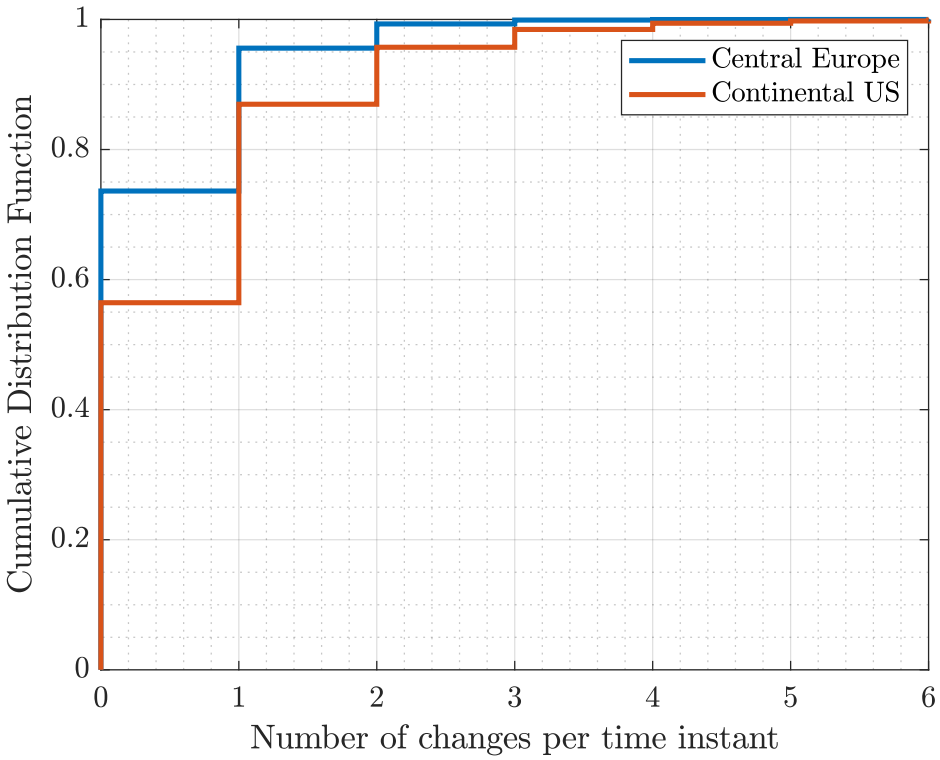

Figure 5.3: Distribution of the number of link changes per BS per time instant.

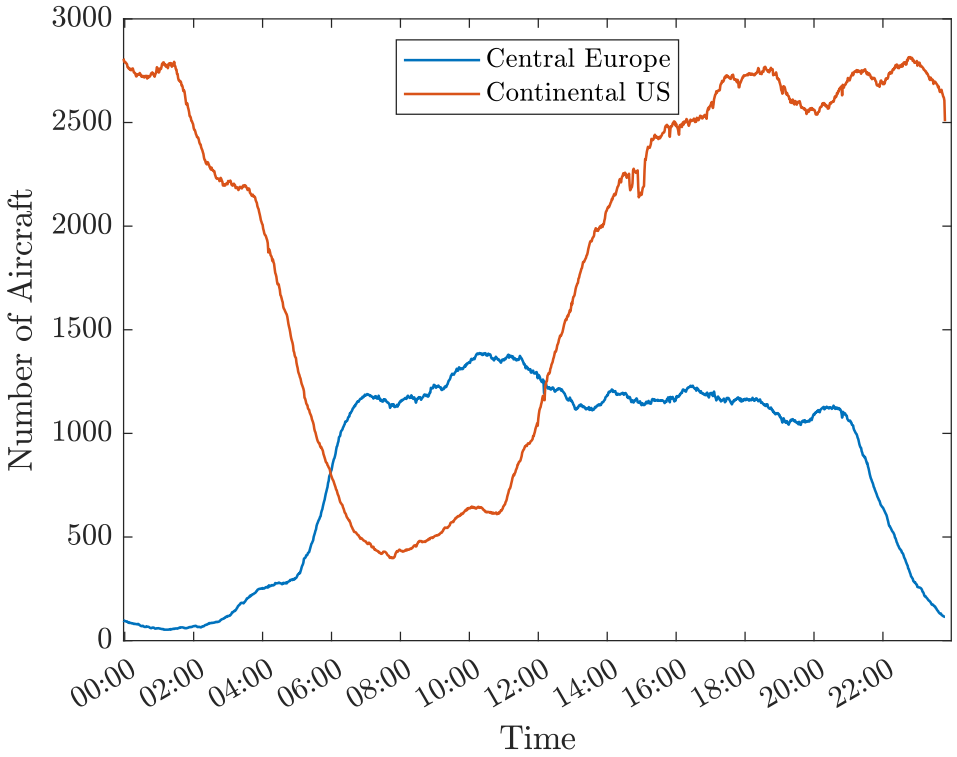

Figure 5.4: Number aircraft for continental US and central Europe scenarios.

In Section 5.4.4, aircraft are separated into four groups of light, medium, heavy and super aircraft. In the Central Europe scenario, 85.6% of all aircraft are medium aircraft. The second largest group are heavy aircraft, which are 13.2% of all aircraft. Super and light aircraft are the smallest groups with 0.9% and 0.3%, respectively. This is reasonable for a continental scenario, as most flights are short-haul flights. For the Continental US scenario, the groups are are similar. The largest group are medium aircraft with 84.1%, while 10.1% are heavy aircraft, 0.2% super aircraft and 5.6% light aircraft. Compared with the Continental Europe scenario, the percentage of light aircraft is increased, cf. [P4].

Lastly, the algorithm execution time is studied. The execution times for the Central Europe scenario are presented in Figure 5.5. The figure depicts the median and maximum calculation times per BS and time instant. The median times can be up to 6 milliseconds, while the maximum time is 0.6 seconds. In the Continental US scenario, the execution times are slightly higher, as more aircraft are connected per BS. Hence, the median times can be up to 0.6 seconds with a maximum time of 8.9 seconds. Compared with the one minute time intervals, the execution times are small. Hence, the load balancing algorithms can easily be computed once every minute. Multiple changes per minute could be handled as well, cf. [P4].

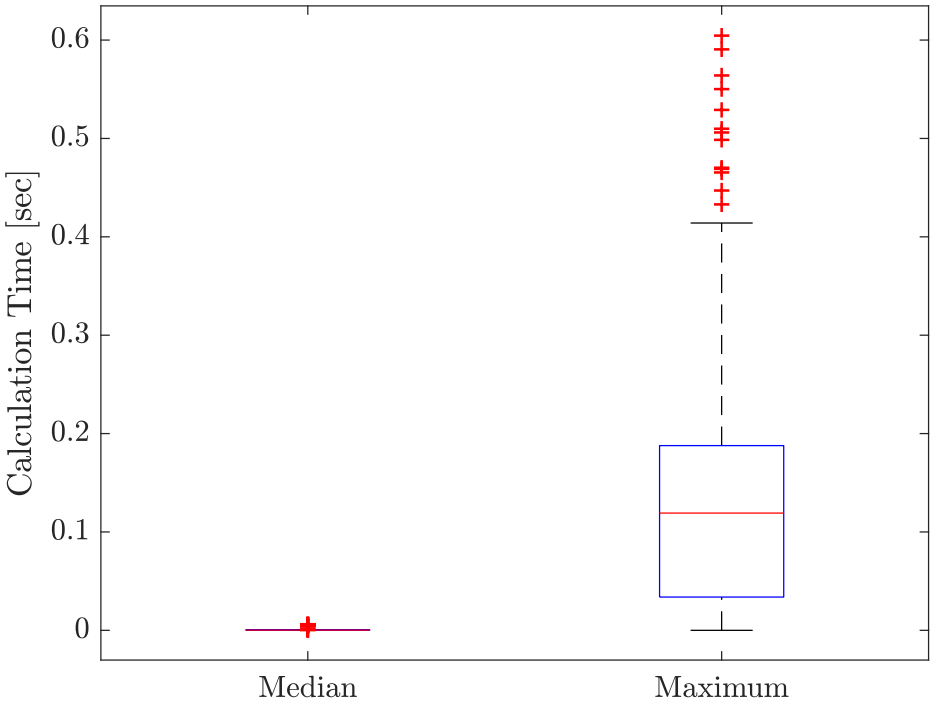

Figure 5.5: Algorithm execution times per BS and time instant in the reference scenario.

5.5.2 Comparison with optimal solution

In order to compare the results of the heuristic and the optimal solution, both have been executed using the same parameter setup. The scenario is the Urban Europe scenario as defined in Section 4.1.4. All other parameters are based on the heuristic reference scenario as presented in Table 5.3. The difference between the optimal and the heuristic solution in percent is presented in Figure 5.6. It can be seen that there is no difference in 44.4% of the time instants. The large differences occur during the low-aircraft-density times. During high-aircraft-density times between 8:00 and 20:00, the maximum absolute difference is 0.8 Mbps, which is 3.1%. The larger differences during low-aircraft-density times are due to the aircraft allocation as detailed in Section 5.5.3. Therefore, the heuristic algorithm is able to achieve a near optimal throughput allocation. In the following, the heuristic throughput allocation will be studied for the defined large geographic scenarios.

5.5.3 Distributed throughput allocation

This section studies the results for the distributed throughput allocation for the two geographic scenarios. Figure 5.7 presents the load balancing results for the reference scenario.

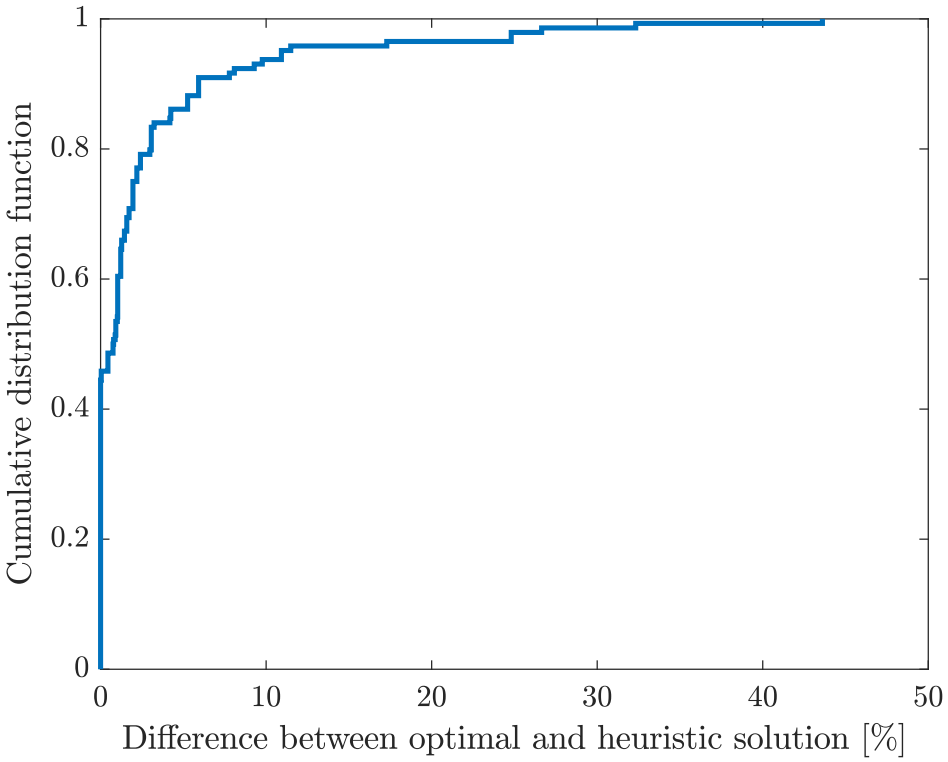

Figure 5.6: Comparison between optimal and heuristic solution.

The performance of the throughput allocation is studied in terms of the max-min throughput per aircraft, as stated in the problem formulation in Section 3.2. The max-min throughput is compared with the mean available throughput per aircraft, which can be stated as $\sum(c_{BS} + c_{sat})/\sum w_a$. If the max-min throughput equals the mean throughput, the capacity is optimally partitioned among all aircraft. Additionally, Figure 5.7 includes the maximum throughput of one single aircraft at each time. The figure shows that the difference between max-min and mean throughput is small during most of the time instants. For times with high aircraft density between 08:00 and 20:00, the difference is up to 1.1 Mbps which is equal to 3.9%. During times with a low aircraft density, the difference increases. This is the case, as the effect of moving one aircraft to another BS is larger with two connected aircraft than with ten connected aircraft. This effect is visible in particular at 4:00, where one part of the BSs is connected to one aircraft (yellow line) and the other part of the BSs is connected to two aircraft (blue line). Since aircraft can only be connected to one BS at a time, the throughput cannot be further improved on the ground. At the same time, the satellite capacity is insufficient to cover this large difference in throughput. However, in these cases the overall throughput is still higher than during the high-aircraft-density times, where 22.9 Mbps to 30.5 Mbps can be provided to each aircraft, cf. [P4].

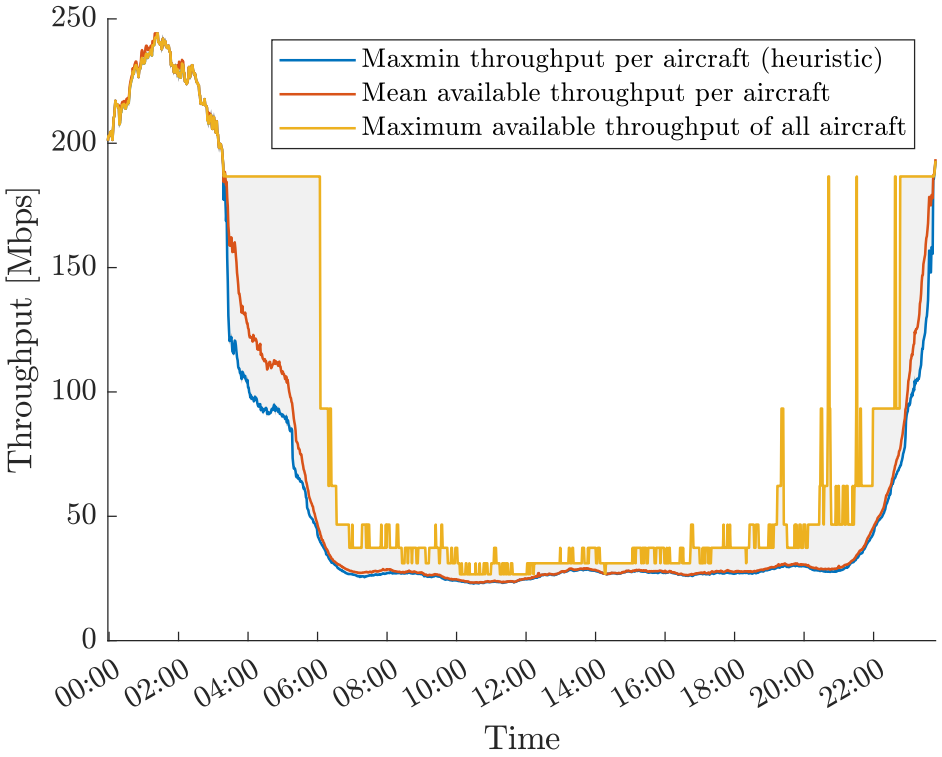

Figure 5.7: Achievable throughput per aircraft for the reference scenario [P4].

The result for the Continental US scenario is presented in Figure 5.8. The results are similar to the Central Europe scenario, except that the high-aircraft-density times are shifted to 16:00 - 4:00 UTC, corresponding to 8:00 - 20:00 Pacific time. In this case, the maximum difference during high-aircraft-density times is 0.45 Mbps, which is lower compared with the Central Europe scenario. With an absolute throughput between 13.81 Mbps and 19.73 Mbps, the achievable throughput is also lower. However, the result is close to the mean throughput during most times of the day. Hence, it can be concluded that the heuristic algorithm is properly distributing the capacity among the aircraft. Compared with the optimal solution in Table 4.6, the throughput of the reference scenario slightly increased compared with the small European scenarios. For the Continental US scenario, the achievable throughput lies between the urban and rural US scenarios. Hence, the available capacity can be successfully transferred from low demand areas to high demand areas, cf. [P4].

One factor for the performance of the algorithm is the freedom in choosing A2G links. In particular, this is influenced by the inter-site distance between BSs and the maximum communication distances of DA2G and A2A. These relations are studied in Table 5.4. The maximum throughput difference during high-aircraft-density times is compared with different maximum communication distances. It can be seen that the throughput difference in-

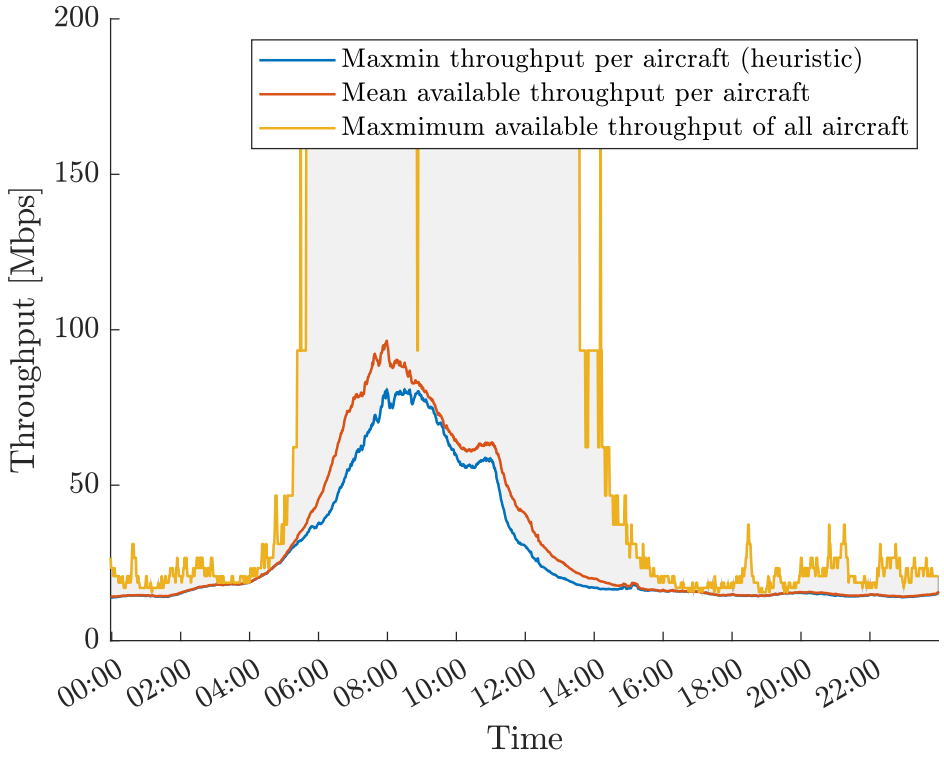

Figure 5.8: Throughput per aircraft without weights in the continental US scenario.

creases with decreasing DA2G distance. When decreasing the DA2G distance from 350 km to 100 km, the difference increases from 1.1% to 12.56%. This is due to a decreasing number of handover options. Nevertheless, decreasing the maximum A2A distance yields an insignificant throughput difference. This relation is also found in the results of the optimal solution in Section 4.2.2, i.e. during high-aircraft-density times, short range A2A links are sufficient, cf. [P4].

Figure 5.9 presents the results using weights. It can be seen that the throughput is distributed proportionally according to the weights. This also holds for the difference between the mean and the max-min throughput. Compared with the previous results without weights

Table 5.4: Maximum difference in throughput during high-aircraft-density times in terms of DA2G and A2A maximum communication distance (extended version from [P4]).

Throughput diff. [Mbps]		DA2G distance [km]				
		100	150	200	250	350
A2A distance [km]	100	12.56	7.65	4.4	2.95	1.01
	350	11.63	7.29	4.46	2.86	1.07
	700	10.85	7.42	4.46	2.84	1.1

in Figure 5.7, the throughput during high-aircraft-density times for $w_a = 1$ decreased from 28 Mbps to 18.9 Mbps. This result is expected, as a higher throughput needs to be provided for large weights. Nevertheless, the difference in throughput is small, as 85.6% of the aircraft belong to $w_a = 1$. The advantage of introducing weights is to provide a fair throughput allocation with respect to the aircraft size, i.e. the number of users. However, during low-aircraft-density times, the throughput cannot be ideally distributed according to the weights. For instance at 2:00, the throughput for aircraft with $w_a = 1$ is even higher than expected. The reason is that aircraft which are alone in one cell receive the full cell throughput, which is higher than the weighted throughput. Nevertheless, during low-aircraft-density times, the throughput is comparatively high for all aircraft. Hence, a non-optimal distribution can be tolerated. During high-aircraft-density times, where a fair throughput allocation is critical, this can be achieved as presented in Figure 5.9, cf. [P4].

The result with weighted throughput allocation for the Continental US scenario is depicted in Figure 5.10. Also in this scenario, the throughput can be distributed well among aircraft with different weights. The drop for $w_a = 3$ between 10:00 and 12:00 is due to aircraft of this type being absent at that time. Also the weight factors of 0.05, 1,2 and 3 are clearly visible, as aircraft with $w_a = 3$ (purple line) receive three times the throughput of aircraft with $w_a = 1$ (red line). Therefore, introducing weights efficiently distributes the throughput among the different groups. Nevertheless, the factors implemented in this analysis are exemplary and other weights such as per passenger or per flow can be implemented as well. As a conclusion, introducing weights enables fair throughput allocation on a per user basis compared with per aircraft. The ideal values for the weights need to be determined depending on a specific implementation, cf. [P4].

5.6 Conclusion

This chapter introduces the distributed A2G load balancing concept. It is based on the A2G resource allocation problem as stated in Section 3.2 using a distributed approach. Instead of the need of having a centralized view of the network, the procedures can be executed distributedly on each BS and satellite. The proposed A2G network is based on a 5G network architecture. The 5G network already includes features such as ATSSS, non-3GPP access and D2D, which enable the implementation of the distributed A2G load balancing concept. A heuristic algorithm is developed to execute the load balancing among BSs and satellites.

The results show that the distributed load balancing concept is feasible and performs well. Especially during high-aircraft-density times, the achievable throughput is close to the optimal solution. The high-aircraft-density times are the most challenging times of the day, as a

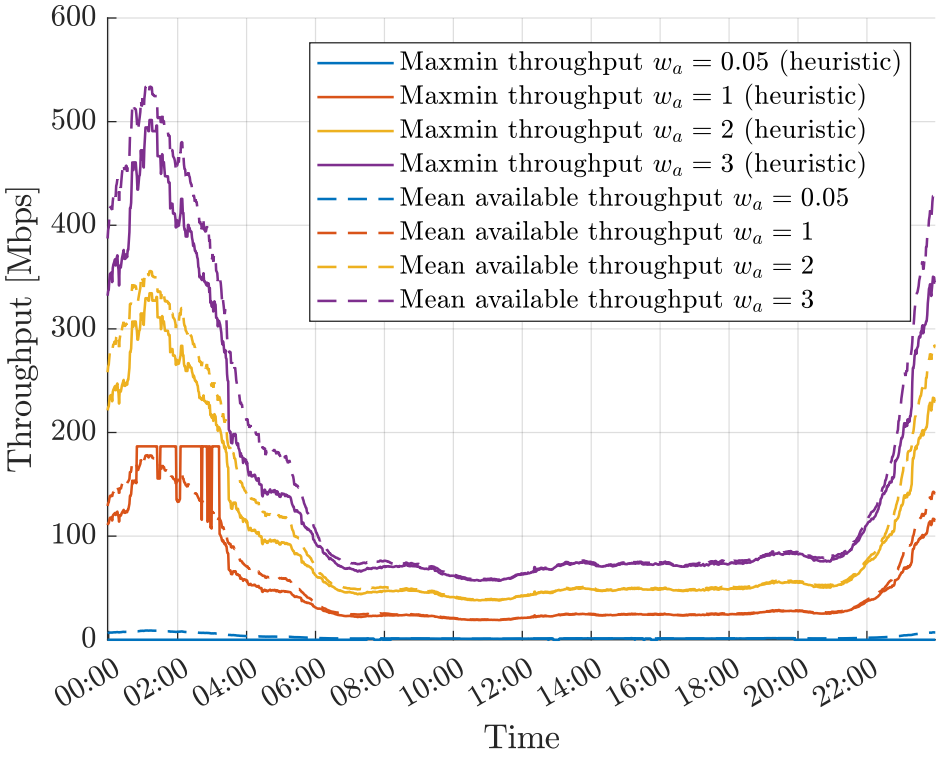

Figure 5.9: Achievable throughput per aircraft in the reference scenario using weighted throughput allocation [P4].

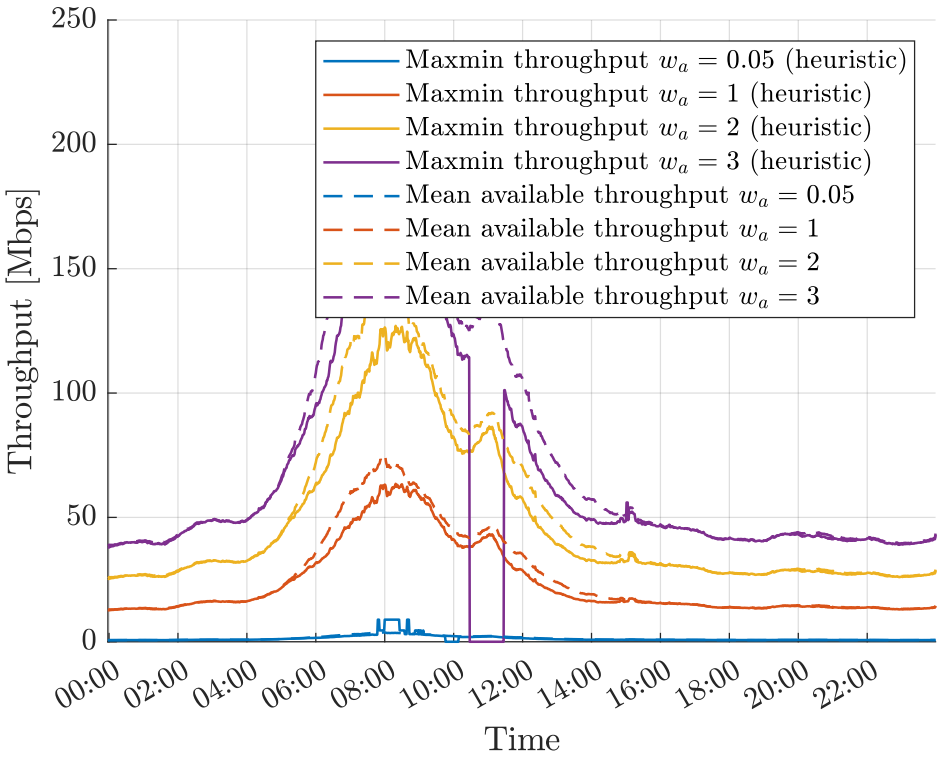

Figure 5.10: Achievable throughput per aircraft in the continental US scenario using weighted throughput allocation.

large number of aircraft demand connectivity simultaneously. For the reference scenario, the throughput during high density times is between 22.9 Mbps and 30.5 Mbps, which is slightly higher than the optimal throughput in the small European scenarios investigated in Chapter 4. Hence, the throughput can be successfully distributed over the increased area. The maximum difference to the mean throughput is only 1.1 Mbps. Additionally, in comparison with the optimal reference scenario, the differences are marginal during high-aircraft-density times. However, in low-aircraft-density times, the heuristic result performs worse, as the link options are more limited. Nevertheless, the absolute throughput during these times is still the highest one during the day, therefore a non-optimal solution is also sufficient.

The heuristic algorithm also enables to study large regions. In the study, time instants with up to 2816 aircraft were calculated, and it is also feasible to increase this number further. The limit in terms of calculation time is the input topology calculation. Additionally, for very large scenarios, spanning over multiple continents, separated DA2G and satellite networks need to be taken into account. It is unreasonable that an aircraft flying over one continent shares the capacity with an aircraft flying over a different continent. Hence, the maximum size of a scenario needs to be limited to areas that are connected to each other. Therefore, the size of the studied European and American scenarios can be used as a reference.

Additionally, the concept includes a weighted approach to the throughput allocation. The share of throughput provided to an aircraft depends on the weight assigned to this aircraft. The implementation assumes an aircraft size based approach, as large aircraft include more users than small aircraft. The result of the weighting approach shows that the throughput can be successfully distributed based on the predefined weights. While one specific weight setup is tested, other parameters for weights, such as number of passengers or number of flows are also feasible. The applicability depends on the specific implementation of the A2G network. The introduction of weights enables an even fairer throughput allocation, as the demand of single users can be taken into account.

6 Discussion and conclusion

High-throughput A2G connectivity has been studied in this thesis. The study investigates the achievable multi-link throughput per aircraft, while ensuring a weighted-fair throughput allocation to aircraft. The flight-traces-based throughput analysis presented in Chapter 2 concludes that one A2G network is unable to provide sufficient throughput to all aircraft. It is shown that for a spot size of 200 km, the 95^{th} percentile throughput is 8.33% of the peak throughput. With maximum capacities of 100 Mbps, as stated in Chapter 1, this is clearly insufficient. Moreover, it is shown that the separate A2G links have limitations in terms of coverage for DA2G and in terms of minimum spot size for satellites. Therefore, an integrated A2G network is proposed and the respective A2G connectivity architecture is detailed. Open challenges and possible solutions are investigated and it is shown that there are existing solutions for the majority of the identified challenges. One remaining challenge is the fair throughput allocation, which is studied in this work.

To study the fair throughput allocation, an A2G model is developed in Chapter 3. The model is based on time snapshots which are extracted from captured flight traces. Additionally, different geographical scenarios can be studied, as the aircraft density highly depends on the region. The model includes various parameters, which are modeled realistically to the largest extent, while staying implementation independent. Therefore, DA2G and satellite link capacities are the primary parameter for providing a high throughput. The problem is formulated as a MILP and includes two objectives, max-min-based and threshold-based. Two solutions are proposed, a centralized optimal solution to obtain a benchmark of the achievable throughput and a distributed heuristic solution.

The centralized optimal solution is introduced in Chapter 4. To obtain a benchmark on the achievable throughput, an extensive parameter study is conducted. This includes different available combinations of A2G links as well as other parameters, such as maximum link distance or capacity. The results show that the achievable throughput is highly limited by the

capacity of the DA2G and satellite links. In the studied reference scenario with 187 Mbps DA2G capacity and 100 Mbps satellite capacity with LEO satellites, the mean throughput per aircraft during high-aircraft-density times is 20 Mbps from DA2G and 4 Mbps from the satellite. Nevertheless, the results show that the available throughput can be optimally distributed among all aircraft, given a sufficient number of aircraft. Additionally, it is shown that single-hop relaying is sufficient over the continent, multi-hop A2A links are only relevant over the ocean. The time of the day is also highly relevant for the achievable throughput. In the reference scenario, the throughput varies between 14.39 Mbps and 191.78 Mbps depending on the time of day. Therefore, high-aircraft-density times are most critical to deliver a high throughput. Moreover, some assumptions of the A2G model, such as the maximum link distance can be relaxed, as the parameter variation shows. Additionally, the influence of the geographic area is presented. For optimal throughput allocation, aircraft need to be able to connect to multiple links.

The presented approach to compute the optimal solution yields two disadvantages. Firstly, it is limited in the number of aircraft that can be present in the scenario. Secondly, a centralized view on the network is necessary, which is unlikely to be available in a deployed network. Therefore, a distributed heuristic is introduced in Chapter 5. The results show that the heuristic provides close-to-optimal results, in particular during high-aircraft-density times. For the extended reference scenario, a minimum of 22.9 Mbps can be provided to all aircraft during high-aircraft-density times. This throughput is slightly higher compared with the small reference scenario. Hence, the throughput can be successfully distributed over a larger area. The possibility to study large regions with several thousands of aircraft enables to study scenarios of the size of a continent. Additionally, the weighted-fair throughput allocation is included into the heuristic algorithm. It is shown that the throughput can be successfully distributed according to the weight. Hence, using weights, fairness can also be adapted to some aircraft obtaining a higher throughput than others.

The achievable throughput during high-aircraft-density times is low compared with the requirement of 1.2 Gbps stated by NGMN [5]. Therefore, the A2G throughput needs to be improved. The throughput of one user is unsteady, in contrast to the assumption of an average throughput as presented here. Each user's throughput is varying with time, due to different packet sizes and the packet intervals. Therefore, a peak in the throughput of one user can meet a minima of another user. Hence, adding 10 users on one link yields an increase in the throughput with a factor smaller than 10. Nevertheless, this is insufficient to achieve a 60-fold increase in throughput from approximately 20 Mbps to 1.2 Gbps. Therefore, other measures have to be implemented. Firstly, the A2G link capacity can be improved. This can be achieved by improving the transmission efficiency, using additional spectrum or using other means of signal transmission. These parameters are already covered by the

presented model. Another mean of signal transmission could be for instance free space optics, which offers significantly higher link capacities in the order of Gbps. This has already been proposed in the related work for AANETs and the satellite links of integrated space-aerial-terrestrial networks. Secondly, the throughput demand could be reduced. This can be achieved by caching a part of the content on-board the aircraft. Smart caching can include mechanisms such as steering users toward cached content or predict popular content to be cached. Additionally, the same content requested by two users should only be sent once via the A2G link. This could also be extended to multiple aircraft. Hence, content could be fetched from other aircraft instead of the ground, as the A2A link is less limited. Moreover, popular content could be broadcasted to multiple aircraft simultaneously. While caching is only applicable to non-real-time traffic, these are also the most demanding services in terms of throughput. Consequently, a smart caching approach could significantly reduce the throughput demand of one aircraft. Thirdly, the obtained throughput also depends on the number of aircraft which are part of the A2G network. While the results in Chapters 4 and 5 are based on current aircraft traces, the effect of an increased or decreased number of aircraft is studied in Chapter 2. The achievable throughput scales inversely with the number of aircraft being part of the network.

The second further research topic is the user-centric view, as introduced in Chapter 2. As the aircraft is a user of the A2G network and contains a network itself, the requirements of the users have to be taken into account. The weight introduced in Chapter 5 ensures that the throughput can be distributed according to the defined weight of the aircraft. As mentioned there, the best parameter for the weight needs to be investigated, which can be for instance aircraft size, number of passengers or number of active flows. Moreover, the presented throughput allocation defines the throughput as a sum of the throughput on the separate links. However, the delay on the different links and the delay requirements of the services differ. Therefore, sufficient throughput could be available while a service is still unable to meet delay requirements. For instance, this can be the case when an aircraft is only connected to a satellite, which is unsuitable for some services due to the high delay as stated in Chapter 1. Furthermore, user behavior is varying, for instance during a long flight some users might be sleeping or users stop their video stream during meals. The user demand also changes with different flight phases and the type of the flight, as for instance passengers on long flights are more likely to watch movies compared with passengers on short flights. Additionally, in the case of insufficient throughput, some services should be prioritized, in particular crew and aircraft services. Consequently, the next step is to extend the study from an aircraft-centric view to a user-centric view. For this, different models need to be developed. Firstly, a user traffic model defines the traffic pattern of the services and the percentage of services among the aircraft users. Secondly, a user activeness model defines the amount of active users at any point in time during the flight depending on the type and duration of the flight. Lastly,

this information needs to be combined for all aircraft in the scenario, to obtain instantaneous throughput demand per aircraft. This result can be combined with the throughput allocation algorithms defined in this thesis. Hence, the instantaneous throughput demand per aircraft can be added as an additional parameter to distribute throughput according to each aircraft demand. However, this requires a transparent on-board network to communicate the aircraft demand.

As a summary, this thesis introduces an A2G network model as well as a centralized optimal and distributed heuristic throughput allocation scheme to study high-throughput connectivity for aircraft. The results quantify the achievable weighted-fair throughput per aircraft and show that the capacity can be fairly distributed among all aircraft. Consequently, a more stable throughput over the flight time can be provided, as the fluctuation between two time instants is small during high-aircraft-density times. During low-aircraft-density times, the achievable throughput is significantly higher due to the low number of aircraft. Using the model, extensive parameters studies have been conducted and the best parameter settings for obtaining a high throughput per aircraft have been presented. Moreover, the available throughput and the optimal link choices can be calculated. Additionally, further research topics have been identified. These are decreasing the throughput demand per link, e.g. by smart caching, and refining the throughput allocation to a per-user basis, to ensure that all requirements of all services are satisfied.

List of Publications

[P1] ©2019 IEEE. Reprinted, with permission, from S. Hofmann, A. E. Garcia, D. Schupke, H. E. Gonzalez, and F. H. P. Fitzek, "Connectivity in the Air: Throughput Analysis of Air-to-Ground Systems," in *IEEE International Conference on Communications (ICC)*. IEEE, May 2019.

[P2] ©2019 IEEE. Reprinted, with permission, from S. Hofmann, V. Megas, M. Ozger, D. Schupke, F. H. P. Fitzek, and C. Cavdar, "Combined Optimal Topology Formation and Rate Allocation for Aircraft to Aircraft Communications," in *IEEE International Conference on Communications (ICC)*. IEEE, May 2019.

[P3] ©2020 IEEE. Reprinted, with permission, from S. Hofmann, D. Schupke, and F. H. P. Fitzek, "Optimal Throughput Allocation in Air-to-Ground Networks," in *IEEE Global Communications Conference (GLOBECOM)*. IEEE, Dec 2020.

[P4] S. Hofmann, D. Schupke, and F. H. P. Fitzek, "Distributed Resource Allocation and Load Balancing in Air-to-Ground Networks," in *18th ACM International Symposium on Mobility Management and Wireless Access (MobiWac'20), November 16–20, 2020, Alicante, Spain*. New York, NY, USA: ACM, Nov 2020. [Online]. Available: https://doi.org/10.1145/3416012.3424635

[P5] S. Hofmann, S. Duhovnikov, and D. Schupke, "Massive Data Transfer from and to Aircraft on Ground: Feasibility and Challenges," *accepted at IEEE Aerospace & Electronics Systems Magazine*, 2021.

[P6] A. Varasteh, S. Hofmann, N. Deric, M. He, D. Schupke, W. Kellerer, and C. M. Machuca, "Mobility-Aware Joint Service Placement and Routing in Space-Air-Ground Integrated Networks," in *IEEE International Conference on Communications (ICC)*. IEEE, May 2019.

[P7] A. Varasteh, S. Hofmann, N. Deric, A. Blenk, D. Schupke, W. Kellerer, and C. M. Machuca, "Toward Optimal Mobility-Aware VM Placement and Routing in Space-Air-Ground Inte-

grated Networks," in *IEEE Conference on Computer Communications Workshops (INFOCOM WKSHPS)*. IEEE, Apr 2019.

[P8] M. Vondra, E. Dinc, M. Prytz, M. Frodigh, D. Schupke, M. Nilson, S. Hofmann, and C. Cavdar, "Performance Study on Seamless DA2GC for Aircraft Passengers Toward 5G," *IEEE Communications Magazine*, vol. 55, no. 11, pp. 194–201, 2017.

[P9] E. Dinc, M. Vondra, S. Hofmann, D. Schupke, M. Prytz, S. Bovelli, M. Frodigh, J. Zander, and C. Cavdar, "In-Flight Broadband Connectivity: Architectures and Business Models for High Capacity Air-to-Ground Communications," *IEEE Communications Magazine*, vol. 55, no. 9, pp. 142–149, 2017.

[P10] V. Megas, S. Hofmann, M. Ozger, D. Schupke, and C. Cavdar, "A Combined Topology Formation and Rate Allocation Algorithm for Aeronautical Ad Hoc Networks," *submitted to IEEE Transactions on Mobile Computing*.

[P11] D. Tomic, S. Hofmann, M. Ozger, D. Schupke, and C. Cavdar, "Quality of Service Aware Traffic Management for Aircraft Communications," in *IEEE 91st Vehicular Technology Conference: VTC2020-Spring*. IEEE, May 2020.

[P12] C. Cavdar, D. Gera, A. Ghosh, S. Hofmann, and A. Nordlöw, "Demonstration of an Integrated 5G Network in an Aircraft Cabin Environment," in *Digital Avionics Systems Conference*, 2018.

[P13] A. Exposito Garcia, S. Hofmann, C. Sous, L. Garcia, A. Baltaci, C. Bach, R. Wellens, D. Gera, D. Schupke, and H. E. Gonzalez, "Performance Evaluation of Network Slicing for Aerial Vehicle Communications," in *IEEE International Conference on Communications Workshops (ICC Workshops)*. IEEE, May 2019.

[P14] A. Exposito Garcia, M. Ozger, A. Baltaci, S. Hofmann, D. Gera, M. Nilson, C. Cavdar, and D. Schupke, "Direct Air to Ground Communications for Flying Vehicles: Measurement and Scaling Study for 5G," in *IEEE 2nd 5G World Forum (5GWF)*. IEEE, Sep 2019.

Bibliography

[1] Cisco, "Cisco Annual Internet Report (2018–2023)," 2020, Accessed: 2020-06-25. [Online]. Available: https://www.cisco.com/c/en/us/solutions/collateral/executive-perspectives/annual-internet-report/white-paper-c11-741490.pdf

[2] International Telecommunication Union, "Minimum requirements related to technical performancefor IMT-2020 radiointerface(s)," International Telecommunication Union, Report ITU-R M.2410-0, 11 2017.

[3] ViaSat, "Fastest In-flight Wi-Fi," Accessed: 2019-11-13. [Online]. Available: https://www.viasat.com/sites/default/files/legacy/EXEDE_InTheAir_Datasheet_011_web_pages.pdf

[4] J. P. Rula, J. Newman, F. E. Bustamante, A. M. Kakhki, and D. Choffnes, "Mile High WiFi: A First Look At In-Flight Internet Connectivity," in *2018 World Wide Web Conference*, 2018.

[5] NGMN Alliance, "5G White Paper," 2015, Accessed: 2020-06-22. [Online]. Available: https://www.ngmn.org/wp-content/uploads/NGMN_5G_White_Paper_V1_0.pdf

[6] Seamless Air Alliance, "Introduction to SR1," 2020, Accessed: 2020-06-25. [Online]. Available: https://www.seamlessalliance.com/wp-content/uploads/SAA-White-Paper-Design-Layout-Final-Spreads.pdf

[7] SITA, "The Future of In-Flight Cellular," 2020, Accessed: 2020-06-25. [Online]. Available: https://www.sitaonair.aero/src/Cabin-Connectivity-Services/Mobile-ONAIR/SITAFORAIRCRAFT_Whitepaper_5G.pdf

[8] Inmarsat, "Global Mobile Broadband," 2012, Accessed: 2019-11-13. [Online]. Available: https://www.itu.int/dms_pub/itu-r/md/12/iturka.band/c/R12-ITURKA.BAND-C-0002!!PDF-E.pdf

[9] "Inmarsat's New Global Broadband Network Hits 330 Mbps in Satellite Speed Tests," 2017, Accessed: 2019-11-13. [Online]. Available: https://gcaptain.com/inmarsats-new-global-broadband-network-hits-330-mbps-during-live-tests/

[10] "Viasat preps big insurance claim for ViaSat-2 antenna anomaly," 2018, Accessed: 2019-11-13. [Online]. Available: https://spacenews.com/viasat-preps-big-insurance-claim-for-viasat-2-antenna-anomaly/

[11] Eutelsat, "Future Satellites," Accessed: 2019-11-13. [Online]. Available: https://www.eutelsat.com/en/satellites/future-launches.html

[12] Thales, "SES and Thales reach record speed and enhanced coverage via integrated GEO/MEO network," 2019, Accessed: 2019-11-13. [Online]. Available: https://www.thalesgroup.com/en/group/journalist/press-release/ses-and-thales-reach-record-speed-and-enhanced-coverage-integrated

[13] E. Kulu, "NewSpace Index," 2019, Accessed: 2019-11-14. [Online]. Available: https://www.newspace.im/

[14] OneWeb, "OneWeb - An Introduction," 2019, Accessed: 2019-11-13. [Online]. Available: https://www.oneweb.world/assets/news/media/OneWeb-Introduction-May2019.pdf

[15] "OneWeb's low-Earth satellites hit 400Mbps and 32ms latency in new test," 2019, Accessed: 2019-11-13. [Online]. Available: https://arstechnica.com/information-technology/2019/07/onewebs-low-earth-satellites-hit-400mbps-and-32ms-latency-in-new-test/

[16] "OneWeb and SatixFy to launch new payload for demand-based targeting," 2020, Accessed: 2020-06-21. [Online]. Available: https://www.getconnected.aero/2020/02/oneweb-satixfy-new-payload/

[17] "Big promise of LEO satellite broadband will require big bucks," 2018, Accessed: 2019-11-13. [Online]. Available: https://www.spaceitbridge.com/big-promise-of-leo-satellite-broadband-will-require-big-bucks.htm

[18] "Musk's satellite project testing encrypted internet with military planes," 2019, Accessed: 2019-11-13. [Online]. Available: https://www.reuters.com/article/us-spacex-starlink-airforce/musks-satellite-project-testing-encrypted-internet-with-military-planes-idUSKBN1X12KM

[19] "Press Release: ThinKom phased array tested over Telesat LEO satellite," 2019, Accessed: 2019-11-13. [Online]. Available: https://runwaygirlnetwork.com/2019/07/02/press-release-thinkom-phased-array-tested-over-telesat-leo-satellite/

[20] "AIX: Inmarsat eyes up satellites for polar coverage," 2019, Accessed: 2019-11-13. [Online]. Available: https://www.getconnected.aero/2019/04/aix-inmarsat-eyes-up-satellites-for-polar-coverage/

[21] Airbus Defence and Space, "Zephyr Pioneering the Stratosphere," 2019, Accessed: 2020-06-22. [Online]. Available: https://www.airbus.com/content/dam/corporate-topics/publications/brochures/Datasheet-Zephyr-February-2019.pdf

[22] Loon LLC, "Loon," 2020, Accessed: 2020-06-22. [Online]. Available: https://loon.com/

[23] A. Mohammed, A. Mehmood, F. N. Pavlidou, and M. Mohorcic, "The role of high-altitude platforms (HAPs) in the global wireless connectivity," *Proceedings of the IEEE*, vol. 99, no. 11, pp. 1939–1953, 2011.

[24] International Telecommunication Union, "WRC-19 identifies additional frequency bands for High Altitude Platform Station systems," 2019, Accessed: 2020-06-22. [Online]. Available: https://news.itu.int/wrc-19-identifies-additional-frequency-bands-for-high-altitude-platform-station-systems/

[25] Intelsat, "A Look Forward: Inflight Connectivity in 2022," 2017, Accessed: 2019-11-13. [Online]. Available: http://www.intelsat.com/intelsat-insider-newsletter/q4-nov-2017/a-look-forward-inflight-connectivity-in-2022/

[26] Eutelsat Broadband, "Eutelsat communications via Ka-Sat," Accessed: 2019-11-13. [Online]. Available: https://de.eutelsat.com/files/live/sites/eutelsatv2/files/contributed/products/pdf/Eutelsat-Broadband.pdf

[27] HughesNet, "Why choose HughesNet Gen5?" Accessed: 2019-11-13. [Online]. Available: https://www.hughesnet.com/frequently-asked-questions

[28] Iridium, "FlytLINK by Thales," Accessed: 2019-11-13. [Online]. Available: https://www.iridium.com/products/flytlink-by-thales/

[29] Globalstar, "Globalstar Overview," 2017, Accessed: 2019-11-13. [Online]. Available: https://www.globalstar.com/Globalstar/media/Globalstar/Downloads/Spectrum/GlobalstarOverviewPresentation.pdf

[30] Gilat Satellite Networks, "Gilat Achieves Fastest Ever Modem Speeds of 1.2Gbps Total Throughput over Telesat's Phase 1 LEO Satellite," 2019, Accessed: 2019-12-04. [Online]. Available: https://www.gilat.com/wp-content/uploads/2019/11/Gilat-PR-2019-11-21-Technology-Telesat-LEO-test-1.2Gbps.pdf

[31] Leosat, "A NEW TYPE OF SATELLITE CONSTELLATION," Accessed: 2019-11-13. [Online]. Available: http://leosat.com/technology/

[32] Gogo Inc., "Gogo ATG-4 – what is it, and how does it work?" 2014, Accessed: 2019-11-13. [Online]. Available: http://concourse.gogoair.com/gogo-atg-4-work/

[33] "Battle hotting up for US air-to-ground inflight connectivity," 2018, Accessed: 2019-11-13. [Online]. Available: https://www.getconnected.aero/2018/04/us-air-to-ground-inflight-connectivity/

[34] European Aviation Network, "The European aviation network," 2015, Accessed: 2019-02-21. [Online]. Available: https://www.telekom.com/resource/blob/390304/.../dl-150929-datenblatt-data.pdf

[35] International Civil Aviation Organization, "4G/5G MOBILE TECHNOLOGY APPLICATION IN CIVIL AVIATION," 2018.

[36] International Telecommunication Union, "Systems for public mobile communications with aircraft," International Telecommunication Union, Report ITU-R M.2282-0, 12 2013.

[37] CEPT, "ECC Report 214," no. May, 2014.

[38] "Airborne Wireless Network updates on Infinitus Super Highway," 2018, Accessed: 2019-11-14. [Online]. Available: https://www.getconnected.aero/2018/10/airborne-wireless-network-update-infinitus-super-highway/

[39] N. Larrieu and A. Varet, *Rapid Prototyping of Software for Avionics Systems*. Hoboken, NJ, USA: John Wiley & Sons, Inc., Oct 2014.

[40] J. Liu, Y. Shi, Z. M. Fadlullah, and N. Kato, "Space-Air-Ground Integrated Network : A Survey," *IEEE Communications Surveys Tutorials*, no. c, pp. 1–28, 2018.

[41] X. Cao, P. Yang, M. Alzenad, X. Xi, D. Wu, and H. Yanikomeroglu, "Airborne Communication Networks: A Survey," *IEEE Journal on Selected Areas in Communications*, vol. 36, no. 9, pp. 1907–1926, 2018.

[42] X. Zhang, L. Zhu, T. Li, Y. Xia, and W. Zhuang, "Multiple-User Transmission in Space Information Networks: Architecture and Key Techniques," *IEEE Wireless Communications*, vol. 26, no. 2, pp. 17–23, 2019.

[43] S. Zhou, G. Wang, S. Zhang, Z. Niu, Xuemin, and Shen, "Bi-Directional Mission Offloading for Agile Space-Air-Ground Integrated Networks," *IEEE Wireless Communications*, vol. 26, no. April, pp. 38–45, 2019.

[44] V. P. Hubenko, R. A. Raines, R. F. Mills, R. O. Baldwin, and B. E. Mullins, "Improving the Global Information Grid ' s Performance through Satellite Communications Layer Enhancements," *IEEE Communications Magazine*, no. November, pp. 66–72, 2006.

[45] D. Li, X. Shen, N. Chen, and Z. Xiao, "Space-based information service in Internet Plus Era," *Science China Information Sciences*, vol. 60, no. 10, 2017.

[46] Y. Shi, Y. Cao, J. Liu, and N. Kato, "A Cross-Domain SDN Architecture for Multi-Layered Space-Terrestrial Integrated Networks," *IEEE Network*, vol. 33, no. 1, pp. 29–35, 2019.

[47] N. Zhang, S. Zhang, P. Yang, O. Alhussein, W. Zhuang, and X. Shen, "Software Defined Space-Air-Ground Integrated Vehicular Networks: Challenges and Solutions," no. July, pp. 1–19, 2017.

[48] X. Huang, J. A. Zhang, R. P. Liu, Y. J. Guo, and L. Hanzo, "Airplane-aided integrated networking for 6g wireless: Will it work?" *IEEE Vehicular Technology Magazine*, vol. 14, no. 3, pp. 84–91, 2019.

[49] Y. Shi, J. Liu, Z. M. Fadlullah, and N. Kato, "Cross-layer data delivery in satellite-aerial-terrestrial communication," *IEEE Wireless Communications*, vol. 25, no. 3, pp. 138–143, 2018.

[50] N. Kato, Z. M. Fadlullah, F. Tang, B. Mao, S. Tani, A. Okamura, and J. Liu, "Optimizing space-air-ground integrated networks by artificial intelligence," *IEEE Wireless Communications*, vol. 26, no. 4, pp. 140–147, 2019.

[51] X. Zhang, W. Cheng, and H. Zhang, "Heterogeneous statistical QoS provisioning over airborne mobile wireless networks," *IEEE Journal on Selected Areas in Communications*, vol. 36, no. 9, pp. 2139–2152, 2018.

[52] M. Sheng, D. Zhou, R. Liu, Y. Wang, and J. Li, "Resource Mobility in Space Information Networks: Opportunities, Challenges, and Approaches," *IEEE Network*, vol. 33, no. 1, pp. 128–135, 2019.

[53] Y. Peng, T. Dong, R. Gu, Q. Guo, J. Yin, Z. Liu, T. Zhang, and Y. Ji, "A review of dynamic resource allocation in integrated satellite and terrestrial networks," *Proceedings - 2018 International Conference on Networking and Network Applications, NaNA 2018*, pp. 127–132, 2019.

[54] H. Liu, J. Zhang, and L. L. Cheng, "Application examples of the network fixed point theory for space-air-ground integrated communication network," *2010 International Congress on Ultra Modern Telecommunications and Control Systems and Workshops, ICUMT 2010*, pp. 989–993, 2010.

[55] Z. Yang, B. Xiao, and Y. Chen, "Modeling and Verification of Space-Air-Ground Integrated Networks on Requirement Level Using STeC," *Proceedings - 2015 International Symposium on Theoretical Aspects of Software Engineering, TASE 2015*, pp. 131–134, 2015.

[56] N. Cheng, W. Quan, W. Shi, H. Wu, Q. Ye, H. Zhou, W. Zhuang, X. S. Shen, and B. Bai, "A comprehensive simulation platform for space-air-ground integrated network," *IEEE Wireless Communications*, vol. 27, no. 1, pp. 178–185, 2020.

[57] É. Bouttier, R. Dhaou, F. Arnal, C. Baudoin, E. Dubois, and A. L. Beylot, "Analysis of content size based routing schemes in hybrid satellite / terrestrial networks," *2016 IEEE Global Communications Conference, GLOBECOM 2016 - Proceedings*, 2016.

[58] W. Qi, W. Hou, L. Guo, Q. Song, and A. Jamalipour, "A Unified Routing Framework for Integrated Space/Air Information Networks," *IEEE Access*, vol. 4, pp. 7084–7103, 2016.

[59] M. Vondra, M. Ozger, D. Schupke, and C. Cavdar, "Integration of Satellite and Aerial Communications for Heterogeneous Flying Vehicles," *IEEE Network*, vol. 32, no. 5, pp. 62–69, 2018.

[60] D. Medina and F. Hoffmann, "The Airborne Internet," *Future Aeronautical Communications*, 2011.

[61] J. Zhang, T. Chen, S. Zhong, J. Wang, W. Zhang, X. Zuo, R. G. Maunder, and L. Hanzo, "Aeronautical Ad Hoc Networking for the Internet-Above-The-Clouds," *Proceedings of the IEEE*, vol. 107, no. 5, pp. 868–911, 2019.

[62] O. S. Oubbati, M. Atiquzzaman, P. Lorenz, M. H. Tareque, and M. S. Hossain, "Routing in flying Ad Hoc networks: Survey, constraints, and future challenge perspectives," *IEEE Access*, vol. 7, pp. 81 057–81 105, 2019.

[63] Y. Wang, M. C. Erturk, H. Arslan, R. Sankar, and S. Morgera, "Throughput analysis in aeronautical data networks," *2011 IEEE 12th Annual Wireless and Microwave Technology Conference, WAMICON 2011*, pp. 1–5, 2011.

[64] Y. Wang, M. C. Ertürk, H. Arslan, R. Sankar, I. H. Ra, and S. Morgera, "Throughput and delay analysis in aeronautical data networks," *2012 International Conference on Computing, Networking and Communications, ICNC'12*, pp. 771–775, 2012.

[65] Y. Wang, M. C. Ertürk, J. Liu, I. H. Ra, R. Sankar, and S. Morgera, "Throughput and delay of single-hop and two-hop aeronautical communication networks," *Journal of Communications and Networks*, vol. 17, no. 1, pp. 58–66, 2015.

[66] J. Yan, C. Hua, C. Chen, and X. Guan, "The capacity of aeronautical ad-hoc networks," *Wireless Networks*, vol. 20, no. 7, pp. 2123–2130, 2014.

[67] S. Ghosh and A. Nayak, "ACPM : An Associative Connectivity Prediction Model for AANET," pp. 605–610, 2016.

[68] H. Zhang, X. Chen, B. Zheng, and Y. Wang, "Analysis of connectivity requirement for aeronautical Ad hoc networks," *Proceedings of 2011 International Conference on Electronic and Mechanical Engineering and Information Technology, EMEIT 2011*, vol. 8, pp. 3943–3946, 2011.

[69] K. D. Büchter, "Availability of aeronautical ad-hoc network in different global air transport fleet scenarios," *2017 32nd General Assembly and Scientific Symposium of the International Union of Radio Science, URSI GASS 2017*, vol. 2017-Janua, no. August, pp. 1–4, 2017.

[70] ——, "Availability of airborne Ad-hoc communication network in global air traffic simulation," *2016 10th International Symposium on Communication Systems, Networks and Digital Signal Processing, CSNDSP 2016*, pp. 8–11, 2016.

[71] K.-d. Büchter, "Modeling of High-capacity Aeronautical Communication Networks with Free-space Optical Links," in *4th International Workshop on Optical Wireless Communications (IWOW) Modeling*, 2015, pp. 21–25.

[72] K.-D. Büchter, N. Randt, and A. Sizmann, "Capacity scaling in airborne communication networks based on air traffic scenario modeling," in *Deutscher Luft-und Raumfahrtkongress*, 2013, pp. 1–10.

[73] B. Newton, J. Aikat, and K. Jeffay, "Analysis of topology algorithms for commercial airborne networks," *Proceedings - International Conference on Network Protocols, ICNP*, pp. 368–373, 2014.

[74] F. Besse, A. Pirovano, F. Garcia, and J. Radzik, "Aeronautical ad hoc networks: A new Datalink for ATM," *Proceedings of the 9th Innovative Research Workshop and Exhibition, INO 2010*, pp. 37–43, 2010.

[75] C. Petersen, K. Fuger, and A. Timm-Giel, "Analytical Model for Aircraft-to-Aircraft Link Probability Over the North Atlantic Corridor," in *2018 IEEE 88th Vehicular Technology Conference (VTC-Fall)*. IEEE, Aug 2018, pp. 1–5.

[76] R. W. Kingsbury, "Mobile Ad Hoc Networks for Oceanic Aircraft Communications," M.S. Thesis, Massachusetts Institute of Technology, Massachusetts, USA, 2009.

[77] Q. Vey, "Access and Routing in Aeronautical Ad-hoc Networks," in *16e Congrès des Doctorants EDSYS (École Doctorale Systèmes)*, no. May 2015, 2015.

[78] Q. Vey, A. Pirovano, J. Radzik, and F. Garcia, "Aeronautical Ad Hoc Network for Civil Aviation," 2014, pp. 81–93.

[79] G. Hadynski, S. B. Lee, G. Rajappan, R. Sundaram, X. Wang, and F. Zhou, "Optimization of directional antenna network topology in airborne networks," *Proceedings - IEEE Military Communications Conference MILCOM*, no. April, pp. 68–73, 2010.

[80] B. N. Cheng, R. Charland, P. Christensen, L. Veytser, and J. Wheeler, "Evaluation of a multihop airborne ip backbone with heterogeneous radio technologies," *IEEE Transactions on Mobile Computing*, vol. 13, no. 2, pp. 299–310, 2014.

[81] S. Ghosh and A. Nayak, "Multi-dimensional clustering and network monitoring system for aeronautical ad hoc networks," *International Conference on Ubiquitous and Future Networks, ICUFN*, vol. 2015-August, pp. 772–777, 2015.

[82] K. Karras, T. Kyritsis, M. Amirfeiz, and S. Baiotti, "Aeronautical mobile ad hoc networks," *EW2008 - 14th European Wireless Conference 2008, Electronic Proceedings*, 2008.

[83] A. Numani, S. J. Nawaz, and M. A. Javed, "Architecture and Routing Protocols for Airborne Internet Access," *2018 IEEE International Conference on Consumer Electronics - Asia, ICCE-Asia 2018*, pp. 206–212, 2018.

[84] Q. Vey, A. Pirovano, and J. Radzik, "Routing protocol assessment for AANETs," vol. 181, no. 5-7, pp. 268–275, 2010.

[85] F. Besse, F. Garcia, A. Pirovano, and J. Radzik, "Wireless Ad Hoc Networks Access For Aeronautical Communications," in *28th AIAA International Communications Satellite Systems Conference (ICSSC-2010)*. Reston, Virigina: American Institute of Aeronautics and Astronautics, Aug 2010.

[86] F. Besse, A. Pirovano, F. Garcia, and J. Radzik, "Interference estimation in an aeronautical ad hoc network," *AIAA/IEEE Digital Avionics Systems Conference - Proceedings*, 2011.

[87] F. Hoffmann, D. Medina, and A. Wolisz, "Joint routing and scheduling in mobile aeronautical Ad Hoc networks," *IEEE Transactions on Vehicular Technology*, vol. 62, no. 6, pp. 2700–2712, 2013.

[88] D. Medina, F. Hoffmann, F. Rossetto, and C. H. Rokitansky, "A crosslayer geographic routing algorithm for the airborne internet," *IEEE International Conference on Communications*, pp. 1–6, 2010.

[89] K. Peters, A. Jabbar, E. K. Cetinkaya, and J. P. Sterbenz, "A geographical routing protocol for highly-dynamic aeronautical networks," *2011 IEEE Wireless Communications and Networking Conference, WCNC 2011*, pp. 492–497, 2011.

[90] Z. Zheng, A. K. Sangaiah, and T. Wang, "Adaptive Communication Protocols in Flying Ad Hoc Network," *IEEE Communications Magazine*, vol. 56, no. 1, pp. 136–142, 2018.

[91] M. Iordanakis, D. Yannis, K. Karras, G. Bogdos, G. Dilintas, M. Amirfeiz, G. Colangelo, and S. Baiotti, "Ad-hoc routing protocol for aeronautical mobile ad-hoc networks," *Fifth International Symposium on Communication Systems, Networks and Digital Signal Processing (CSNDSP)*, pp. 1–5, 2006.

[92] D. Medina, F. Hoffmann, S. Ayaz, and C. H. Rokitansky, "Feasibility of an aeronautical mobile ad hoc network over the north atlantic corridor," *2008 5th Annual IEEE Communications Society Conference on Sensor, Mesh and Ad Hoc Communications and Networks, SECON*, pp. 109–116, 2008.

[93] A. Tiwari, A. Ganguli, A. Sampath, D. S. Anderson, B. H. Shen, N. Krishnamurthi, J. Yadegar, M. Gerla, and D. Krzysiak, "Mobility aware routing for the airborne network backbone," *Proceedings - IEEE Military Communications Conference MILCOM*, no. December, 2008.

[94] H. Tu and S. Shimamoto, "Mobile ad-hoc network based relaying data system for oceanic flight routes in aeronautical communications," *International Journal of Computer Networks and Communications*, vol. 1, no. 1, pp. 33–44, 2009.

[95] N. Krishnamurthi, A. Ganguli, A. Tiwari, B. H. Shen, J. Yadegar, and G. Hadynski, "Topology control for future airborne networks," *Proceedings - IEEE Military Communications Conference MILCOM*, pp. 1–7, 2009.

[96] S. U. Hyeon, K. I. Kim, and S. W. Yang, "A new geographic routing protocol for aircraft ad hoc networks," *AIAA/IEEE Digital Avionics Systems Conference - Proceedings*, pp. 1–8, 2010.

[97] K. Saifullah and K. I. Kim, "A new geographical routing protocol for heterogeneous aircraft Ad Hoc Networks," *AIAA/IEEE Digital Avionics Systems Conference - Proceedings*, pp. 1–9, 2012.

[98] Q. Vey, S. Puechmorel, A. Pirovano, and J. Radzik, "Routing in aeronautical ad-hoc networks," *AIAA/IEEE Digital Avionics Systems Conference - Proceedings*, pp. 1–10, 2016.

[99] Q. Vey, A. Pirovano, S. Puechmorel, and J. Radzik, "Performance assessment of a new routing protocol in AANET," *Lecture Notes in Computer Science (including subseries Lecture Notes in Artificial Intelligence and Lecture Notes in Bioinformatics)*, vol. 10222 LNCS, pp. 3–14, 2017.

[100] E. Sakhaee and A. Jamalipour, "The Global In-Flight Internet," *IEEE Journal on Selected Areas in Communications*, vol. 24, no. 9, pp. 1748–1757, Sep 2006.

[101] E. Sakhaee, A. Jamalipour, and N. Kato, "Aeronautical ad hoc networks," *Wireless Communications and Networking Conference, 2006. WCNC 2006. IEEE*, vol. 00, no. c, pp. 246–251, 2006.

[102] W. Gu, J. Li, F. He, F. Cai, and F. Yang, "A Delay-aware Stable Routing Protocol for Aeronautical Ad Hoc Networks," vol. 2, no. 2009, pp. 347–359, 2012.

[103] S. Wang, C. Fan, C. Deng, W. Gu, Q. Sun, and F. Yang, "A-GR: A novel geographical routing protocol for AANETs," *Journal of Systems Architecture*, vol. 59, no. 10 PART B, pp. 931–937, 2013.

[104] L. Lei, D. Wang, L. Zhou, X. Chen, and S. Cai, "Link availability estimation based reliable routing for aeronautical ad hoc networks," *Ad Hoc Networks*, vol. 20, pp. 53–63, 2014.

[105] E. Sakhaee, A. Jamalipour, and N. Kato, "Multipath doppler routing with QoS support in pseudo-linear highly mobile Ad Hoc networks," *IEEE International Conference on Communications*, vol. 8, pp. 3566–3571, 2006.

[106] F. Hoffmann, D. Medina, and A. Wolisz, "Two-step delay based internet gateway selection scheme for aeronautical ad hoc networks," *IEEE International Symposium on Personal, Indoor and Mobile Radio Communications, PIMRC*, pp. 2638–2642, 2009.

[107] S. H. Bouk and I. Sasase, "Multiple end-to-end QoS metrics gateway selection scheme in mobile ad hoc networks," *2009 International Conference on Emerging Technologies, ICET 2009*, no. June 2014, pp. 446–451, 2009.

[108] Q. Luo and J. Wang, "Multiple QoS Parameters-Based Routing for Civil Aeronautical Ad Hoc Networks," *IEEE Internet of Things Journal*, vol. 4, no. 3, pp. 804–814, 2017.

[109] K. Chen, S. Zhao, N. Lv, W. Gao, X. Wang, and X. Zou, "Segment Routing Based Traffic Scheduling for the Software-Defined Airborne Backbone Network," *IEEE Access*, vol. 7, 2019.

[110] K. Sampigethaya, R. Poovendran, S. Shetty, T. Davis, and C. Royalty, "Future E-enabled aircraft communications and security: The next 20 years and beyond," *Proceedings of the IEEE*, vol. 99, no. 11, pp. 2040–2055, 2011.

[111] K. Büchter, A. Reinhold, G. Stenz, and A. Sizmann, "Drivers and Elements of Future Airborne Communication Networks," pp. 1–10, 2012.

[112] K. Büchter and A. Sizmann, "High-Bandwidth Aeronautical Telecommunication Options," 2014.

[113] T. Graupl and M. Ehammer, "Simulation results and final recommendations of the SANDRA concept for integrated IP-based aeronautical networking," *Integrated Communications, Navigation and Surveillance Conference, ICNS*, 2013.

[114] S. Plass, "Seamless networking for aeronautical communications: One major aspect of the SANDRA concept," *IEEE Aerospace and Electronic Systems Magazine*, vol. 27, no. 9, pp. 21–27, 2012.

[115] S. Plass, R. Hermenier, O. Lucke, D. Depoorter, T. Tordjman, M. Chatterton, M. Amirfeiz, S. Scotti, Yongqiang Cheng, P. Pillai, T. Graupl, F. Durand, K. Murphy, A. Marriott, and A. Zaytsev, "Flight trial demonstration of seamless aeronautical networking," *IEEE Communications Magazine*, vol. 52, no. 5, pp. 119–128, May 2014.

[116] O. Lucke, D. G. Depoorter, T. Tordjman, and F. Kuhnde, "The SANDRA testbed for the future aeronautical communication network," *Integrated Communications, Navigation and Surveillance Conference, ICNS*, 2013.

[117] T. Mcparland, "A Common Mobility Solution for ATN OSI and Internet Protocol Stacks," 2004.

[118] C. Bauer and M. Zitterbart, "A survey of protocols to support IP mobility in aeronautical communications," *IEEE Communications Surveys and Tutorials*, vol. 13, no. 4, pp. 642–657, 2011.

[119] A. Jahn, M. Holzbock, J. Müller, R. Kebel, M. De Sanctis, A. Rogoyski, E. Trachtman, O. Franzrahe, M. Werner, and F. Hu, "Evolution of aeronautical communications for personal and multimedia services," *IEEE Communications Magazine*, vol. 41, no. 7, pp. 36–43, 2003.

[120] J. Zambrano, O. Yeste, and R. Landry, "Requirements for communication systems in future passenger air transportation," *AIAA AVIATION 2014 -14th AIAA Aviation Technology, Integration, and Operations Conference*, no. June, pp. 1–18, 2014.

[121] H. Gonzalez, X. Prats, and C. Bes, "Capacity modelling for future aeronautical safety communications over wide areas," in *The 26th Congress of ICAS and 8th AIAA ATIO*, 2008.

[122] A. Mishra, "Performance Analysis of Multipath Data Transport in Tactical Networks," *2018 6th IEEE International Conference on Wireless for Space and Extreme Environments, WiSEE 2018*, pp. 95–100, 2018.

[123] D. Gomez Depoorter and W. Kellerer, "Designing the air-ground data links for future air traffic control communications," *IEEE Transactions on Aerospace and Electronic Systems*, vol. 55, no. 1, pp. 135–146, 2019.

[124] C. Zhang, Y. Zhang, J. Xiao, and J. Yu, "Aeronautical central cognitive broadband air-to-ground communications," *IEEE Journal on Selected Areas in Communications*, vol. 33, no. 5, pp. 946–957, 2015.

[125] M. Hoyhtya, J. Huusko, M. Kiviranta, K. Solberg, and J. Rokka, "Connectivity for autonomous ships: Architecture, use cases, and research challenges," *International Conference on Information and Communication Technology Convergence: ICT Convergence Technologies Leading the Fourth Industrial Revolution, ICTC 2017*, vol. 2017-December, no. October, pp. 345–350, 2017.

[126] R. Goyal, S. Kota, R. Jain, S. Fahmy, B. Vandalore, and J. Kallaus, "Analysis and Simulation of Delay and Buffer Requirements of Satellite- ATM Networks for TCP / IP Traffic," pp. 1–24, 1998.

[127] N. V. Wambeke and M. Gineste, "The role of satellite systems in future aeronautical communications," *Future Aeronautical Communications*, pp. 1–15, 2011.

[128] R. Ferrús, H. Koumaras, O. Sallent, G. Agapiou, T. Rasheed, M. A. Kourtis, C. Boustie, P. Gélard, and T. Ahmed, "SDN/NFV-enabled satellite communications networks: Opportunities, scenarios and challenges," *Physical Communication*, vol. 18, pp. 95–112, 2016.

[129] D. Fischer, D. Basin, and T. Engel, "Topology dynamics and routing for predictable mobile networks," *Proceedings - International Conference on Network Protocols, ICNP*, no. 2, pp. 207–217, 2008.

[130] D. Fischer, K. Eckstein, D. Basin, and T. Engel, "Increasing the efficiency of next-generation space operations by exploiting predictability," *Proceedings - 2009 3rd IEEE International Conference on Space Mission Challenges for Information Technology, SMC-IT 2009*, pp. 315–322, 2009.

[131] D. Fischer, D. Basin, K. Eckstein, and T. Engel, "Predictable mobile routing for spacecraft networks," *IEEE Transactions on Mobile Computing*, vol. 12, no. 6, pp. 1174–1187, 2013.

[132] J. Jurski and J. Wozniak, "Routing decisions independent of queuing delays in broadband LEO networks," *GLOBECOM - IEEE Global Telecommunications Conference*, 2009.

[133] H. Nishiyama, Y. Tada, N. Kato, N. Yoshimura, M. Toyoshima, and N. Kadowaki, "Toward Optimized Traffic Distribution for Efficient Network Capacity Utilization in Two-Layered Satellite Networks," *IEEE Transactions on Vehicular Technology*, vol. 62, no. 3, pp. 1303–1313, 2013.

[134] T. Taleb, D. Takaishi, A. Jamalipour, N. Kato, and Y. Nemoto, "Explicit Load Balancing Technique for NGEO Satellite IP Networks With On-Board Processing Capabilities," *IEEE/ACM Transactions on Networking*, vol. 17, no. 1, pp. 281–293, 2009.

[135] J. A. Ruiz de Azua, A. Calveras, and A. Camps, "Internet of Satellites (IoSat): Analysis of Network Models and Routing Protocol Requirements," *IEEE Access*, vol. 6, 2018.

[136] M. Schmidt and W. Schütz, "Radio Frequency Spectrum Requirement Calculations for Future Aeronautical Mobile (Route) System," pp. 1–60, 2003. [Online]. Available: https://eurocontrol.int/sites/default/files/content/documents/communications/radio-frequency-spectrum-requirement-calculations-for-future-aeronautical-mobile-system-amrs.pdf

[137] N. Tadayon, G. Kaddoum, and R. Noumeir, "Inflight Broadband Connectivity Using Cellular Networks," *IEEE Access*, vol. 4, no. c, pp. 1595–1606, 2016.

[138] Nokia, "Using air-to-ground LTE for in-flight ultra-broadband," pp. 1–18, 2016.

[139] M. Sakamoto and S. Kawato, "Four-dimensional network simulation of direct air to ground LTE networks," *2016 1st International Workshop on Link- and System Level Simulations, IWSLS 2016*, pp. 7–12, 2016.

[140] S.-p. Chen, "Perfomance Analysis and Optimization of DA2GC using LTE Advanced Technology," in *GLOBAL WIRELESS SUMMIT*, 2014, pp. 2–6.

[141] M. Vondra, E. Dinc, and C. Cavdar, "Coordinated Resource Allocation Scheme for 5G Direct Air-to-Ground Communication," in *European Wireless 2018; 24th European Wireless Conference*, 2018, pp. 137–143.

[142] H. N. Qureshi and A. Imran, "Towards Designing Systems with Large Number of Antennas for Range Extension in Ground-to-Air Communications," *IEEE International Symposium on Personal, Indoor and Mobile Radio Communications, PIMRC*, vol. 2018-Septe, 2018.

[143] E. Dinc, M. Vondra, and C. Cavdar, "Multi-user Beamforming and Ground Station Deployment for 5G Direct Air-to-Ground Communication," *IEEE Global Communications Conference (GLOBECOM)*, 2017.

[144] X. Lin, A. Furuskär, O. Liberg, and S. Euler, "Sky high 5G: New radio for air-to-ground communications," *arXiv preprint arXiv:2003.06361*, 2020.

[145] Q. Sun, D. Wang, Y. Wang, M. Gao, and G. Zhao, "Handoff rate analysis of aircraft in the aeronautical network," in *Proceedings of the 2019 8th International Conference on Networks, Communication and Computing*. Association for Computing Machinery, 2019, p. 109–115.

[146] L. Wang and G. S. G. Kuo, "Mathematical modeling for network selection in heterogeneous wireless networks - A tutorial," *IEEE Communications Surveys and Tutorials*, vol. 15, no. 1, pp. 271–292, 2013.

[147] X. Xi, X. Cao, P. Yang, Z. Xiao, and D. Wu, "Efficient and fair network selection for integrated cellular and drone-cell networks," *IEEE Transactions on Vehicular Technology*, vol. 68, no. 1, pp. 923–937, 2019.

[148] D. Wang, G. Huang, S. Dong, Y. Wang, J. Liu, and W. Gao, "Network-Assisted Optimal Datalink Selection Scheme for Heterogeneous Aeronautical Network," *Wireless Communications and Mobile Computing*, vol. 2018, pp. 1–13, 2018.

[149] D. Wang, Y. Wang, S. Dong, G. Huang, J. Liu, and W. Gao, "Exploiting Dual Connectivity for Handover Management in Heterogeneous Aeronautical Network," *IEEE Access*, vol. 7, pp. 62 938–62 949, 2019.

[150] A. S. Alam, Y. F. Hu, P. Pillai, K. Xu, and J. Baddoo, "Optimal Datalink Selection for Future Aeronautical Telecommunication Networks," *IEEE Transactions on Aerospace and Electronic Systems*, vol. 53, no. 5, pp. 2502–2515, 2017.

[151] F. Mendoza, R. Ferrus, and O. Sallent, "A traffic distribution scheme for 5G resilient backhauling using integrated satellite networks," *2017 13th International Wireless Communications and Mobile Computing Conference, IWCMC 2017*, pp. 1671–1676, 2017.

[152] "FlightRadar24," Accessed: 2019-12-02. [Online]. Available: https://www.flightradar24.com/

[153] Federal Communications Commission, "OneWeb Non-Geostationary Satellite System," 2018.

[154] OneWeb, "How OneWeb's system works," 2020, Accessed: 2020-03-17. [Online]. Available: https://www.youtube.com/watch?v=YIrIt0R47Z8

[155] International Air Transport Association, "2036 Forecast Reveals Air Passengers Will Nearly Double to 7.8 Billion," 2017, Accessed: 2019-02-21. [Online]. Available: http://www.iata.org/pressroom/pr/Pages/2017-10-24-01.aspx

[156] 3GPP, "Study on New Radio (NR) to support non-terrestrial networks," 3rd Generation Partnership Project (3GPP), Technical Report (TR) 38.811, 12 2019, version 15.2.0.

[157] ——, "Study on architecture aspects for using satellite access in 5G," 3rd Generation Partnership Project (3GPP), Technical Report (TR) 23.737, 12 2019, version 17.0.0.

[158] ——, "Study on access traffic steering, switch and splitting support in the 5G system architecture," 3rd Generation Partnership Project (3GPP), Technical Report (TR) 23.793, 12 2018, version 16.0.0.

[159] ——, "Proximity-based services (ProSe)," 3rd Generation Partnership Project (3GPP), Technical Specification (TS) 23.303, 06 2018, version 15.1.0.

[160] U. N. Kar and D. K. Sanyal, "A Critical Review of 3GPP Standardization of Device-to-Device Communication in Cellular Networks," *SN Computer Science*, vol. 1, no. 1, pp. 1–18, 2020.

[161] 3GPP, "Evolved Universal Terrestrial Radio Access (E-UTRA) and Evolved Universal Terrestrial Radio Access Network (E-UTRAN)," 3rd Generation Partnership Project (3GPP), Technical Specification (TS) 36.300, 12 2019, version 16.0.0.

[162] ——, "Evolved Universal Terrestrial Radio Access (E-UTRA); Physical layer procedures," 3rd Generation Partnership Project (3GPP), Technical Specification (TS) 36.213, 03 2020, version 16.1.0.

[163] S. O. Elbassiouny and A. S. Ibrahim, “Link level performance evaluation of higher order modulation in Small Cells,” *IWCMC 2014 - 10th International Wireless Communications and Mobile Computing Conference*, pp. 850–855, 2014.

[164] J. Zyren, “Overview of the 3GPP Long Term Evolution Physical Layer,” 2007, Accessed: 2019-02-22. [Online]. Available: https://www.nxp.com/docs/en/white-paper/3GPPEVOLUTIONWP.pdf

[165] 3GPP, “NR; User equipment (UE radio access capabilities,” 3rd Generation Partnership Project (3GPP), Technical Specification (TS) 38.306, 03 2020, version 16.0.0.

[166] J. Parsons, *The Mobile Radio Propagation Channel*. Wiley, Nov 2001.

[167] V. Megas, “Aircraft to aircraft connectivity analysis,” Master thesis, KTH Royal Institute of Technology, Stockholm, Sweden, 2018.

[168] H. Friis, “A Note on a Simple Transmission Formula,” *Proceedings of the IRE*, vol. 34, no. 5, pp. 254–256, May 1946.

[169] National Oceanic and Atmospheric Administration, “U.S. Standard Atmosphere,” 1976.

[170] D. Minoli, *Satellite Systems Engineering in an IPv6 Environment*. Auerbach Publications, Feb 2009.

[171] European Telecommunications Standards Institute, “Broadband Direct Air-to-Ground Communications; Equipment operating in the 1900 MHz to 1920 MHz and 5855 MHz to 5875 MHz frequency bands; Fixed pattern antennas; Harmonised Standard covering the essential requirements of article 3.2 of Directive 2014/5,” vol. 1, pp. 1–37, 2016.

[172] ThinAir, “Delivering High Performance from Every Orbit,” 2018, Accessed: 2020-05-10. [Online]. Available: https://www.thinkom.com/wp-content/uploads/2018/09/ka2517-datasheet_9_18_web.pdf

[173] Deutsche Telekom AG, “EAN LTE-basiertes Bodennetz,” 2019, Accessed: 2019-12-15. [Online]. Available: https://www.telekom.com/resource/blob/513890/.../dl-ean-07-ean-lte-basiertes-bodennetz-karte-data.jpg

[174] Travel Skills Group, “How we use inflight wi-fi,” 2013, Accessed: 2019-12-15. [Online]. Available: https://travelskills.com/2013/03/08/how-we-use-inflight-wi-fi-infographic/

[175] 3GPP, “Evolved Universal Terrestrial Radio Access (E-UTRA); LTE Positioning Protocol (LPP),” 3rd Generation Partnership Project (3GPP), Technical Specification (TS) 36.355, 09 2019, version 15.5.0.